DISTRIBUTION AGREEMENT

In presenting this thesis or dissertation as a partial fulfillment of the requirements for an advanced degree from Emory University, I hereby grant to Emory University and its agents the non-exclusive license to archive, make accessible, and display my thesis or dissertation in whole or in part in all forms of media, now or hereafter known, including display on the world wide web. I understand that I may select some access restrictions as part of the online submission of this thesis or dissertation. I retain all ownership rights to the copyright of the thesis or dissertation. I also retain the right to use in future works (such as articles or books) all or part of this thesis or dissertation.

Signature:

_____ _____

Sarah L. Lebeis Date

STRIKING A BALANCE: ANALYSIS OF THE PROTECTIVE AND DESTRUCTIVE CONSEQUENCES OF INNATE IMMUNITY AGAINST THE A/E PATHOGEN *CITROBACTER RODENTIUM*

By

Sarah L. Lebeis
Doctor of Philosophy

Graduate Division of Biological and Biomedical Sciences
Program in Microbiology and Molecular Genetics

_____
Daniel Kalman
Advisor

_____
William Shafer
Committee Member

_____
Melanie A. Sherman
Committee Member

_____
Samuel Speck
Committee Member

_____
Ifor R.Williams
Committee Member

Accepted:

_____
Lisa A. Tedesco, Ph.D.
Dean of the Graduate School

_____
Date

STRIKING A BALANCE: ANALYSIS OF THE PROTECTIVE AND DESTRUCTIVE CONSEQUENCES OF INNATE IMMUNITY AGAINST THE A/E PATHOGEN *CITROBACTER RODENTIUM*

By

Sarah L. Lebeis
B.S, Michigan State University, 2002

Advisor: Daniel Kalman

An abstract of

A dissertation submitted to the Faculty of the Graduate

School of Emory University in partial fulfillment

of the requirements for the degree of

Doctor of Philosophy

in

Program in Microbiology and Molecular Genetics

Graduate Division of Biological and Biomedical Sciences

2008

ABSTRACT

STRIKING A BALANCE: ANALYSIS OF THE PROTECTIVE AND DESRTUCTIVE EFFECTS OF INNATE IMMUNITY IN RESPONSE TO THE A/E PATHOGEN *CITROBACTER RODENTIUM*

By Sarah L. Lebeis

Attaching and effacing (A/E) pathogens such as enteropathogenic *Escherichia coli* (EPEC) and Citrobacter *rodentium* adhere to intestinal epithelia and destroy absorptive microvilli. In mice, *C. rodentium* breach the intestinal epithelial barrier, leading to colitis via vigorous inflammation. Ultimately, a protective antibody response clears the infection. Here I explore the regulatory mechanisms that orchestrate a balanced innate immune response that facilitate both destructive effects, such as inflammation, and protective effects during a *C. rodentium* infection. More specifically, I demonstrate that the signaling cascades activated by the type I IL-1 receptor and MyD88, a signaling adaptor protein utilized by several innate immune receptors including TLRs and IL-1R, protect mice from lethal intestinal damage induced by *C. rodentium*. Interestingly, although the intestinal damage prevented by MyD88 signaling is associated with many complex and interrelated phenotypes including induction of epithelial repair, neutrophil recruitment, and control of pathogen load, IL-1R signaling appears to only regulate sensitivity of intestinal epithelia to damage caused by *C. rodentium*. Finally, I show that a slow growing variant of *C. rodentium* induces equally low levels of disease in wild type and MyD88$^{-/-}$ mice, suggesting that the increased intestinal damage seen in infected MyD88$^{-/-}$ animals is pathogen-induced, rather than host-induced. Together these studies indicate that IL-1R, TLR, and MyD88 signaling mediate a balanced innate immune response in which the protective effects outweigh the destructive effects during infection with *C. rodentium*.

STRIKING A BALANCE: ANALYSIS OF THE PROTECTIVE AND DESTRUCTIVE EFFECTS OF INNATE IMMUNITY IN RESPONSE TO THE A/E PATHOGEN *CITROBACTER RODENTIUM*

By

Sarah L. Lebeis
B.S., Michigan State University, 2002

Advisor: Daniel Kalman

A dissertation submitted to the Faculty of the Graduate

School of Emory University in partial fulfillment

of the requirements for the degree of

Doctor of Philosophy

in

Program in Microbiology and Molecular Genetics

Graduate Division of Biological and Biomedical Sciences

2008

TABLE OF CONTENTS

CHAPTER I:

INTRODUCTION

Table I and II were previously published as part of Lebeis et al. 2008.

Introduction:

Pathogenic strains of *Escherichia coli*, including enteropathogenic *E. coli* (EPEC) and enterohemorrhagic *E. coli* (EHEC), pose a significant public health risk especially in developing countries where they contaminate food and water supplies. EPEC causes infantile diarrhea (1) and leads to severe dehydration, which contributes to as many as one million infant deaths per year (2). EHEC infections cause hemorrhagic colitis and can lead to hemolytic-uremic syndrome (HUS), a potentially fatal disease (3, 4). EPEC, EHEC, and the murine pathogen *Citrobacter rodentium* are classified as attaching and effacing (A/E) pathogens based on the ability of these extracellular bacteria to intimately attach to intestinal epithelium, induce actin rearrangements called pedestals, and flatten absorptive microvilli (effacement). These actions require a ~35 kB pathogenicity island called the locus of enterocyte effacement (LEE) (5). All A/E pathogens have the LEE, which contains genes encoding a type III secretion system (TTSS), several translocated effector proteins, a bacterial outer-membrane protein intimin, and translocated intimin receptor (Tir) (1). Both the secretion system itself and many of the LEE effectors are required for disease in a mouse model of A/E infection (6). Additional effectors and toxins encoded elsewhere in the genome have also been recognized to play a critical role in disease (7).

Upon infection, A/E pathogens displace the commensal flora (8) and cause intestinal inflammation characterized by crypt hyperplasia, goblet cell depletion, cellular necrosis, infiltration of immune cells and damage to the lumen of the epithelium (9, 10). Following detection of pathogens by innate immune receptors, signaling pathways are triggered and the immune response against the pathogen is initiated. Innate immune

signaling pathways ultimately lead to activation of transcription factors (e.g. NF-κB and IRF-3), which regulate expression of cytokines and chemokines (e.g. IL-6, IFN-γ, TNF-α, IL-8, etc.). Following their production, cytokine and chemokines facilitate recruitment and activation of innate immune cells, such as macrophages, neutrophils, and dendritic cells (11, 12). Dendritic cells present antigens found in the intestinal lumen to naïve T cells in draining secondary lymphatic tissues such as Peyer's patches and mesenteric lymph nodes (12). The innate immune response helps to initiate a robust antibody response, which is required for clearance of the infection (13) and to lower disease severity upon reinfection (14). Much of the pathology observed during an infection with A/E pathogens appears to result from a host response to the bacteria following disruption of epithelial barrier, such as the formation of crypt abscesses upon neutrophil infiltration (15). In summary, for infections caused by A/E pathogens, the activation of innate immune cells leads to both stimulation of a protective antibody response and deleterious inflammation. In this dissertation, I will evaluate both the protective and destructive roles the innate immune system plays during an infection with *C. rodentium*.

A. Innate immune recognition of microbes

1. Host-pathogen interactions

The relationship between a host and its pathogen is not static in an evolutionary sense. However, adaptations cannot occur unless each has the ability to sense the presence of the other. In fact, this interaction is so imperative that both hosts and pathogens have acquired numerous systems of detection for the other. In hosts, several sets of innate immune sensors called pattern recognition receptors (PRR) detect pathogen associated molecular patterns (PAMPs) (16). PAMPs are conserved motifs associated with a wide variety of pathogens, allowing the host to detect bacteria, virus, and fungal pathogens (17). Notably, PRRs are remarkably similar in plants, insect, and mammals in structure and function (18), suggesting that host-pathogen interactions are a driving force during evolution. The first of these receptors, Toll, was discovered in *Drosophila melanogaster*. Initially Toll was identified for its role in embryonic development (19), but later it was discovered that flies lacking Toll had increased susceptibility to fungal and Gram-positive infections (20, 21). Soon afterward, mammalian homologs of Toll were discovered, and thus the importance of innate immune PRRs was uncovered (22-24).

2. Pattern recognition receptors (PRRs)

There are several sets of germline encoded PRRs that have been identified in animals to defend against invading pathogens. Probably the best characterized family of PRRs is Toll-like receptors (TLRs). To date, thirteen of these type I transmembrane proteins have been discovered in mammalian systems (25). There have been ten TLRs identified in humans (TLR1-10) and twelve TLRs identified in mice (TLR 1-9 and TLR

11-13) (25). TLRs recognize and respond to conserved motifs associated with microbes, which include proteins (e.g. flagellin), lipids (e.g. lipid A of LPS), and nucleic acids (e.g. CpG DNA) (26). TLRs bind to with their ligands by extracellular leucine rich repeat (LRR) domain. Innate immune signaling cascades are mediated by adaptor proteins, which interact with TLRs via a protein domain present in both TLRs and IL-1 receptor family members called the Toll/IL-1R homologous (TIR) domain. Another group of PRRs found in mammalian systems are cytolsolic receptors known as nucleotide-binding oligomerization domain (NODs) and their other family members NOD-like receptors (NLRs), which include: NOD1, NOD2, NALP, CIITA, IPAF and NAIP (18). Although NLRs contain LRR regions to bind their ligands similar to TLRs, the rest of the structure is more related to resistance (R) proteins in plants than to TLRs (27). Both NLRs and R proteins contain a central nucleotide binding site (NBS or NACHT) domain and at least one protein-protein interaction domain, such as caspase-activating and recruitment domain (CARD), TIR domain, or a pyrine N-terminal homology domain (PYD) (28).

Signaling cascades initiated by engagement of PRRs with their ligands requires protein-protein interactions of receptors with signaling adaptor proteins. For example, the TIR domains of TLRs associate with the TIR domains of their adaptor proteins (25). Stimulation of TLRs can potentially activate several signaling cascades. The pattern of signaling pathways stimulated depends largely on which adaptor proteins associate with the TLR that has been activated. The most commonly utilized adaptor protein amongst TLRs is myeloid differentiation primary response gene 88 (MyD88) (26). A/E pathogens contain many TLR ligands, which could potentially induce production of pro-inflammatory cytokines, such as IL-6, IFN-γ, TNF-α, and IL-8. In fact, most of these

cytokines are strongly induced during an infection with A/E pathogens (15, 29), suggesting the TLR signaling pathways may partially mediate these responses to A/E infections *in vivo*.

B. Model systems for exploring the innate immune response to A/E pathogens.

1. *In vitro* models of A/E infection.

Several *in vitro* and *in vivo* experimental systems exist to study A/E pathogens, and the innate immune response they elicit. The intestinal epithelia are the first host cells to encounter A/E pathogens and respond to the infection. Intestinal epithelial cells derived from human intestinal cancer patients, such as Caco-2 (small intestine) and T84 (colon) are passaged as immortal cell lines and can be grown as polarized monolayers. These and other cultured cell types have been exploited to define initial steps in EPEC pathogenesis such as pedestal formation (30-32), mechanisms of barrier disruption (33, 34), the host response to EPEC, and bacterial immunoevasive measures. With regards to innate immune responses, Savkovic et al. have shown that EPEC infection of T84 cells induces production of IL-8, a potent neutrophil chemokine, through the NF-κB pathway (29). More specifically, EPEC flagellin alone or supernatant from EPEC cultures, which contain flagellin, potently induce IL-8 production (35, 36). However, IL-8 production can be induced by EPEC lacking flagellin suggesting that additional innate immune receptors contribute to pro-inflammatory cytokine production (36). *In vitro*, TLR5 is sufficient to activate NF-kB in response to EPEC flagellin, though it remains unclear whether TLR5 participates in innate immune detection *in vivo*. Recent reports indicate that prior to barrier breach, an unknown secreted EPEC effector can inhibit NF-κB activation *in vitro*

by suppressing the IκB kinase, MAP kinase, and PI-3 kinase pathways (37). Thus, although EPEC flagellin is capable of inducing pro-inflammatory cytokine production, such an effector may dampen the response, perhaps limiting inflammation.

In vitro experiments have identified a similar immune evasion strategy in EHEC. In EHEC, an unknown secreted EHEC effector inhibits STAT-1 signaling (38), and thus inhibits cytokine production by altering IFN-γ receptor localization in epithelial cell lines (39). Further, many strains of EHEC encode a metalloprotease, which specifically cleaves C1 esterase inhibitor, a regulator of classical complement cascade (40), although its role in pathogenesis *in vivo* has not been determined. While *in vitro* experiments allow mechanistic characterization of virulence factors, insights gained from evaluating innate immune responses require validation via *in vivo* studies.

2. *In vivo* models of A/E pathogen infection.

A variety of small animal models have been developed to study A/E pathogens *in vivo*. Rabbit diarrheagenic *E. coli* (RDEC-1 (also called REPEC)) is a natural rabbit A/E pathogen that causes disease closely resembling that seen in humans with EPEC (41) (reviewed in Table I). REPEC causes increases in pro-inflammatory cytokines such as IL-1β, TNF-α, IL-6 and IL-8 in infected rabbits (42), recapitulating *in vitro* data. At initial stages of the infection (8-12 hours post-infection (p.i.)), bacteria adhere to M-cells in the intestine, which translocate RDEC-1 molecules and antigens across the barrier into Peyer's patches (43). At 12 hours p.i., neutrophils begin infiltrating the colon. Luminal neutrophils often contain phagocytosed bacteria, indicating direct killing of RDEC-1 (43); thus neutrophil infiltration facilitated by M-cell translocation appears to be an

important innate immune defense against RDEC-1. Together, these studies suggest that neutrophils are recruited to the site of infection by chemokines where they directly kill A/E pathogens.

The newborn gnotobiotic pig has been used as a model host organism for both EPEC and EHEC infection, and recapitulates severe manifestations of the human disease including diarrhea, anorexia, rapid wasting, and often death within several days (44). Although the immune system is not fully developed in these animals, it may mimic that in newborn humans, who are highly susceptible to EPEC infection. Both EPEC and EHEC form prototypic A/E lesions in the piglet small intestine. The formation of these lesions following EHEC infection is dependent upon intimin (45) and Tir (46), and correlates with epithelial damage and diarrhea. Although disease in the gnotobiotic pig model is very similar to that seen in humans, its use has been limited primarily due to cost.

Many laboratories have attempted to establish an EPEC infection model in mice, which are a genetically tractable host, and thus capable of defining host factors that mediate the innate immune response against A/E pathogens. Infection of mice with EPEC causes low levels of colonization in the small intestine, cecum, and colon, and some pathology consistent with an A/E lesion, and, in accordance with the rabbit model, neutrophils are recruited to the site of infection (47). Unfortunately, this model has proven challenging to replicate in many laboratories. Anecdotal evidence indicates that administration of antibiotics may improve colonization. However, even with such measures, pathological symptoms are difficult to achieve on a consistent basis. Several explanations are possible, perhaps the simplest being that EPEC strains are not adapted to

cause disease in mice, and only colonize the cecum (48). Additionally, differences in adhesins and regulation of virulence account for lack of disease. Mundy et al. report that intimin and the TTSS appear to regulate persistence of the infection, as EPEC strains lacking intimin or an ATPase that regulates TTSS, persisted for significantly less time than the wild type strain (48). However, other nonpathogenic strains that lack TTSS or intimin can persist as long as EPEC. Thus, it is unclear whether pleiotropic effects associated with growth in the context of other bacteria, or differences in gene expression account for the observed effects. EPEC can colonize gnotobiotic mice for up to 60 days, but with no detectable disease (K. Eaton, personal communication). By contrast, EHEC causes significant morbidity and mortality in gnotobiotic mice, with disease ascribed to the plasmid-encoded Shiga toxins present in this organism (49, 50).

Recently models have been developed to study the innate immune responses to EHEC in human colons using *in vitro* organ culture (51), or human tissue xenografted into mice (52). In the latter model, human fetal colonic tissue was transplanted subcutaneously onto the backs of severe combined immunodeficiency (SCID) mice and allowed to mature. It was found that infecting the graft with EHEC induced IL-8 production and neutrophil infiltration, and that inflammatory responses were induced in flagellin-dependent, and Shiga toxin-independent manner. It should be noted that the geometry of the graft is not identical to that seen in colon, and perhaps as a result, the distribution of TLR5, an innate immune receptor for flagellin, was not the same as that reported in polarized Caco-2 cells (53). Moreover, the route of infection is unnatural and no commensal flora is present. Nevertheless, the model has interesting potential for assessing both the innate and adaptive responses to EHEC. For example, it is possible to

reconstitute these mice with a human immune system (SCID-Hu mice) (54) prior to engraftment, raising the possibility of investigating human-specific innate and adaptive responses to EHEC, and correlating such responses with those seen in human patients (55).

Schauer and colleagues developed a model of inflammatory disease that can be induced in mice by infection with the murine-specific pathogen *C. rodentium*, the causative agent of transmissible murine colonic hyperplasia (TMCH) (9, 56). Disease caused by *C. rodentium* in mice recapitulates many crucial aspects of that caused by EPEC or EHEC infection in humans (57), including colonization, hyperplasia, and diarrhea which is characterized by soft stools in mice, together with innate and adaptive immune responses. The effect is specific to the pathogen, because addition or overgrowth of non-pathogenic bacteria alone does not cause inflammation in mice (8). Some minor differences compared to EPEC infection in humans are evident. Among them, *C. rodentium*, like EHEC, colonizes the colon while EPEC colonizes small intestine. In addition, *C. rodentium* causes a much more robust inflammatory response compared to infection with EPEC in humans.

This model has proven extremely important in understanding many aspects of the A/E pathogenic infection *in vivo*. *C. rodentium* shares approximately half its genes with EHEC, and contains a LEE pathogenicity island nearly identical to that found in EPEC. *C. rodentium* pathogenesis in mice requires both an intact TTSS and secreted effectors encoded both within and outside the LEE (8, 56). There exist considerable conservation of virulence factors between EPEC, EHEC and *C. rodentium*, and the model has been used both to characterize *C. rodentium* virulence factors first identified in EPEC and

EHEC (6), as well as to screen for novel factors by signature tagged mutagenesis (58, 59). The *C. rodentium* model has been used to understand bacterial virulence factors (e.g. EspF and MAP) that contribute to barrier disruption (60-62), and cellular factors (e.g. aquaporins 2 and 3; (63)) that contribute to diarrhea. Of importance for this dissertation, the model has been used extensively in conjunction with extant mouse mutants to understand the innate immune responses (64-68), the mechanisms of dissemination throughout the body (64, 66), and adaptive responses that resolve the infection (13, 69, 70). The model may prove useful in understanding whether colitis induced by a pathogen contributes to the development of a chronic disease, such as that seen in inflammatory bowel disease (IBD) (71). Moreover, the model may also be used to evaluate candidate therapeutic agents, such as those directed against factors regulating the expression of LEE effectors (72). The characteristics of infection caused by each pathogen and the advantages and disadvantage of the various *in vivo* models are summarized in Tables I and II, respectively.

3. Mechanism of the innate immune response against A/E pathogens

It has long been recognized that the host inflammatory response causes much of the pathology associated with A/E pathogen infection (15). Activation of TLRs and other bacterial recognition receptors in epithelial cells induces production of cytokines and chemokines via NF-κB activation, which in turn recruit neutrophils to the site of infection. Lipopolysaccharide (LPS) is abundant on the surface of *C. rodentium*, and serves as a ligand for the TLR4 receptor complex, comprised of TLR4, LPS-binding protein (LBP), CD14, and MD-2 (73). LPS binding to its receptor complex triggers activation of NF-κB and production of pro-inflammatory cytokines (73). Infection of

TLR4$^{-/-}$ mice with *C. rodentium* results in less TLR stimulated pro-inflammatory cytokine production and therefore a slower, less severe inflammatory response and reduced mortality (66). Production of the murine neutrophil chemokine MIP-2, and the macrophage chemokine MCP-1 (66) require TLR4 signaling. Accordingly, recruitment of neutrophils and macrophages to the site of infection is slower in TLR4$^{-/-}$ mice. This delay in inflammation may reduce the gap between the onset of pathology and the initiation of clearance by an adaptive response, resulting in less disease overall. Thus, TLR4 signaling facilitates induction of inflammation and exacerbates disease.

These data raise the question of how much of the innate immune response can be safely eliminated. This has been addressed by the work performed by myself and others using mice lacking MyD88 (see CHAPTER II) (64, 67), a signaling intermediary used by most TLRs (26). In MyD88$^{-/-}$ mice, little innate immune detection of *C. rodentium* is apparent. Thus, compared to wild type mice, MyD88$^{-/-}$ mice exhibit decreased production of pro-inflammatory cytokines such as IL-6 and the mouse neutrophil chemokine KC, and increased *C. rodentium* colonization both in the colon and peripheral organs. MyD88$^{-/-}$ mice also exhibit more severe pathology, and higher mortality rates (64, 67). Notably, the absence of MyD88 signaling leads to gangrenous mucosal necrosis associated with uncontrolled pathogen growth in the colon (67). Furthermore, the severe colitis and necrosis seen in MyD88$^{-/-}$ colonic tissue is evident prior to neutrophil infiltration and is therefore likely caused by bacteria, and not a harmful host response. Death occurs when bacterial dissemination continues unabated, and overwhelms the animal before an effective adaptive response can be mounted (67). Notably, immunized MyD88$^{-/-}$ mice have a suboptimal adaptive response (67), indicating a role for innate immune signaling

in establishing effective antibody production. Recently, dendritic cells, an innate immune cell type important for antigen presentation, were found to be recruited to the colonic epithelia during *C. rodentium* infection (36). Together these data suggest that innate immune signaling via MyD88 is required to protect mice from increased pathology during an infection with *C. rodentium*, and to initiate an effective adaptive response.

Although many innate immune receptors utilize MyD88, the absence of TLR2 signaling alone appears to lead to severe disease phenotypes. Upon infection with *C. rodentium*, TLR2$^{-/-}$ mice suffer colonic mucosal ulcerations, bleeding, and increased apoptosis, resulting in 75% mortality (65). Previously, a protective role in response to intestinal damage has been demonstrated for TLR2 and its ligand, even from commensal strains (74). However, by seven days p.i. most of the bacteria present in the colon are *C. rodentium* (8), therefore indicating that commensals likely play a minor role during the course of this infection. Interestingly, the phenotype of TLR2$^{-/-}$ mice is not as severe as that seen in MyD88$^{-/-}$ mice; MyD88$^{-/-}$ mice suffer 100% mortality and severe hypercolonization throughout the body (65, 67). Hence, TLR2 signaling is required to prevent the increase in pathology, but not to limit colonization of *C. rodentium*. Further, these data indicate that innate immune receptors other than TLR2 that act through MyD88 provide additional protection during an infection with *C. rodentium*.

It is also important to consider the roles that other innate immune receptors besides TLRs, especially those that signal via MyD88, might play during an infection with *C. rodentium*. Interestingly, the type I IL-1 receptor (IL-1R) utilizes MyD88 in its signaling pathway to activate NF-κB and one of the IL-1R ligands, IL-1β is produced in a MyD88-dependent fashion (26, 75). This positive feedback circuit has been hypothesized to

amplify the NF-κB response leading to a localized inflammatory response (76). Upon infection, mice lacking IL-1R (IL-1R$^{-/-}$ mice) exhibit increased mortality together with severe colitis characterized by intramural colonic bleeding and intestinal damage including gangrenous mucosal necrosis (CHAPTER III), phenotypes also evident in MyD88$^{-/-}$ mice (CHAPTER II). However, unlike MyD88$^{-/-}$ mice, IL-1R$^{-/-}$ mice do not exhibit increased pathogen loads, delays in recruitment of neutrophils, or defects in the capacity to replace damaged enterocytes. Together, these data suggest that IL-1R signaling regulates susceptibility to intestinal damage caused by *C. rodentium* possibly contributing to the increased mortality.

Together my research, along with the work of others, demonstrates that the innate immune response is complex causing both protective and deleterious outcomes. The data from TLR-deficient mice raises the possibility that particular TLR signaling cascades mediate either protective (e.g. TLR2) or destructive (e.g. TLR4) responses (Figure 1A). However, several lines of evidence suggest that such a model may be too simplistic. For instance, not all TLRs appear to be involved in response to every pathogen. Indeed, *in vitro* infection with *C. rodentium* lacking flagellin causes similar cytokine production as that seen with wild-type strains (36). Likewise, disease induced by infection of mice deficient in TLR5 with *C. rodentium* was identical to that seen in wild type mice (see CHAPTER II). Furthermore, different TLRs utilize slightly different combinations of signaling intermediates (26). Thus, in response to an intact pathogen, several receptors activate convergent and divergent signaling pathways within the same host cell (Figure 1B). Adding to the complexity of the innate immune response, different pathogens may express different concentrations of TLR ligands, and different cell types have distinct

repertoires of TLRs. Other innate immune receptors such as NOD-like receptors (NLRs) recognize bacterial motifs found in the cytosol of host cells. For example, IPAF and NAIP-5 are associated with the detection of intracellular flagellin (77, 78). Although their involvement in A/E pathogenic infections has not been investigated, it has been established that NLRs mediate innate immune responses to other intestinal pathogens and to non-pathogenic bacteria (79). In such a "combinatorial" model many TLRs may contribute to a "threshold" of signaling, which determines whether the overall response is protective or deleterious (Figure 1C). Such signaling can be seen as analogous to the threshold of depolarization that, when surpassed, triggers an action potential. Thus, particular microbes may induce low levels of signaling that result in limited response by the host cell. Others may produce an optimal level of innate immune signaling, resulting in a balance innate immune response. Finally, some pathogens, such as *C. rodentium*, may over-stimulate innate immune signaling, which may induce deleterious inflammation that exacerbates the infection and itself constitutes disease. Such a combinatorial signaling cascade may lead to a unique innate immune response that differs from the response stimulated by any single receptor alone would generate. Moreover, the complexity of the signaling may not be reflected in knockouts of particular TLRs. Indeed, systems analytic approaches to TLR signaling may be a useful complement to knockout approaches (80).

C. Cell types that mediate the innate immune response to A/E pathogens

1. Intestinal Epithelium

The intestinal epithelium serves as the first site where A/E pathogens and the host interact, causing A/E lesions and pedestals to form. The tight adherence of bacteria to the

epithelium allows the bacteria to remain firmly attached (81) as diarrhea displaces commensal microflora (8). Thus, diarrhea may create a niche for A/E pathogens and facilitate colonization in the intestine. Once colonization is established, the intestinal epithelium produces a number of pro-inflammatory cytokines and subsequently incurs significant damage and cell death characteristic of infections with A/E pathogens. EPEC also causes increased epithelial paracellular permeability through its virulence factors EspF (60-62, 82), Map (60), and EspG proteins (63, 83, 84). Compromising the epithelial barrier integrity may allow the bacteria access to the basolateral side of the epithelium and contribute to the development of diarrhea. Moreover, disruption of the barrier may cause redistribution of innate immune receptors such as TLRs, which are designed to detect the bacteria, perhaps facilitating the development of over-stimulation of innate immune signaling pathways and deleterious inflammation.

The host response to this epithelial damage requires TLR4 and MyD88 signaling (66, 67). MyD88 signaling on macrophages is required to replenish damaged epithelium following treatment with dextran sodium sulfate (DSS) (85). In this process, stem cells at the base of intestinal crypts differentiate into enterocytes, divide, and migrate along the crypt to the site of damage (86). Crypt hyperplasia, measured as an increase in crypt length, is also a hallmark feature of A/E pathogen infection (9, 56), and is indicative of repair to damaged intestinal epithelium. Bone marrow transplants between wild type and MyD88$^{-/-}$ mice indicate that signaling in hematopoietic cells, including macrophages, and non-hematopoietic cells including intestinal epithelium, may both contribute in a significant way to repair of damaged intestinal enterocytes following *C. rodentium*

infection (67). Thus, protection may in part be mediated by wound repair of epithelial barrier breach, contributing to containment of the infection within the colon.

MyD88 signaling in non-hematopoietic cells, which likely include epithelial cells is required for protection following infection with *C. rodentium* (67). Moreover, epithelial cells are also a potent source of antimicrobial factors such as C-type lectin RegIIIγ and cathelicidin-related antimicrobial peptide (CRAMP) in mice, both of which contribute to protective responses against A/E pathogens *in vivo* (87, 88). Vallance and colleagues demonstrated that epithelial cells significantly upregulate the production of nitric oxide during infection, which is also an important component of innate host defense against bacterial pathogens (89). Importantly, iNOS was not expressed by epithelial cells with attached bacteria, but only by neighboring uninfected cells, suggesting that A/E pathogens can selectively inhibit iNOS production via a translocated effector molecule (89). This observation was confirmed *in vitro* using cultured Caco-2 cells and EPEC (90). Together, these data suggest that epithelial cells play an important protective role in the innate immune response to A/E pathogens.

2. M cells

The epithelium associated with intestinal lymphoid follicles includes specialized M cells, which have a high capacity for transcytosis, facilitating access of luminal antigens to lymphocytes. As mentioned previously, RDEC-1 has been shown to selectively adhere to rabbit M cells (43), although the antiphagocytosis activity of EPEC bacteria appears to inhibit uptake of EPEC-specific antigen by M cells (91). Despite this apparent mechanism to elude detection by the immune system, antibody responses to

EPEC are readily generated in infected children over one year of age and are effectively protective (92, 93).

3. Dendritic Cells

There are several ways antigen can cross the intestinal epithelium, and dendritic cells may play a large role in providing antigen to drive the immune response to A/E pathogens. Dendritic cells located below M cells can sample antigens in the proximity of lymphoid follicles (94), but they are also dispersed throughout the intestinal tract and can sample luminal contents by extending dendrites through the epithelium (12). Moreover, dendritic cells can migrate to inflamed areas and are recruited to colonic epithelium infected by *C. rodentium* (36). Importantly, dendritic cell-associated cytokines such as IL-10 have been demonstrated to strongly influence the host immune response to *C. rodentium* . Dendritic cells can also be the source of TGF-β (95), which is essential for T_H17-dependent host protection from *C. rodentium* infection (96). Thus, dendritic cells bridge the innate and adaptive responses to *C. rodentium*.

4. Neutrophils

Neutrophils are the first cell type recruited to the site of infection. While neutrophils are often associated with tissue damage, several lines of evidence suggest that neutrophils act together with intestinal epithelium in a protective manner. First, neutrophil chemokines are produced by intestinal epithelia early in the infection (66, 67). Second, neutrophils are capable of directly killing *C. rodentium in vitro* (67, 68). Finally,

depletion of neutrophils in wild-type mice results in increased levels of bacterial colonization in peripheral organs and mortality (67). A protective role for neutrophils in a *C. rodentium* infection is in accordance with evidence for phagocytosed RDEC-1 within neutrophils of infected rabbits (43).

5. Macrophages

In addition to their role in repair of the intestinal barrier, macrophages also phagocytose bacteria and process antigen for presentation to T cells. Interestingly, *in vitro* experiments suggest that EPEC inhibits macrophage phagocytosis. Antiphagocytic activity may require blocking PI-3 kinase activity (97), in line with the known role for the PI-3 kinase product, PIP3 in macrophage phagocytosis (98). Moreover, antiphagocytic activity requires an intact TTSS, suggesting the involvement of a secreted effector (97). Recent evidence indicates that the secreted EPEC effector EspB mediates antiphagocytic activity. EspB binds to the actin-binding domain of several members of the myosin superfamily, which mediate phagocytosis (99). More specifically, myosin-10 is recruited to the phagocytic cup following its association with PIP3 (98). Thus, inhibition of myosin function by EspB accounts for the antiphagocytic activity of EPEC. Recent results demonstrate that EspJ in EPEC and EHEC is responsible for trans-inhibition of opsonophagocytosis (100). Ectopic expression of EspJ in macrophages inhibits both IgG- and C3bi-mediated phagocytosis, suggesting that EspJ targets a critical regulatory host protein that is downstream of these distinct signaling receptors. It seems likely that macrophages provide significant selective pressure on EPEC for such specific mechanisms to have evolved. The antiphagocytic action of EPEC and EHEC may

contribute to colonization of the intestine by evading immune detection early in the infection, and to bacterial dissemination by inhibiting phagocytosis of infected cells in the blood and lymph system.

6. Mast Cells

Mast cells contribute to intestinal disease by their reactivity to bacterial products and ability to release antimicrobial peptides (AMPs) and potent inflammatory mediators (e.g. TNF-α). Because of the strong inflammatory responses induced by mast cells, their role in allergy often overshadows their bactericidal functions. However, evidence from the *C. rodentium* model has brought the focus back to a protective role for these cells. Infection of mast cell-deficient mice has demonstrated that mast cells are necessary to prevent bacteremia and death. Mast cells are situated in the perivascular space in most organs, and may serve to prevent dissemination by secreting factor(s) into interstitial tissues that directly kill bacteria, including *C. rodentium* (68), perhaps including AMPs (101). Indeed, mice deficient in cathelicidin-related AMP show elevated levels of colonization upon infection with *C. rodentium* (88), raising the possibility that mast cell mediated protection results from secretion of AMPs.

7. Intestinal Microbiota

Several lines of evidence suggest that the normal microbiota comprise a critical innate immune defense against enteropathogenic infection. Intestinal microbiota contributes to epithelial barrier integrity and development (102, 103). Intestinal flora provides competition to an invading pathogen, and may even inhibit their growth (104)

via secreted antimicrobial factors, such as AMPs. In this regard, administration of *Lactobacillus acidophilus* NCFM reduced hyperplasia and inflammation following *C. rodentium* infection (105). Likewise, *L. acidophilus* and *Lactobacillus rhamnosis* enhanced bacterial killing and prevented attachment of *C. rodentium* (106). The innate immune response induced by A/E pathogens may, however, induce changes in the host microbiota that in turn may affect disease and exacerbate inflammation. Lupp and colleagues have recently reported the effects on intestinal microbiota upon infection with *C. rodentium*, or by chemicals and deficiencies in host cytokines (e.g. IL-10) that exacerbate inflammation (8). *C. rodentium* eliminates host microbiota in accordance with previous reports. Importantly, exacerbated inflammation induced by DSS or by nonpathogenic bacteria in $IL10^{-/-}$ mice caused overgrowth of resident or introduced nonpathogenic bacteria, particularly aerotolerant ones. Lupp and colleagues conclude that inflammation alone can promote overgrowth of bacteria (8). Together, these data suggest that inflammation induced upon infection with A/E pathogens may in part facilitate colonization, and that normal intestinal microbiota may antagonize such overgrowth.

The work described in this dissertation, in addition to that presented by others, demonstrates that the innate immune response to A/E pathogens is complex and comprises both protective and destructive elements. A/E pathogens cause lesions on intestinal epithelia and disruption of the epithelial barrier and diarrhea. Bacteria are detected by TLRs (35, 36) and possibly other receptors on both epithelial cells and dendritic cells. TLR-dependent signaling leads to recruitment of innate immune cells such as neutrophils and macrophages via release of chemokines (64-67). Although

damage caused by neutrophils can further facilitate bacterial dissemination and overgrowth of the pathogen , the bactericidal capabilities of neutrophils and macrophages ultimately restrict bacterial load and prevent death (67). In response, EPEC has developed antiphagocytic effectors to prevent such killing (97, 99). Furthermore, the repair of epithelial barrier breach is mediated by macrophages (85). Mast cells induce inflammation by secreting pro-inflammatory factors and induce vascular permeability (107, 108), but they also kill bacteria and prevent dissemination (68). Lastly, an effective innate immune response perhaps initiated by dendritic cells facilitates a robust antibody response, which is required to clear the infection (10, 13).

Literature Cited:

1. Frankel, G., A. D. Phillips, I. Rosenshine, et al.: Enteropathogenic and enterohaemorrhagic Escherichia coli: more subversive elements. *Mol Microbiol*. 30(5), 911-921(1998).
2. Mead, P. S., L. Slutsker, V. Dietz, et al.: Food-related illness and death in the United States. *Emerg Infect Dis*. 5(5), 607-625(1999).
3. Karch, H., P. I. Tarr, and M. Bielaszewska: Enterohaemorrhagic Escherichia coli in human medicine. *Int J Med Microbiol*. 295(6-7), 405-418(2005).
4. Noel, J. M., and E. C. Boedeker: Enterohemorrhagic Escherichia coli: a family of emerging pathogens. *Dig Dis*. 15(1-2), 67-91(1997).
5. McDaniel, T. K., K. G. Jarvis, M. S. Donnenberg, and J. B. Kaper: A genetic locus of enterocyte effacement conserved among diverse enterobacterial pathogens. *Proc Natl Acad Sci U S A*. 92(5), 1664-1668(1995).
6. Deng, W., J. L. Puente, S. Gruenheid, et al.: Dissecting virulence: systematic and functional analyses of a pathogenicity island. *Proc Natl Acad Sci U S A*. 101(10), 3597-3602(2004).
7. Klapproth, J. M., M. Sasaki, M. Sherman, et al.: Citrobacter rodentium lifA/efa1 is essential for colonic colonization and crypt cell hyperplasia in vivo. *Infect Immun*. 73(3), 1441-1451(2005).
8. Lupp, C., M. L. Robertson, M. E. Wickham, et al.: Host-mediated inflammation disrupts the intestinal microbiota and promotes the overgrowth of Enterobacteriaceae. *Cell Host Microbe*. 2(3), 204(2007).
9. Luperchio, S. A., and D. B. Schauer: Molecular pathogenesis of Citrobacter rodentium and transmissible murine colonic hyperplasia. *Microbes Infect*. 3(4), 333-340(2001).
10. Donnenberg, M. S.: Enteropathogenic Escherichia coli. In: *Infections of the gastrointestinal tract*. M. Blaser, P. Smith, J. Ravdin, H. Greenberg, and R. Guerranteds). Lippincott Williams & Wilkins, Philadelphia, PA, 595-612(2002).
11. Niess, J. H., and H. C. Reinecker: Dendritic cells in the recognition of intestinal microbiota. *Cell Microbiol*. 8(4), 558-564(2006).
12. Niess, J. H., and H. C. Reinecker: Lamina propria dendritic cells in the physiology and pathology of the gastrointestinal tract. *Curr Opin Gastroenterol*. 21(6), 687-691(2005).
13. Maaser, C., M. P. Housley, M. Iimura, et al.: Clearance of Citrobacter rodentium requires B cells but not secretory immunoglobulin A (IgA) or IgM antibodies. *Infect Immun*. 72(6), 3315-3324(2004).
14. Donnenberg, M. S., C. O. Tacket, G. Losonsky, et al.: Effect of prior experimental human enteropathogenic Escherichia coli infection on illness following homologous and heterologous rechallenge. *Infect Immun*. 66(1), 52-58(1998).
15. Higgins, L. M., G. Frankel, G. Douce, G. Dougan, and T. T. MacDonald: Citrobacter rodentium infection in mice elicits a mucosal Th1 cytokine response and lesions similar to those in murine inflammatory bowel disease. *Infect Immun*. 67(6), 3031-3039.(1999).

16. Nurnberger, T., and F. Brunner: Innate immunity in plants and animals: emerging parallels between the recognition of general elicitors and pathogen-associated molecular patterns. *Curr Opin Plant Biol*. 5(4), 318-324(2002).
17. Leulier, F., and B. Lemaitre: Toll-like receptors--taking an evolutionary approach. *Nat Rev Genet*. 9(3), 165-178(2008).
18. Philpott, D. J., and S. E. Girardin: The role of Toll-like receptors and Nod proteins in bacterial infection. *Mol Immunol*. 41(11), 1099-1108(2004).
19. Anderson, K. V., L. Bokla, and C. Nusslein-Volhard: Establishment of dorsal-ventral polarity in the Drosophila embryo: the induction of polarity by the Toll gene product. *Cell*. 42(3), 791-798(1985).
20. Lemaitre, B., J. M. Reichhart, and J. A. Hoffmann: Drosophila host defense: differential induction of antimicrobial peptide genes after infection by various classes of microorganisms. *Proc Natl Acad Sci U S A*. 94(26), 14614-14619(1997).
21. Lemaitre, B., E. Nicolas, L. Michaut, J. M. Reichhart, and J. A. Hoffmann: The dorsoventral regulatory gene cassette spatzle/Toll/cactus controls the potent antifungal response in Drosophila adults. *Cell*. 86(6), 973-983(1996).
22. Medzhitov, R., P. Preston-Hurlburt, and C. A. Janeway, Jr.: A human homologue of the Drosophila Toll protein signals activation of adaptive immunity. *Nature*. 388(6640), 394-397(1997).
23. Poltorak, A., X. He, I. Smirnova, et al.: Defective LPS signaling in C3H/HeJ and C57BL/10ScCr mice: mutations in Tlr4 gene. *Science*. 282(5396), 2085-2088(1998).
24. Rock, F. L., G. Hardiman, J. C. Timans, R. A. Kastelein, and J. F. Bazan: A family of human receptors structurally related to Drosophila Toll. *Proc Natl Acad Sci U S A*. 95(2), 588-593(1998).
25. Takeda, K., and S. Akira: Toll-like receptors. *Curr Protoc Immunol*. Chapter 14(Unit 14 12(2007).
26. Kaisho, T., and S. Akira: Pleiotropic function of Toll-like receptors. *Microbes Infect*. 6(15), 1388-1394(2004).
27. Gomez-Gomez, L.: Plant perception systems for pathogen recognition and defence. *Mol Immunol*. 41(11), 1055-1062(2004).
28. Werts, C., S. E. Girardin, and D. J. Philpott: TIR, CARD and PYRIN: three domains for an antimicrobial triad. *Cell Death Differ*. 13(5), 798-815(2006).
29. Savkovic, S. D., A. Koutsouris, and G. Hecht: Activation of NF-kappaB in intestinal epithelial cells by enteropathogenic Escherichia coli. *Am J Physiol*. 273(4 Pt 1), C1160-1167(1997).
30. Campellone, K. G., D. Robbins, and J. M. Leong: EspFU is a translocated EHEC effector that interacts with Tir and N-WASP and promotes Nck-independent actin assembly. *Dev Cell*. 7(2), 217-228(2004).
31. Bommarius, B., D. Maxwell, A. Swimm, et al.: Enteropathogenic Escherichia coli Tir is an SH2/3 ligand that recruits and activates tyrosine kinases required for pedestal formation. *Mol Microbiol*. 63(6), 1748-1768(2007).
32. Swimm, A. I., and D. Kalman: Cytosolic extract induces Tir translocation and pedestals in EPEC-infected red blood cells. *PLoS Pathog*. 4(1), e4(2008).

33. Stein, M. A., D. A. Mathers, H. Yan, K. G. Baimbridge, and B. B. Finlay: Enteropathogenic Escherichia coli markedly decreases the resting membrane potential of Caco-2 and HeLa human epithelial cells. *Infect Immun*. 64(11), 4820-4825.(1996).
34. Canil, C., I. Rosenshine, S. Ruschkowski, et al.: Enteropathogenic Escherichia coli decreases the transepithelial electrical resistance of polarized epithelial monolayers. *Infect Immun*. 61(7), 2755-2762(1993).
35. Zhou, X., J. A. Giron, A. G. Torres, et al.: Flagellin of enteropathogenic Escherichia coli stimulates interleukin-8 production in T84 cells. *Infect Immun*. 71(4), 2120-2129(2003).
36. Khan, M. A., S. Bouzari, C. Ma, et al.: Flagellin-dependent and -independent inflammatory responses following infection by enteropathogenic Escherichia coli (EPEC) and Citrobacter rodentium. *Infect Immun*2008).
37. Ruchaud-Sparagano, M. H., M. Maresca, and B. Kenny: Enteropathogenic Escherichia coli (EPEC) inactivate innate immune responses prior to compromising epithelial barrier function. *Cell Microbiol*. 9(8), 1909-1921(2007).
38. Ceponis, P. J., D. M. McKay, J. C. Ching, P. Pereira, and P. M. Sherman: Enterohemorrhagic Escherichia coli O157:H7 disrupts Stat1-mediated gamma interferon signal transduction in epithelial cells. *Infect Immun*. 71(3), 1396-1404(2003).
39. Jandu, N., P. J. Ceponis, S. Kato, et al.: Conditioned medium from enterohemorrhagic Escherichia coli-infected T84 cells inhibits signal transducer and activator of transcription 1 activation by gamma interferon. *Infect Immun*. 74(3), 1809-1818(2006).
40. Lathem, W. W., T. Bergsbaken, S. E. Witowski, N. T. Perna, and R. A. Welch: Acquisition of stcE, a C1 esterase inhibitor-specific metalloprotease, during the evolution of Escherichia coli O157:H7. *J Infect Dis*. 187(12), 1907-1914(2003).
41. DeVinney, R., A. Gauthier, A. Abe, and B. B. Finlay: Enteropathogenic Escherichia coli: a pathogen that inserts its own receptor into host cells. *Cell Mol Life Sci*. 55(6-7), 961-976(1999).
42. Ramirez, K., R. Huerta, E. Oswald, et al.: Role of EspA and intimin in expression of proinflammatory cytokines from enterocytes and lymphocytes by rabbit enteropathogenic Escherichia coli-infected rabbits. *Infect Immun*. 73(1), 103-113(2005).
43. Inman, L. R., and J. R. Cantey: Specific adherence of Escherichia coli (strain RDEC-1) to membranous (M) cells of the Peyer's patch in Escherichia coli diarrhea in the rabbit. *J Clin Invest*. 71(1), 1-8(1983).
44. Tzipori, S., R. Gibson, and J. Montanaro: Nature and distribution of mucosal lesions associated with enteropathogenic and enterohemorrhagic Escherichia coli in piglets and the role of plasmid-mediated factors. *Infect Immun*. 57(4), 1142-1150.(1989).
45. Donnenberg, M. S., C. O. Tacket, S. P. James, et al.: Role of the eaeA gene in experimental enteropathogenic Escherichia coli infection. *J Clin Invest*. 92(3), 1412-1417(1993).

46. Campellone, K. G., A. J. Roe, A. Lobner-Olesen, et al.: Increased adherence and actin pedestal formation by dam-deficient enterohaemorrhagic Escherichia coli O157:H7. *Mol Microbiol*. 63(5), 1468-1481(2007).
47. Savkovic, S. D., J. Villanueva, J. R. Turner, K. A. Matkowskyj, and G. Hecht: Mouse model of enteropathogenic Escherichia coli infection. *Infect Immun*. 73(2), 1161-1170(2005).
48. Mundy, R., F. Girard, A. J. FitzGerald, and G. Frankel: Comparison of colonization dynamics and pathology of mice infected with enteropathogenic Escherichia coli, enterohaemorrhagic E. coli and Citrobacter rodentium. *FEMS Microbiol Lett*. 265(1), 126-132(2006).
49. Taguchi, H., M. Takahashi, H. Yamaguchi, et al.: Experimental infection of germ-free mice with hyper-toxigenic enterohaemorrhagic Eschichia coli 0157:H7, strain 6. *J. Med. Microbiol.* 51(336-343(2002).
50. Aiba, Y., H. Ishikawa, K. Shimizu, et al.: Role of internalization in the pathogenicity of Shiga toxin-producing Escherichia coli infection in a gnotobiotic murine model. *Microbiol Immunol*. 46(11), 723-731(2002).
51. Chong, Y., R. Fitzhenry, R. Heuschkel, et al.: Human intestinal tissue tropism in Escherichia coli O157 : H7--initial colonization of terminal ileum and Peyer's patches and minimal colonic adhesion ex vivo. *Microbiology*. 153(Pt 3), 794-802(2007).
52. Miyamoto, Y., M. Iimura, J. B. Kaper, A. G. Torres, and M. F. Kagnoff: Role of Shiga toxin versus H7 flagellin in enterohaemorrhagic Escherichia coli signalling of human colon epithelium in vivo. *Cell Microbiol*. 8(5), 869-879(2006).
53. Gewirtz, A. T., T. A. Navas, S. Lyons, P. J. Godowski, and J. L. Madara: Cutting edge: bacterial flagellin activates basolaterally expressed tlr5 to induce epithelial proinflammatory gene expression. *J Immunol*. 167(4), 1882-1885.(2001).
54. McCune, J. M.: Development and applications of the SCID-hu mouse model. *Semin Immunol*. 8(4), 187-196(1996).
55. Westerholt, S., A. K. Pieper, M. Griebel, et al.: Characterization of the cytokine immune response in children who have experienced an episode of typical hemolytic-uremic syndrome. *Clin Diagn Lab Immunol*. 10(6), 1090-1095(2003).
56. Borenshtein, D., M. E. McBee, and D. B. Schauer: Utility of the Citrobacter rodentium infection model in laboratory mice. *Curr Opin Gastroenterol*. 24(1), 32-37(2008).
57. Schauer, D. B., and S. Falkow: The eae gene of Citrobacter freundii biotype 4280 is necessary for colonization in transmissible murine colonic hyperplasia. *Infect Immun*. 61(11), 4654-4661(1993).
58. Mundy, R., D. Pickard, R. K. Wilson, et al.: Identification of a novel type IV pilus gene cluster required for gastrointestinal colonization of Citrobacter rodentium. *Mol Microbiol*. 48(3), 795-809(2003).
59. Kelly, M., E. Hart, R. Mundy, et al.: Essential role of the type III secretion system effector NleB in colonization of mice by Citrobacter rodentium. *Infect Immun*. 74(4), 2328-2337(2006).
60. Dean, P., and B. Kenny: Intestinal barrier dysfunction by enteropathogenic Escherichia coli is mediated by two effector molecules and a bacterial surface protein. *Mol Microbiol*. 54(3), 665-675(2004).

61. Guttman, J. A., Y. Li, M. E. Wickham, et al.: Attaching and effacing pathogen-induced tight junction disruption in vivo. *Cell Microbiol*. 8(4), 634-645(2006).
62. McNamara, B. P., A. Koutsouris, C. B. O'Connell, et al.: Translocated EspF protein from enteropathogenic Escherichia coli disrupts host intestinal barrier function. *J Clin Invest*. 107(5), 621-629(2001).
63. Guttman, J. A., F. N. Samji, Y. Li, et al.: Aquaporins contribute to diarrhoea caused by attaching and effacing bacterial pathogens. *Cell Microbiol*. 9(1), 131-141(2007).
64. Gibson, D. L., C. Ma, K. S. Bergstrom, et al.: MyD88 signalling plays a critical role in host defence by controlling pathogen burden and promoting epithelial cell homeostasis during Citrobacter rodentium-induced colitis. *Cell Microbiol*. 10(3), 618-631(2008).
65. Gibson, D. L., C. Ma, C. M. Rosenberger, et al.: Toll-like receptor 2 plays a critical role in maintaining mucosal integrity during Citrobacter rodentium-induced colitis. *Cell Microbiol*. 10(2), 388-403(2008).
66. Khan, M. A., C. Ma, L. A. Knodler, et al.: Toll-like receptor 4 contributes to colitis development but not to host defense during Citrobacter rodentium infection in mice. *Infect Immun*. 74(5), 2522-2536(2006).
67. Lebeis, S. L., B. Bommarius, C. A. Parkos, M. A. Sherman, and D. Kalman: TLR signaling mediated by MyD88 is required for a protective innate immune response by neutrophils to Citrobacter rodentium. *J Immunol*. 179(1), 566-577(2007).
68. Wei, O. L., A. Hilliard, D. Kalman, and M. Sherman: Mast cells limit systemic bacterial dissemination but not colitis in response to Citrobacter rodentium. *Infect Immun*. 73(4), 1978-1985(2005).
69. Bry, L., and M. B. Brenner: Critical role of T cell-dependent serum antibody, but not the gut-associated lymphoid tissue, for surviving acute mucosal infection with Citrobacter rodentium, an attaching and effacing pathogen. *J Immunol*. 172(1), 433-441(2004).
70. Simmons, C. P., S. Clare, M. Ghaem-Maghami, et al.: Central role for B lymphocytes and CD4+ T cells in immunity to infection by the attaching and effacing pathogen Citrobacter rodentium. *Infect Immun*. 71(9), 5077-5086(2003).
71. Nenci, A., C. Becker, A. Wullaert, et al.: Epithelial NEMO links innate immunity to chronic intestinal inflammation. *Nature*. 446(7135), 557-561(2007).
72. Hughes, D. T., and V. Sperandio: Inter-kingdom signalling: communication between bacteria and their hosts. *Nat Rev Microbiol*. 6(2), 111-120(2008).
73. Fitzgerald, K. A., D. C. Rowe, and D. T. Golenbock: Endotoxin recognition and signal transduction by the TLR4/MD2-complex. *Microbes Infect*. 6(15), 1361-1367(2004).
74. Rakoff-Nahoum, S., J. Paglino, F. Eslami-Varzaneh, S. Edberg, and R. Medzhitov: Recognition of commensal microflora by toll-like receptors is required for intestinal homeostasis. *Cell*. 118(2), 229-241(2004).
75. Adachi, O., T. Kawai, K. Takeda, et al.: Targeted disruption of the MyD88 gene results in loss of IL-1- and IL-18-mediated function. *Immunity*. 9(1), 143-150(1998).

76. Barnes, P. J., and M. Karin: Nuclear factor-kappaB: a pivotal transcription factor in chronic inflammatory diseases. *N Engl J Med*. 336(15), 1066-1071(1997).
77. Ren, T., D. S. Zamboni, C. R. Roy, W. F. Dietrich, and R. E. Vance: Flagellin-deficient Legionella mutants evade caspase-1- and Naip5-mediated macrophage immunity. *PLoS Pathog*. 2(3), e18(2006).
78. Miao, E. A., E. Andersen-Nissen, S. E. Warren, and A. Aderem: TLR5 and Ipaf: dual sensors of bacterial flagellin in the innate immune system. *Semin Immunopathol*. 29(3), 275-288(2007).
79. Kim, Y. G., J. H. Park, M. H. Shaw, et al.: The cytosolic sensors Nod1 and Nod2 are critical for bacterial recognition and host defense after exposure to Toll-like receptor ligands. *Immunity*. 28(2), 246-257(2008).
80. Brown, K. L., C. Cosseau, J. L. Gardy, and R. E. Hancock: Complexities of targeting innate immunity to treat infection. *Trends Immunol*. 28(6), 260-266(2007).
81. Kenny, B., R. DeVinney, M. Stein, et al.: Enteropathogenic E. coli (EPEC) transfers its receptor for intimate adherence into mammalian cells. *Cell*. 91(4), 511-520(1997).
82. Nougayrede, J. P., and M. S. Donnenberg: Enteropathogenic Escherichia coli EspF is targeted to mitochondria and is required to initiate the mitochondrial death pathway. *Cell Microbiol*. 6(11), 1097-1111(2004).
83. Tomson, F. L., V. K. Viswanathan, K. J. Kanack, et al.: Enteropathogenic Escherichia coli EspG disrupts microtubules and in conjunction with Orf3 enhances perturbation of the tight junction barrier. *Mol Microbiol*. 56(2), 447-464(2005).
84. Elliott, S. J., E. O. Krejany, J. L. Mellies, et al.: EspG, a novel type III system-secreted protein from enteropathogenic Escherichia coli with similarities to VirA of Shigella flexneri. *Infect Immun*. 69(6), 4027-4033(2001).
85. Pull, S. L., J. M. Doherty, J. C. Mills, J. I. Gordon, and T. S. Stappenbeck: Activated macrophages are an adaptive element of the colonic epithelial progenitor niche necessary for regenerative responses to injury. *Proc Natl Acad Sci U S A*. 102(1), 99-104(2005).
86. Radtke, F., and H. Clevers: Self-renewal and cancer of the gut: two sides of a coin. *Science*. 307(5717), 1904-1909(2005).
87. Zheng, Y., P. A. Valdez, D. M. Danilenko, et al.: Interleukin-22 mediates early host defense against attaching and effacing bacterial pathogens. *Nat Med*. 14(3), 282-289(2008).
88. Iimura, M., R. L. Gallo, K. Hase, et al.: Cathelicidin mediates innate intestinal defense against colonization with epithelial adherent bacterial pathogens. *J Immunol*. 174(8), 4901-4907(2005).
89. Vallance, B. A., W. Deng, M. De Grado, et al.: Modulation of inducible nitric oxide synthase expression by the attaching and effacing bacterial pathogen citrobacter rodentium in infected mice. *Infect Immun*. 70(11), 6424-6435(2002).
90. Maresca, M., D. Miller, S. Quitard, P. Dean, and B. Kenny: Enteropathogenic Escherichia coli (EPEC) effector-mediated suppression of antimicrobial nitric oxide production in a small intestinal epithelial model system. *Cell Microbiol*. 7(12), 1749-1762(2005).

91. Martinez-Argudo, I., C. Sands, and M. A. Jepson: Translocation of enteropathogenic Escherichia coli across an in vitro M cell model is regulated by its type III secretion system. *Cell Microbiol*. 9(6), 1538-1546(2007).
92. Martinez, M. B., C. R. Taddei, A. Ruiz-Tagle, L. R. Trabulsi, and J. A. Giron: Antibody response of children with enteropathogenic Escherichia coli infection to the bundle-forming pilus and locus of enterocyte effacement-encoded virulence determinants. *J Infect Dis*. 179(1), 269-274(1999).
93. Carbonare, C. B., S. B. Carbonare, and M. M. Carneiro-Sampaio: Early acquisition of serum and saliva antibodies reactive to enteropathogenic Escherichia coli virulence-associated proteins by infants living in an endemic area. *Pediatr Allergy Immunol*. 14(3), 222-228(2003).
94. Iwasaki, A., and B. L. Kelsall: Freshly isolated Peyer's patch, but not spleen, dendritic cells produce interleukin 10 and induce the differentiation of T helper type 2 cells. *J Exp Med*. 190(2), 229-239(1999).
95. McGeachy, M. J., K. S. Bak-Jensen, Y. Chen, et al.: TGF-beta and IL-6 drive the production of IL-17 and IL-10 by T cells and restrain T(H)-17 cell-mediated pathology. *Nat Immunol*. 8(12), 1390-1397(2007).
96. Mangan, P. R., L. E. Harrington, D. B. O'Quinn, et al.: Transforming growth factor-beta induces development of the T(H)17 lineage. *Nature*. 441(7090), 231-234(2006).
97. Celli, J., M. Olivier, and B. B. Finlay: Enteropathogenic Escherichia coli mediates antiphagocytosis through the inhibition of PI 3-kinase-dependent pathways. *Embo J*. 20(6), 1245-1258.(2001).
98. Cox, D., J. S. Berg, M. Cammer, et al.: Myosin X is a downstream effector of PI(3)K during phagocytosis. *Nat Cell Biol*. 4(7), 469-477(2002).
99. Iizumi, Y., H. Sagara, Y. Kabe, et al.: The enteropathogenic E. coli effector EspB facilitates microvillus effacing and antiphagocytosis by inhibiting myosin function. *Cell Host Microbe*. 2(6), 383-392(2007).
100. Marches, O., V. Covarelli, S. Dahan, et al.: EspJ of enteropathogenic and enterohaemorrhagic Escherichia coli inhibits opsono-phagocytosis. *Cell Microbiol*. 10(5), 1104-1115(2008).
101. Di Nardo, A., A. Vitiello, and R. L. Gallo: Cutting edge: mast cell antimicrobial activity is mediated by expression of cathelicidin antimicrobial peptide. *J Immunol*. 170(5), 2274-2278(2003).
102. Hooper, L. V., T. Midtvedt, and J. I. Gordon: How host-microbial interactions shape the nutrient environment of the mammalian intestine. *Annu Rev Nutr*. 22(283-307(2002).
103. Stappenbeck, T. S., L. V. Hooper, and J. I. Gordon: Developmental regulation of intestinal angiogenesis by indigenous microbes via Paneth cells. *Proc Natl Acad Sci U S A*. 99(24), 15451-15455(2002).
104. Servin, A. L.: Antagonistic activities of lactobacilli and bifidobacteria against microbial pathogens. *FEMS Microbiol Rev*. 28(4), 405-440(2004).
105. Chen, C. C., S. Louie, H. N. Shi, and W. A. Walker: Preinoculation with the probiotic Lactobacillus acidophilus early in life effectively inhibits murine Citrobacter rodentium colitis. *Pediatr Res*. 58(6), 1185-1191(2005).

106. Johnson-Henry, K. C., M. Nadjafi, Y. Avitzur, et al.: Amelioration of the effects of Citrobacter rodentium infection in mice by pretreatment with probiotics. *J Infect Dis*. 191(12), 2106-2117(2005).
107. Majno, G., and G. E. Palade: Studies on inflammation. 1. The effect of histamine and serotonin on vascular permeability: an electron microscopic study. *J Biophys Biochem Cytol*. 11(571-605(1961).
108. Malaviya, R., and S. N. Abraham: Clinical implications of mast cell-bacteria interaction. *J Mol Med*. 76(9), 617-623(1998).

Figure Legend:

Figure 1: Models for how innate immune signaling can be both protective and destructive. (A) Displays the potential of an intact pathogen to activate both protective and destructive innate immune responses; thus resulting in a balanced response. (B) The Combinatorial Response Model adds in the complexity of different innate immune detectors utilizing slightly different patterns of signaling adaptor proteins. In response to an intact pathogen which could trigger a specific set of innate immune receptors this would create a "tuned response" specific to the pathogen. (C) The Threshold Response Model illustrates the hypothesis that certain signaling cascades are not detrimental or protective, but instead that there is an optimal level of innate immune signaling that must be reached for protection to be ensured during *C. rodentium* infection.

Table I

Disease caused by A/E pathogens

Pathogen	GI tract targeting	Host	Pathology	Selected secreted effectors that impact innate immunity
EPEC[10]	Small Intestine	Human	- A/E lesion - Diarrhea - Hyperplasia - Immune cell infiltration	- EspF[60-62,81], EspG[63,82,83], & Map[60] (disrupt epithelial barrier) - EspB[98] & EspJ[99] (inhibit phagocytosis) - Unknown effector[40] (inhibits NF-KB activation)
EHEC[3,4]	Colon	Human	- A/E lesion - Bloody diarrhea - HUS - Hyperplasia - Immune cell infiltration	- EspJ[99] (inhibits phagocytosis) - StcE[39] (alters complement cascade) - Unknown effector[38] (inhibits STAT-1 signaling)
		Bovine	None	N/A
RDEC-1[41-43]	Small Intestine	Rabbit	- A/E lesion - Diarrhea (age-dependent)[43] - Immune cell infiltration	N/A
C. rodentium[9,56]	Colon Cecum	Mouse	- A/E lesion - Diarrhea (soft stool) - Hyperplasia - Immune cell infiltration	EspF[6,61] (disrupts epithelial barrier)

Table II

Advantages and Disadvantages of *in vivo* A/E models

Pathogen	Animal	Recapitulate human disease?	Advantages	Disadvantages
EPEC	Mouse[49]	-	Potential host genetic manipulation, inexpensive, accurate early infection	Low colonization, inconsistent disease
	Newborn Gnotobiotic pig[44]	+	Both disease and immune system are similar to infant humans	Expensive, no host genetic manipulation
EHEC	Gnotobiotic mouse[50]	+/-	Recapitulates toxin based disease, potential genetic manipulation, inexpensive	Requires a gnotobiotic mouse facility, no non-toxin based disease
	Newborn Gnotobiotic pig[44]	+	Both disease and immune system are similar to infant humans	Expensive, no host genetic manipulation
RDEC-1[41-43]	Rabbit	+	Natural host, accurate disease	Expensive, no genetic manipulation
C. rodentium[9,56]	Mouse	+/-	Natural host, potential host genetic manipulation, inexpensive, A/E lesion formation is accurate	Many aspects of disease are different from EPEC, and EHEC (see table I)

Figure 1

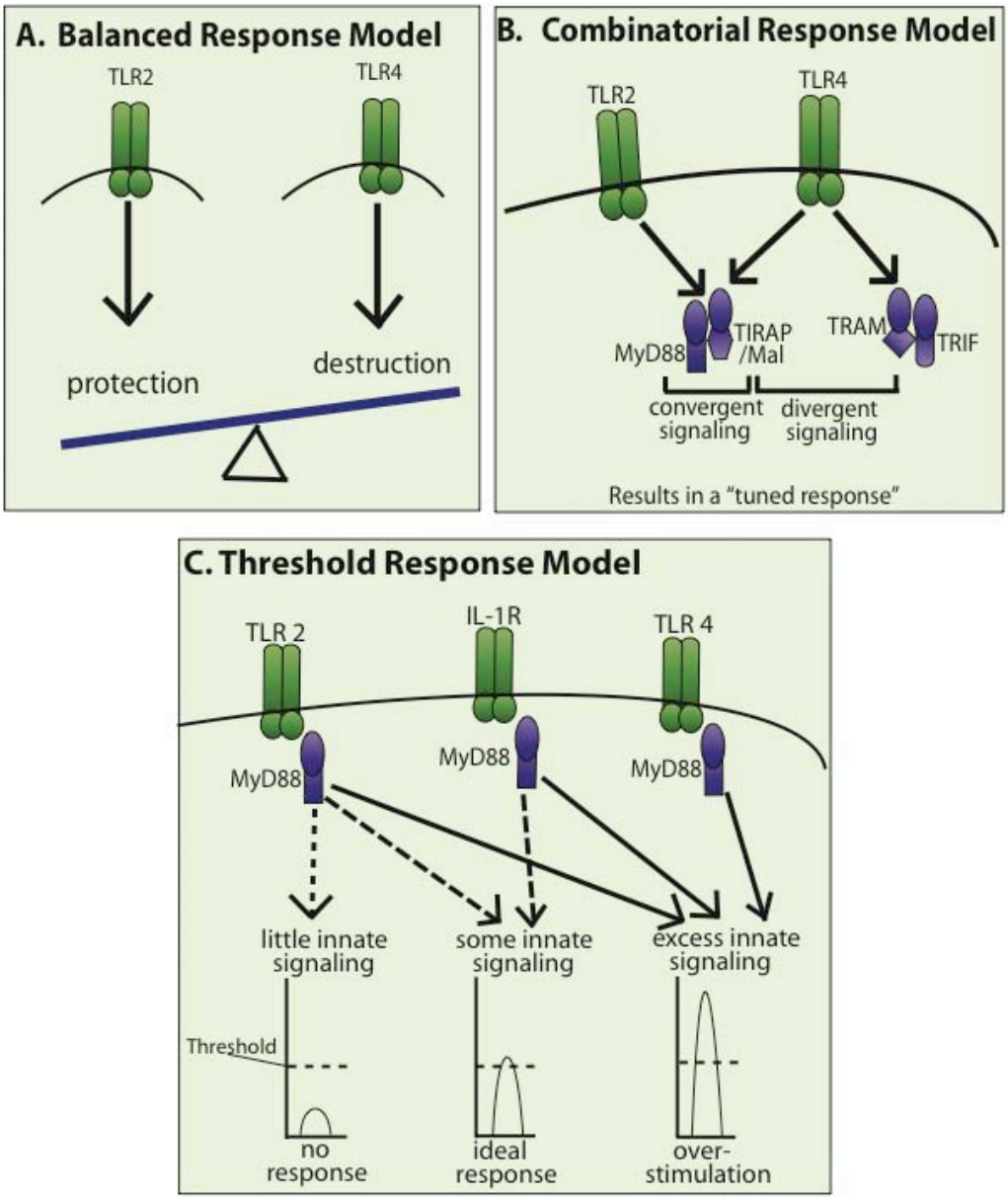
A. Balanced Response Model
TLR2
TLR4
protection
destruction
B. Combinatorial Response Model
TLR2
TLR4
MyD88
TIRAP /Mal
TRAM
TRIF
convergent signaling
divergent signaling
Results in a "tuned response"
C. Threshold Response Model
TLR 2
IL-1R
TLR 4
MyD88
MyD88
MyD88
little innate signaling
some innate signaling
excess innate signaling
Threshold
no response
ideal response
over-stimulation

CHAPTER II:

Innate immune signaling mediated by MyD88 is required for a protective innate immune response by neutrophils to *Citrobacter rodentium*.

Figures 2 and 4-9 were previously published as part of Lebeis et al. 2007.
All experiments were performed by Sarah Lebeis, except for the pedestal assays on 3T3 cells, which were performed by Bettina Bommarius. The pathology observations were made by Charles Parkos, and the TUNEL assay scoring was performed by Melanie Sherman.

Abstract:

Enteropathogenic *E. coli* (EPEC), enterohemorrhagic *E. coli* (EHEC) and *Citrobacter rodentium* are classified as attaching and effacing (A/E) pathogens based on their ability to adhere to intestinal epithelium via actin-filled membranous protrusions (pedestals). Infection of mice with *C. rodentium* causes breach of the colonic epithelial barrier, a vigorous T_H1 inflammatory response, and colitis. Ultimately, an adaptive immune response leads to clearance of the bacteria. Whereas much is known about the adaptive response to *C. rodentium*, the role of the innate immune response remains unclear. Here we demonstrate for the first time that the TLR adaptor MyD88 is essential for survival and optimal immunity against *C. rodentium* infection. MyD88$^{-/-}$ mice suffer from bacteremia, gangrenous mucosal necrosis, severe colitis, and death following infection with *C. rodentium*. Although an adaptive response occurs, MyD88 signaling is necessary for efficient clearance of the pathogen. Based on reciprocal bone marrow transplants in conjunction with assessment of intestinal mucosal pathology, repair, and cytokine production, our findings suggest a model in which TLR signaling in hematopoietic and non-hematopoietic cells mediate three distinct processes: (i) induction of an epithelial repair response that maintains the protective barrier and limits access of bacteria to the lamina propria; (ii) production of KC or other chemokines that attract neutrophils and thus facilitate killing of bacteria; and (iii) efficient activation of an adaptive response that facilitates antibody-mediated clearance of the infection. Together, these experiments provide evidence for a protective role of innate immune signaling during infections caused by A/E pathogens.

Introduction:

Enteropathogenic *Escherichia coli* (EPEC), enterohemorrhagic *E. coli* (EHEC), and a closely related mouse pathogen *C. rodentium* are classified as attaching and effacing (A/E) pathogens based on their ability to attach intimately to intestinal epithelium and flatten absorptive microvilli (effacement). EPEC causes infantile diarrhea (1) and leads to dehydration and death in 25-70% of infected infants (2). EHEC infections cause hemorrhagic colitis and hemolytic-uremic syndrome (HUS), a potentially fatal disease (3, 4). *C. rodentium* is the causative agent for transmissible murine colonic hyperplasia (TMCH) (5). Another hallmark feature of A/E pathogens is their ability to induce actin filled membranous protrusions, or "pedestals" at the site of attachment. Pedestal formation is associated with the formation of A/E lesions, breach of the epithelial barrier by the bacteria, and development of disease (6, 7).

Upon infection, A/E pathogens displace the commensal flora and cause intestinal inflammation characterized by crypt hyperplasia, goblet cell depletion, and damage to the epithelium (5). Additionally, infection with these pathogens induces infiltration of immune cells and edema within the lamina propria. An influx of neutrophils is associated with the formation of abundant crypt abscesses (8). Much of the pathology observed in response to A/E pathogens appears to result from a deleterious host response to the bacteria following breach of epithelial barrier; thus, administration of heat killed *C. rodentium* to mice with permeabilized colons has been shown to result in inflammatory disease nearly identical to that seen with live bacteria (8). Ultimately, an antibody response is necessary for clearance of the bacteria (9). Therefore, although host immune

response to infection with *C. rodentium* results in a destructive colitis, it also serves to protect mice.

While much is known about the etiology of A/E pathogen infections, the induction of the host immunity particularly as it relates to controlling the balance between protective and destructive responses is less well understood. To identify signaling cascades responsible for such immune responses to A/E pathogens, we considered the involvement of TLRs. These receptors are highly conserved type-I transmembrane proteins containing leucine rich repeats (LRR) and a conserved toll/interleukin-1 receptor (TIR) domain. TLRs recognize and respond to conserved motifs associated with microbes, which include proteins (e.g. flagellin), lipids (e.g. LPS), and nucleic acids (e.g. CpG DNA) (10). Signaling cascades initiated by engagement of TLRs with their ligands utilizes many adaptor proteins including myeloid differentiation primary response gene 88 MyD88), toll-IL-1 receptor domain-containing adaptor protein/MyD88 adaptor-like (TIRAP/Mal), TIR domain-containing adaptor inducing IFN-β (TRIF), and TRIF related adaptor molecule (TRAM) (10). TLR signaling pathways ultimately lead to activation of transcription factors (e.g. NF-KB and IRF-3), which regulate production of cytokines and chemokines (e.g. IL-6, IFN-γ, TNF-α, IL-8, etc.). Most of these cytokines are strongly induced during an infection with A/E pathogens (8, 11).

Although most studies on TLR signaling have focused on cytokine responses to particular TLR ligands, several recent studies have described a role for MyD88 signaling in detecting intact viruses (12), parasites (13), pathogenic bacteria (14, 15), and even commensal bacteria present in the intestine (16, 17). In these latter studies, dextran

sodium sulfate (DSS) was used to induce epithelial injury and, as a consequence, acute colitis that resembles that seen in patients with Inflammatory Bowel Disease (IBD). Notably, DSS-induced colitis was exacerbated in the absence of MyD88 and TLR4. Thus, TLR signaling appears to be required for innate immune responses to intestinal injury. However, how TLR signaling contributes to containment of pathogens within the intestinal tract is less clear (16) (17).

Several lines of evidence suggest that *C. rodentium* may provide an ideal system for evaluating how TLR signaling and the innate immune response contribute to intestinal inflammation and prevents dissemination of the bacteria out of the colon. *C. rodentium* efficiently out-competes commensal strains in the intestine and can easily be cultured *ex vivo*. Khan and colleagues have provided evidence that TLR4 signaling contributes to inflammation induced by *C. rodentium* (18). By contrast, TLR2 signaling appears to be required for protective responses to *C. rodentium*. Thus, following *C. rodentium* infection of TLR2$^{-/-}$ mice suffer from colonic mucosal ulcerations, bleeding, increased apoptosis, and increased mortality (19). Here we show that MyD88 signaling contributes to intestinal inflammation in response to *C. rodentium*, and is required to protect mice from a disseminated infection. Moreover, we provide evidence that these effects are mediated by both non-hematopoietic and hematopoietic cells, particularly neutrophils. Thus, although TLR signaling via MyD88 mediates a deleterious inflammatory response following infection, such signaling is also required to limit the level of bacterial colonization throughout the body and facilitate timely clearance. Experiments presented here may provide important information on means to mollify the destructive responses while facilitating protective ones.

Materials and Methods:

***In vitro* infections and immunofluorescence analysis:** 3T3 cells were grown in DMEM (Cellgro, Hernadon, VA) containing 10% fetal bovine serum (FBS) (US Biological, Swampscott, MA) and macrophages were grown in RPMI (Cellgro) containing 10% FBS, 1.5g/L sodium bicarbonate (Gibco/Invitrogen, Carlsbad, CA), 1mM sodium pyruvate (Cellgro), 10mM HEPES (Fisher Scientific, Suwanee, GA), and 0.05mM 2-β mercaptoethanol (Sigma-Aldrich, St. Louis, MO). For infections, 3T3 cells were grown on glass coverslips and incubated for 6 to 8 hours at 37ºC with wild type EPEC (strain 2389/69) or *C. rodentium* (ATCC 51116) at a multiplicity of infection of 10. For infections of primary macrophages, cells were isolated from the peritoneal cavity of wild type or MyD88$^{-/-}$ mice two days following injection with 100μg of Con A (Sigma-Aldrich), plated on glass coverslips overnight, and incubated for 3 to 5 hours at 37ºC with EPEC or *C. rodentium* at a multiplicity of infection of 10. For immunofluorescence analysis, cells were fixed in 2% formaldehyde and permeabilized in Triton-X-100 as described previously (20, 21). EPEC was recognized by staining with 4, 6-diamindino-2-phenylindole (DAPI; 10μg/mL; Sigma-Aldrich), and pedestals were recognized by staining with FITC-phalloidin (4U/mL; Molecular Probes, Eugene, OR). TLR antibodies (Abcam, Cambridge, MA), MyD88 antibody (eBioscience, San Diego, CA), and FLAG antibody for the tagged TIRAP (Sigma-Aldrich) were used at a concentration of 5μg/mL. All secondary antibodies (Jackson ImmunoResearch, West Grove, PA) were used at a concentration of 1μg/mL. Images were acquired with a scientific-grade cooled charge-coupled device (Cool-Snap HQ with ORCA-ER chip) on a multi-wavelength wide-field three-dimensional microscopy system (Intelligent Imaging Innovations, Denver, CO),

based on a 200M-inverted microscope using a 63× NA 1.4 objective (Carl Zeiss, Thornwood, NY).

Mouse strains and breeding: MyD88$^{-/-}$ mice on a C57BL/6 background (22) were the generous gift of David Underhill, and were originally generated in the laboratory of Shizuo Akira (23). TIRAP$^{-/-}$ mice (24) were the generous gift of Ruslan Medzhitov (Yale University). These mice were bred at Emory University. TLR5$^{-/-}$ mice were the generous gift of Andrew Gewirtz, and who obtained them from Charles River Laboratories (Wilmington, MA). C57BL/6 mice were used as the control strain for MyD88$^{-/-}$, TLR4$^{-/-}$, and TLR5$^{-/-}$ mice while B129PF2/J mice were used as the control strain for TIRAP$^{-/-}$ mice (25). Control mice were obtained from Jackson Laboratory (Bar Harbor, ME), as were TLR4$^{-/-}$ mice (C57BL6/ScN), μMT mice (B6.129S2-Igh-6^{tm1Cgn}/J), and GFP mice (C57BL/6-Tg(ACTB-EGFP)10sb/J). Animal care was provided in accordance with protocols approved by the Institutional Animal Care and Use Committee of Emory University.

***In vivo* infections:** *C. rodentium* were prepared by overnight culturing (12 to 16 hours) at 37ºC in Luria-Bertani broth (LB; Becton Dickinson, Franklin Lakes, NJ) without shaking. Cultures were harvested by centrifugation and resuspended in 20% sucrose distilled water. For infections of mice, food was withdrawn and drinking water was replaced with *C. rodentium* suspension overnight. Volume of suspension was measured before and after administration and the number of bacteria in the inoculum was calculated following retrospective plating. The average dosage was 4 x 10^8 CFU/mouse. Survival of infected mice and changes in body weight were monitored daily. Mice losing more than 15% of their original weight were euthanized. For immunization studies, drinking water

was supplemented with a neomycin sulfate/polymyxin B sulfate cocktail (Sigma-Aldrich) three days after infection. Clearance of *C. rodentium* was assessed by measuring the number of colonies in fecal samples. Four weeks after initial infection mice were reinfected with 4 x 10^8 CFU *C. rodentium*.

Histology: For histology studies, colons were removed from uninfected or infected mice, fixed in 10% formalin, and embedded in paraffin. Sections (5μm) were cut and stained with H&E by the Translational Research Lab at Emory University. Crypt height was measured by micrometry using a Zeiss 200M microscope, a 20× NA 1.4 lens and Slidebook software (Intelligent Imaging Innovations,). Longitudinal sections, which displayed the entire lengths of crypts, were used for measurements. Two measurements were made on each image, and one image was taken per colon. The number of samples (n) refers to the number of colons measured rather than the number of measurements. Intestinal histopathology was assessed microscopically by Charles Parkos. Samples were coded and the observations made in a blind fashion to avoid bias in the evaluation process.

TUNEL assay staining and scoring: To access level of apoptosis in colonic tissue, sections (5μm) were cut from the same paraffin blocks described above and stained using an ApopTag Fluorescein *In Situ* Apoptosis Detection Kit (S7110) (Millipore, Billerica, MA) according to the manufacturer's instructions. Briefly, the tissue was digested with terminal deoxynucleotidyl transferase (TdT) enzyme, and stained with α-digoxigenin conjugated to fluorescein and DAPI. The intensity of fluorescein staining was assessed from digital images using a Nikon Eclipse 80i microscope, a 20× NA 0.75 and Spot software (Diagnostic Instruments, Sterling Heights, MI). Longitudinal sections, which

displayed the entire lengths of crypts, were used for measurements. Samples were coded and the observations made in a blind fashion to avoid bias in the evaluation process by Melanie Sherman. Samples were given a score of 0, 1, 2, or 3, where a low score represented minimal TdT dUTP nick end labeling (TUNEL) staining and a high score extensive staining. Examples of the scoring criteria are shown in Figure 3.

Colony counts of *C. rodentium*: To measure the CFU of *C. rodentium,* tissue samples of colon, liver, spleen, or mesenteric lymph node (MLN) weighing ~0.1 to 0.3g were homogenized at low speed with a Tissuemizer (Fisher Scientific, Pittsburgh, PA) in 1mL of PBS. The lysate was plated on MacConkey agar plates at various dilutions, and *C. rodentium* colonies were recognized as pink with a white rim as previously described (26). Pink colonies were confirmed as *C. rodentium* by PCR with Tir-specific primers (forward primer 5'-GCGCGAATTCATGCCTATTGGTAATCTTGGTAATAATAAT -3' and reverse primer 5'-GCGCCCCGGGTTAGACGAAACGTTCAACTCCCGGTGT TGT-3'). Reactions were conducted using the Peltier Thermal Cycler-200 from MJ Research (Bio-Rad, Waltham, MA) under the following conditions: 94ºC for 3 minutes; 35 cycles of 94ºC for 30 seconds, 65ºC for 1 minute and 72ºC for 1 minute; and 72ºC for 2 minutes. Pink colonies with white rims were counted after 20 hours of incubation at 37ºC to determine the CFU per gram of tissue.

Passive immunization: To generate immune serum, C57BL/6 or MyD88$^{-/-}$ mice were infected with 4 x 10^8 CFU/mouse *C. rodentium* and rescued with antibiotic treatment as described above. Serum was harvested three or four weeks p.i. from each strain. Samples from each strain were pooled and used to passively immunize naïve μMT mice. To do this, naïve μMT mice were infected with *C. rodentium* and injected daily intraperitoneal

on days 4-7 and 11-14 post-infection (p.i.) with 40μL of serum from infected MyD88$^{-/-}$ or wild type mice or serum from uninfected wild type mice, as previously described (9).

ELISA analysis: For antibody isotype analysis, antibody titers in sera were determined by enzyme-linked immunosorbent assay (ELISA). Plates were coated with 100 μl of 10μg of C. *rodentium* lysate per ml in 0.1 M carbonate buffer and incubated overnight at 4°C. The plates were washed with 0.05% polyoxyethylenesorbitan monolaurate (Tween® 20, Sigma-Aldrich) in phosphate buffered saline (PBS, 50mM K_2HPO_4, 50mM KH_2PO_4, pH 6.0, Sigma-Aldrich) and then blocked with blocking solution (0.2% bovine serum albumin (BSA; Sigma) and 0.05% Tween® 20 in PBS) at room temperature for 2 hours. Dilutions of serum starting at 1:20 were made with blocking solution, and 100 μl of each dilution was added to coated plates. After incubation at 37°C for 2 hours, the coated plates were washed with Tween 20 in PBS and bound immunoglobulin (Ig) was detected with horseradish peroxidase-conjugated goat anti-mouse IgG1 and IgG2b (Roche, Basel, Switzerland) at 37°C for 2 hours. The plates were then washed with Tween 20 in PBS. After incubation, color was developed with tetramethylbenzidine (Promega, Madison, WI), stopped with 0.18 N sulfuric acid, and measured by determination of optical density at 450 nm on a microplate reader (Biotek, Winooski, VT). The antibody titer was defined as the dilution required to reduce a positive signal to threefold above the background. (26). Sandwich ELISA kits were used according to the specifications of the manufacturer to measure levels of IL-6 (Becton Dickinson) and KC (Biosource, Camarillo, CA) in supernatant derived from colon or other tissues.

Bone marrow transplants: MyD88$^{-/-}$→WT chimeric mice were generated essentially as described previously (27). Briefly, C57BL/6 recipient mice were irradiated in two

sessions, separated by three hours, for a total dosage of 11Gy. Bone marrow from donor mice (3 x 10^6 cells in 200μL PBS) was injected into the tail vein the following day. Because MyD88$^{-/-}$ mice are more susceptible to infection by opportunistic pathogens, MyD88$^{-/-}$ recipients received a single dose of irradiation of 6 Gy. For two weeks following the transplant, drinking water was replaced with water containing neomycin sulfate/polymyxin B sulfate cocktail (Sigma-Aldrich). To facilitate confirmation of reconstitution in sublethally irradiated animals, mice received WT marrow from C57BL/6 mice with GFP labeled β-actin. Twelve weeks after reconstitution, blood samples were taken via tail or eye bleed. To confirm reconstitution, lymphocytes were isolated through centrifugation over Histopaque-1077 (Sigma Diagnostics, St. Louis, MO) (28) from whole blood and were identified by GFP fluorescence. Based on flow cytometry measurements, donor marrow comprised 95.93% of the peripheral white blood cells.

Myeloperoxidase (MPO) assays: Tissue samples from colon weighing ~0.2 to 0.3 g were homogenized in ice-cold PBS containing hexadecyltrimethlammonium bromide (0.5% w/v; Sigma-Aldrich). The homogenates were then subjected to three freeze-thaw cycles, followed by sonication (Fisher Scientific) on ice for 10s (power level 5) prior to centrifugation at 14,000 rpm (Forma Scientific, Waltham, MA) for 15 min at 4ºC. Aliquots of each supernatant or MPO standard (14μl; Sigma-Aldrich) were added to 200μl of substrate (0.167mg/mL of o-dianisidine in H_2O, 0.0005% H_2O_2, in potassium phosphate buffer), and the A_{450} was measured with a plate reader (Biotek). Total protein levels were measured by the bicinchoninic acid protein assay (Bio-Rad). MPO activity

was expressed as units per milligram of protein. One unit of enzyme activity was defined as the amount that consumes 1μmol of H_2O_2/min.

Manual neutrophil counts: Crypts were observed in the slides stained with H&E as described above using a 63× NA 1.4 lens on a Zeiss 200M microscope. Neutrophils were identified by their distinctive nuclear morphology and counted in fifteen crypts per colon. The mean number of neutrophils per crypt was calculated for each colon observed. The number of samples (n) refers to the number of colons measured.

Neutrophil killing assays: *C. rodentium* bacteria were cultured overnight in LB. To isolate neutrophils, bone marrow from wild type or MyD88$^{-/-}$ mice was removed, and red blood cells were lysed, 22-30% of cells were positive for GR-1 as measured by flow cytometry with an α-GR-1 antibody conjugated to FITC (BD bioscience, San Jose, CA). Bacteria ($5x10^6$) were added to $5x10^5$ cells in 300uL of RPMI medium without antibiotics. After 1, 2, or 3 hours, the bacterium-cell culture was diluted 1:10 in water for 10 minutes to lyse neutrophils and serial dilutions in PBS were plated on MacConkey agar to determine the number of bacterial colonies remaining. Assays were carried out in triplicate.

α-GR1 antibody treatment: C57BL/6 mice were rendered neutropenic by injection of 100μg of α-GR1 antibody (eBiosource) in 300uL PBS on days 2 and 4 p.i. Peripheral blood samples were taken on days 1 and 5 p.i. to ensure that number of neutrophils decreased. Mice were sacrificed on 7 days p.i. and various disease parameters measured.

Statistical analysis: For mortality curves, a two-sided Fisher's Exact Test determined statistical significance of data. For crypt lengths in Figure 2E, a student T-test assessed statistical significance. For all other experiments, level of statistical significance was

determined by a Mann-Whitney Rank-Sum test. Results were considered significant if the p-value was less than 0.01.

Results:

TLR signaling components localize in actin-filled pedestals beneath A/E bacteria.

Actin filled membranous protrusions or "pedestals", which form beneath A/E bacteria, have previously been characterized on the basis of proteins that facilitate actin polymerization (29). We hypothesized that these structures might also serve as sites of host immune detection and that TLRs might localize within pedestals. To test this, 3T3 cells were infected with EPEC or C. rodentium and indirect immunofluorescence microscopy was used to visualize the pathogens, actin pedestals and various TLRs. Bacterial DNA was stained with DAPI and polymerized actin with FITC-phalloidin. Cells were stained with antibodies against various TLRs. Pedestals were seen as intense actin staining apposed to a bacterium. As shown in Figure 1 (A-C), endogenous proteins resembling TLR1, TLR2, and TLR4 localized within the pedestal apposed to EPEC. 3T3 cells infected with EPEC or C. rodentium (data not shown) were also stained with antibodies that recognize the TLR signaling adaptor proteins MyD88 and TIRAP. As seen in Figure 1D and E, endogenous proteins resembling MyD88 and TIRAP were also present in pedestals and apposed to the bacterium. Pedestal formation did not appear to require TLR signaling because macrophages isolated from mice lacking MyD88 ($MyD88^{-/-}$) or TIRAP ($TIRAP^{-/-}$) formed pedestals upon infection with EPEC or C. rodentium (e.g. Figure 1F). These results demonstrate that TLRs and associated signaling elements are positioned in intimate association with bacteria and suggest that a coordinate signaling response involving multiple TLRs occurs at the site of A/E pathogen attachment *in vitro*.

MyD88 signaling is necessary to survive infection with *C. rodentium*.

To determine whether TLR signaling participates in host response to an A/E pathogen *in vivo*, we infected mice deficient in individual TLRs or in adaptor proteins with *C. rodentium* and assessed survival. Upon infection, mice deficient in TLR4 ($TLR4^{-/-}$) and their control strain, C57BL/6, all survived (data not shown) and appeared healthy four weeks later, the longest time assessed (data not shown). Thus, signaling through TLR4 alone is not required for a protective immune response to *C. rodentium*, a result similar to that reported by Khan et al. (18). Similarly, when mice deficient in TLR5 ($TLR5^{-/-}$) and their control strain, C57BL/6, were also infected with *C. rodentium* all mice survived, and no differences were found between the two strains at seven and fourteen days p.i. These data correlate with the recent findings that *C. rodentium* does not express flagellin, the ligand for TLR5, *in vitro* (30) although its expression *in vivo* remains unknown.

We considered that signaling from several TLRs might coordinate innate immune responses to an infection with *C. rodentium in vivo*. To test this possibility, we infected mice deficient in TIRAP ($TIRAP^{-/-}$), an adaptor protein necessary for MyD88 signaling from TLR2 and TLR4 complexes (24, 31), or MyD88 ($MyD88^{-/-}$), an adaptor protein that mediates signaling from most TLRs (10). In accordance with our results with $TLR4^{-/-}$ mice, $TIRAP^{-/-}$ mice infected with *C. rodentium* survived at a rate comparable to that seen with the control background strain, B129PF2/J (data not shown). Infection of $MyD88^{-/-}$ mice with *C. rodentium* proved much more deleterious. All infected $MyD88^{-/-}$ mice died within thirteen days (Figure 2A); by contrast, all wild type control mice (C57BL/6)

survived. Together these data suggest that MyD88 signaling is required to protect mice from mortality following infection with *C. rodentium*.

MyD88 signaling protects mice from severe intestinal damage and facilitates repair of damaged epithelium in response to *C. rodentium*.

To characterize the pathology associated with *C. rodentium* infection in MyD88$^{-/-}$ mice, colons were removed from wild type and MyD88$^{-/-}$ strains and evaluated for both macroscopic and microscopic appearance, and crypt length. As seen in Figure 2B, colons from MyD88$^{-/-}$ mice but not wild type mice exhibited localized intramural colonic bleeding, which developed between three and seven days p.i. Longitudinal sections of colonic tissue stained with H&E revealed that both wild type and MyD88$^{-/-}$ mice suffer from edema and epithelial injury following infection with *C. rodentium* (Figure 2D and G). However, MyD88$^{-/-}$ colonic tissue additionally displayed pathological features consistent with gangrenous necrosis characterized by foci of mucosal necrosis associated with large colonies of bacteria (Figure 2G). Gangrenous mucosal necrosis was not evident in uninfected MyD88$^{-/-}$ mice (Figure 2F) or in infected wild type mice (Figure 2D). Moreover, neither intramural colonic bleeding nor gangrenous mucosal necrosis was evident in TIRAP$^{-/-}$ mice. Together these data suggest that MyD88 signaling, but not TIRAP signaling, occurring in response to activation of multiple innate immune receptors provides protection from severe colonic pathology associated with unregulated bacterial growth.

Intestinal damage induced by DSS has been reported to induce a repair mechanism that replenishes epithelial cells and restores the integrity of the intestinal barrier in a TLR4- and MyD88-dependent manner (18, 32). In this process, stem cells

present at the base of intestinal crypts differentiate into enterocytes, divide, and migrate along the crypt to the site of damage (33). Such hyperplasia, measured as an increase in crypt length, is also a hallmark feature of A/E pathogen infection (5) and is indicative of restoration of damaged intestinal epithelium enterocytes. We observed that crypts of wild type mice were nearly twice as long seven days following *C. rodentium* infection compared to those of uninfected mice (Figure 2E). However, no increase in crypt length was evident following infection of MyD88$^{-/-}$ mice (Figure 2E). Accordingly, histological examination of colons from infected MyD88$^{-/-}$ mice indicates sustained damage throughout the course of the infection. By contrast, upon infection of TIRAP$^{-/-}$ mice, hyperplasia was evident to the same degree as in the control strain, B129PF2/J (data not shown). Together, these data suggest that MyD88 signaling is required for either sensing *C. rodentium* or for the replacement of damaged epithelia.

We also explored the effect of MyD88 signaling on epithelial apoptosis. TLR4$^{-/-}$ mice show increased apoptosis after intestinal injury with DSS, which can be reversed with exogenous PGE2 (34). Furthermore, mutant *Salmonella* strains that fail to activate TLR5 signaling induce extensive apoptosis, which exacerbates disease (35). These studies raise the possibility that MyD88 signaling protects from *C. rodentium* through blocking epithelial apoptosis and preserving the integrity of the epithelial barrier. To test this, we assessed apoptosis using TUNEL staining of infected colon sections at three and seven days p.i. Examples of each score are shown in Figure 3. Quantitation of these data is shown in Figure 4G. Although some apoptosis was evident in areas of gangrenous mucosal necrosis, overall we observed no significant increase in apoptosis in colonic tissue from MyD88$^{-/-}$ animals compared to wild type animals at three or seven days p.i.

(Compare Figure 4A with B, C with D, and E with F). Together, these data suggest that MyD88 signaling does not contribute to apoptosis in response to *C. rodentium* infection, and the exacerbated pathology seen in infected MyD88$^{-/-}$ mice is likely indicative of increased necrosis, not apoptosis.

Levels of *C. rodentium* colonization correlate with intramural colonic bleeding.

Damage to the colon caused by A/E pathogens can facilitate transit of bacteria across the epithelial barrier and dissemination throughout the body (5). In accordance with this idea, colonic sections with the highest degree of damage, evidenced by isolated intramural colonic bleeding, also contained the highest numbers of *C. rodentium* (Figure 5A). Intramural colonic bleeding in MyD88$^{-/-}$ mice appeared to progress distally over time. Such a progression was correlated with the colonization pattern of *C. rodentium*, which began in the cecal patches, but within days was found in the medial and eventually the distal colon (36). These data suggest that bleeding and high levels of colonization in MyD88$^{-/-}$ colons may facilitate dissemination of *C. rodentium* throughout the body.

MyD88$^{-/-}$ mice fail to control the level of *C. rodentium* colonization.

To test whether colonic damage facilitates bacteremia, we next assessed the extent to which *C. rodentium* disseminates to peripheral organs in MyD88$^{-/-}$ mice. Dissemination of bacteria from the colon to the mesenteric lymph nodes was evident one day after infection (data not shown), and to the liver and spleen by three days p.i. (Figure 5B). The level of *C. rodentium* colonization in various tissues increased until seven days p.i. (Figure 5C), after which time levels began to decrease (data not shown), presumably due to the onset of an adaptive immune response (9, 37). Although no difference in level of colonization was evident between the wild type and MyD88$^{-/-}$ mice three days after

infection (Figure 5B), by seven days p.i., the level of colonization was two to four orders of magnitude higher in MyD88$^{-/-}$ mice compared to that seen in wild type mice (Figure 5C). Administration of a higher infectious dose of *C. rodentium* to wild type mice (8×10^9 CFU) resulted in colonization levels that were similar to those seen in mice infected with the normal dose in all organs tested (data not shown). Together, these data suggest that an innate immune response mediated by MyD88 is required to control the level of colonization in the colon and peripheral organs by killing bacteria and replacing damaged enterocytes. However, these results do not rule out the possibility that MyD88 also mediates development of an efficient adaptive response.

An adaptive antibody response is sufficient to protect MyD88$^{-/-}$ mice from mortality.

Previous studies have shown that MyD88$^{-/-}$ mice mount an effective adaptive immune response to parasites, bacteria and viruses (12-15), but are impaired in their ability to class-switch auto-antibodies in a systemic lupus erythematosus model (38). To assess the efficacy of the adaptive immune response of MyD88$^{-/-}$ mice following infection with *C. rodentium*, we determined whether the antibody produced was sufficient to protect MyD88$^{-/-}$ mice from mortality. To do this, MyD88$^{-/-}$ mice were infected with *C. rodentium* and then treated three days later with antibiotics for four weeks. Ninety-five percent of mice treated with antibiotics survived (22/23 mice; data not shown). The mice were then reinfected with *C. rodentium* and their survival assessed. As seen in Figure 6A, 73% of the reinfected MyD88$^{-/-}$ mice survived the second infection although clearance of *C. rodentium* in reinfected survivors occurred at least two weeks later than in wild type mice. Interestingly, low levels of *C. rodentium* were still present in colonic tissue of 27.7% of MyD88$^{-/-}$ mice after four weeks of continuous antibiotic treatment, and colons

of these mice showed evidence of pathology (see CHAPTER IV, data not shown). Thus, the percentage of mice that succumbed following reinfection was the same as that in which colonization and pathology was evident following antibiotic treatment. Notably, MyD88$^{-/-}$ mice produced decreased levels of IL-6 (Figure 6B), a cytokine required for the efficient induction of an adaptive response at the site of infection (39).

We next verified that antibody was produced in MyD88$^{-/-}$ mice treated with antibiotic. Notably, *C. rodentium* specific IgG_1 and $IgG2_b$ were generated in both wild type and MyD88$^{-/-}$ mice, though the IgG_1 titer was significantly higher in MyD88$^{-/-}$ mice (Figure 6C). We attribute this difference to the higher bacterial loads seen in MyD88$^{-/-}$ animals at this time in infection. To determine whether antibody produced by MyD88$^{-/-}$ animals was sufficient to confer protection against *C. rodentium*, we transferred serum from immunized animals into μMT mice, which lack B cells (40), and are extremely susceptible to infection from this bacteria (37, 41). Notably, the level of *C. rodentium* colonization in μMT mice is lower than that seen in MyD88$^{-/-}$ mice seven days p.i. (data not shown). Furthermore, examination of the colons of μMT mice indicated no evidence of the intramural colonic bleeding or severe colitis seen in MyD88$^{-/-}$ mice. As shown in Figure 6D, serum from immunized MyD88$^{-/-}$ mice conferred survival on 40% of μMT mice infected by C. rodentium. The rate of survival was similar to that seen in μMT mice that received serum from immunized WT mice. Together, these data indicate that MyD88$^{-/-}$ mice can mount a protective *C. rodentium*-specific antibody response. The increased mortality of immunized MyD88$^{-/-}$ mice compared to wild type mice (Figure 6A) suggest a deficiency in another protective process in these mice, such as wound repair or neutrophil response.

MyD88 signaling in both hematopoietic and non-hematopoietic cells is necessary to survive *C. rodentium* infection.

To determine whether MyD88 signaling in hematopoietic cells, in non-hematopoietic cells or in both was necessary for protection from *C. rodentium*, we performed reciprocal bone marrow transplants. Thus, bone marrow from MyD88$^{-/-}$ mice was transferred into lethally irradiated wild type (WT) mice, creating MyD88$^{-/-}$→WT chimeric mice, to determine the necessity of MyD88 signaling in hematopoietic cells. Likewise, we created WT→MyD88$^{-/-}$ chimeric mice, to determine the necessity of MyD88 signaling in non-hematopoietic cells. As controls, we created WT→WT and MyD88$^{-/-}$→MyD88$^{-/-}$ chimeric mice. Reconstitution was confirmed after twelve weeks by flow cytometry.

Upon infection with *C. rodentium*, 100% of MyD88$^{-/-}$→WT mice died within 10 days at a rate similar to that seen in MyD88$^{-/-}$ or MyD88$^{-/-}$→MyD88$^{-/-}$ mice (Figure 7A). By contrast, nearly all control WT→WT mice survived (Figure 7A). Therefore, MyD88 signaling from hematopoietic cells is required for survival in response to infection with *C. rodentium*. Notably, bone marrow from WT mice provided only marginal protection to MyD88$^{-/-}$ mice infected with *C. rodentium* as only 77.8% of WT→MyD88$^{-/-}$ chimeric mice died compared to 100% of MyD88$^{-/-}$ or MyD88$^{-/-}$→MyD88$^{-/-}$ mice (Figure 7A). Moreover, the WT→MyD88$^{-/-}$ mice that survived cleared the infection with kinetics comparable to those seen with WT and WT→WT mice (data not shown). Together these data suggest that both hematopoietic and non-hematopoietic cells are required for survival upon infection with *C. rodentium.*

Pathological examination of infected MyD88$^{-/-}$→WT mice indicated that colons displayed phenotypes characteristic of those induced by *C. rodentium* in MyD88$^{-/-}$ mice. Thus, colons from MyD88$^{-/-}$→WT mice showed evidence of isolated intramural colonic bleeding (compare Figure 7B), a phenotype never observed in WT→WT mice (Figure 7B), or in WT mice (Figure 2B). Colons of uninfected MyD88$^{-/-}$→WT mice likewise showed no evidence of bleeding between crypts or inflammation (Figure 7C). Additionally, histological evaluation of longitudinal sections of colons in MyD88$^{-/-}$→WT mice revealed mucosal and epithelial injury, including gangrenous mucosal necrosis similar to those observed in MyD88$^{-/-}$ animals (Figure 1F). Such findings were not evident in WT→WT mice (Figure 7D). These results indicate that MyD88 signaling on hematopoietic cells is necessary to prevent localized intramural colonic bleeding and severe intestinal pathology.

MyD88 signaling on either hematopoietic or non-hematopoietic cells is sufficient to facilitate repair of intestinal epithelia in response to *C. rodentium* infection.

In contrast to results from MyD88$^{-/-}$ mice (Figure 2E), hyperplasia was evident in colonic tissue from MyD88$^{-/-}$→WT mice infected with *C. rodentium* (Figure 8A). Thus, crypt length was significantly longer than that observed in uninfected MyD88$^{-/-}$→WT colonic tissue (Figure 8A), but not significantly different from that found in infected WT→WT mice (data not shown). As expected, crypt lengths from infected WT→WT mice were significantly longer than those found in infected MyD88$^{-/-}$→MyD88$^{-/-}$ mice (data not shown). These data indicate that MyD88 signaling on non-hematopoietic cells is sufficient for the development of hyperplasia in response to *C. rodentium*. Histological examination of colons from WT→MyD88$^{-/-}$ mice also showed evidence of hyperplasia

(Figure 8A), suggesting that hematopoietic cells also contribute to the development of hyperplasia. Together, these data suggest that MyD88 signaling in either hematopoietic or non-hematopoietic cells is sufficient to facilitate repair of colonic epithelium. However, crypt lengths were significantly longer in WT→MyD88$^{-/-}$ mice compared to those seen in MyD88$^{-/-}$→WT mice, indicating that MyD88 signaling in hematopoietic cells may contribute in a more significant way to the repair process than non-hematopoietic cells. Nevertheless, signaling in both hematopoietic and non-hematopoietic cells is required to protect mice from severe colitis and death upon infection with *C. rodentium*. A similar requirement for MyD88 signaling in multiple cell types has been described in a murine pulmonary inflammation model (27).

Control of *C. rodentium* colonization requires MyD88 signaling in hematopoietic and non-hematopoietic cells.

To further characterize pathology in the chimeric mice, organs were harvested from the mice and bacterial colony counts were measured. In each organ, the degree of colonization of the WT→WT mice was similar to that seen in WT (Figure 8B). Likewise, the degree of colonization in organs of MyD88$^{-/-}$→MyD88$^{-/-}$ mice was similar to that seen in MyD88$^{-/-}$ mice (Figure 7B). The level of colonization seen in organs removed from both MyD88$^{-/-}$→WT and WT→MyD88$^{-/-}$ mice more closely matched that found in MyD88$^{-/-}$ mice and was higher than the levels seen in organs from WT organs or WT→WT mice, especially in peripheral organs (Figure 8C). Taken together, these data suggest that MyD88 signaling on both hematopoietic and non-hematopoietic cells is necessary to control levels of *C. rodentium* colonization.

A role for neutrophils in the protective response to *C. rodentium* infection.

Bone marrow transplants indicated that MyD88 signaling on hematopoietic and non-hematopoietic cells is necessary for protection. We next set out to characterize more precisely which hematopoietic cell types were required. The observation that MyD88$^{-/-}$ mice cannot control *C. rodentium* colonization (Figure 5C) suggested a role for neutrophils, which kill bacteria. To investigate the role of neutrophils, we measured the levels of myeloperoxidase (MPO) activity in colons of wild type and MyD88$^{-/-}$ mice. Because MPO is expressed predominantly in neutrophils and to a lesser extent in macrophages (42), it enabled us to selectively distinguish the role of neutrophils. Levels of MPO in colons of WT mice increased by 13.2 fold at three days p.i., and remained at a high level at seven days p.i. The increase in MPO levels in the medial and distal colon mirrored the increased levels of colonization seen in these regions as the infection progressed (Figure 5C and 9A). By contrast, MPO levels in colons of MyD88$^{-/-}$ mice measured three days p.i. significantly lower (2.7 fold) than those seen in wild type mice (Figure 9A). MPO levels in the colons of MyD88$^{-/-}$ mice did increase by seven days p.i. (Figure 9A) though to a lesser extent than that seen in wild type mice, despite the fact that colonization was two orders of magnitude higher (Figure 5C). Counts of neutrophils in colonic tissues corroborated results of the MPO assays (Figure 9B). Together, these data suggest that recruitment of neutrophils to the colon of MyD88$^{-/-}$ mice was delayed at a time when bacterial numbers at this site were rapidly expanding.

To determine whether there was an intrinsic defect in neutrophils from MyD88$^{-/-}$ mice, we assessed the capacity of neutrophils to migrate and to kill bacteria *in vitro*. As shown in Figure 9C, MyD88$^{-/-}$ neutrophils migrated *in vitro* in response to the

chemoattractant fNLP with the same efficacy as wild type neutrophils, confirming previous observations (16). In addition, bactericidal activity of neutrophils isolated from both MyD88$^{-/-}$ and wild type mice was indistinguishable (Figure 9D). The addition of serum from convalescent wild type or MyD88$^{-/-}$ mice to the killing assay did not influence the efficiency or rate of killing by neutrophils (data not shown). We were unable to measure MPO levels in peripheral organs of wild type and MyD88$^{-/-}$ mice due to limitations in sensitivity of the assay. Thus, neutrophil levels in infected liver samples were below the level of detection, and levels of splenic neutrophils were high in uninfected samples and we could not distinguish an increase upon infection. Together, these data indicate that neutrophils from MyD88$^{-/-}$ mice did not display an intrinsic functional defect, though we cannot rule out the possibility that MyD88 signaling regulates specific neutrophil functions *in vivo*.

The observation that neutrophils from MyD88$^{-/-}$ mice did not display an intrinsic defect led us to hypothesize that chemokines derived from hematopoietic or non-hematopoietic cells or both might facilitate migration of neutrophils to the colon following infection. In this regard, CXC chemokines such as KC are released by epithelial cells and have been shown to participate in the recruitment of neutrophils following infection by a of variety pathogens (43). As shown in Figure 9E, levels of KC were ~3 orders of magnitude higher in colons of wild type mice three days p.i. compared to MyD88$^{-/-}$ mice. By seven days p.i., KC levels in wild type and MyD88 animals were nearly equivalent (data not shown). Together these data suggest that production of KC or other chemokines required for proper recruitment of neutrophils, was significantly

delayed in colons of MyD88$^{-/-}$ mice in response to *C. rodentium*, thus mirroring the changes in MPO levels in these mice.

To determine whether neutrophils are required for innate immune protection from *C. rodentium*, we next set out to deplete neutrophils in wild type mice by injecting the neutralizing monoclonal antibody directed against GR-1. To do this α-GR-1 mAb was injected on days two and four p.i. with *C. rodentium*. Using this protocol, the number of neutrophils was reduced to undetectable levels (data not shown). Injection of α-GR-1 mAb resulted in 22% mortality by day seven p.i. compared to no mortality in PBS-injected controls (data not shown). Moreover, wild type mice injected with α-GR-1 mAb had levels of *C. rodentium* colonization in liver and spleen comparable to that seen in infected MyD88$^{-/-}$ mice, and 2-4 orders of magnitude higher than those of PBS-injected controls (Figure 9F and 5C). Together, these data suggest (i) that efficient migration of neutrophils to the colon depends on MyD88, although neutrophils retain the capacity to migrate *in vitro* in a MyD88-independent manner; (ii) that MyD88-dependent signals derived from hematopoietic cells, non-hematopoietic cells or both contribute to efficient neutrophil recruitment to the colon; and (iii) that neutrophils are required to control bacterial load and promote a protective response in a MyD88-dependent fashion.

Discussion:

A/E pathogens, including EPEC, EHEC, and *C. rodentium*, cause disease characterized by intestinal inflammation and diarrhea. Previous reports suggest that inflammatory responses occur following a breach of the intestinal barrier and are mediated by innate and adaptive immune mechanisms (37, 41, 44). Whereas the adaptive responses to A/E pathogens have been well characterized (9, 37, 41), the role of innate immune responses is less well understood. We initiated this study to determine whether reducing innate immune recognition of the bacteria could mollify the colitis caused by *C. rodentium*. However, data presented here suggest that innate immune signals through the innate immune receptor adaptor protein MyD88 protect the host from bacteremia and severe pathology in the colon including gangrenous mucosal necrosis that is associated with uncontrolled growth of the pathogen. Thus, although an innate immune response associated with inflammation appears deleterious and maladaptive, it also affords significant protection as the adaptive response is generated.

Triggering the innate immune response.

The intestinal epithelium serves as the first site where A/E pathogens interact with the host, inducing formation of characteristic actin-filled "pedestals" and disruption of microvilli. Although there is no direct evidence, pedestals have been traditionally been viewed as adherence sites that allow the bacteria to remain firmly attached (29), perhaps as a means of colonizing the lumen as diarrhea disrupts commensal microflora. Finally, pedestals serve as the site at which virulence factors, such as EspF (45), are introduced via a type III secretion system that disrupt the epithelial barrier and allow the bacteria access to the colonic lamina propria and ultimately to peripheral organs. Our data

suggest that pedestals may also serve as a site that facilitates innate immune recognition of a pathogen. Thus, localization of TLRs and their adaptor proteins in pedestals suggests that immune signaling may occur at this site (Figure 1A-E). The localization of several TLRs within the pedestal suggest that a coordinated signaling cascade or threshold mechanism may be used to detect A/E pathogens, and possibly to distinguish them from commensal strains. Our data with chimeric WT→MyD88$^{-/-}$ mice (Figure 6A) suggest that MyD88 signaling in non-hematopoietic cells, possibly epithelial cells in the crypts or fibroblasts in the submucosa may be required to induce timely neutrophil recruitment (Figure 6A). We speculate that pedestals forming on non-hematopoietic cells may not only serve as sites of adhesion, but the TLRs within pedestals may facilitate chemokine production in these cells that alerts neutrophils to the presence of the pathogen.

Innate and adaptive immune responses control bacterial dissemination.

Khan and colleagues provide evidence that TLR4-dependent responses mediate inflammation and tissue pathology during *C. rodentium* infection (18). Our data with MyD88-deficient mice extend the results of Khan *et al.* and point to MyD88 as a key mediator not only of inflammation, but also of protection from bacteremia and severe colonic pathology. The cell types involved include both hematopoietic cells including neutrophils, and non-hematopoietic cells, most notably the epithelium (Figures 7-9).

Control of bacterial dissemination to peripheral organs following *C. rodentium* infection in the colon appears to be mediated by both innate and adaptive immune responses. For example, infection of mice lacking B cells, T cells, or both have greater pathogen loads in colonic and peripheral tissues (9, 37). However, adaptive responses do not alone appear necessary for survival. A significant proportion of T and B cell-deficient mice survive infection with *C. rodentium* (9, 37, 46), although the infection appears more

severe than in wild type mice. Moreover, mast cell-deficient mice suffer bacteremia and death after infection with *C. rodentium*, although the adaptive response appears unaffected (26). Finally, we provide evidence here that MyD88$^{-/-}$ mice have greater bacterial loads both in the colon and in peripheral tissues (Figure 5C), which strongly correlates with decreased neutrophil infiltration into the colon (Figure 9A and B). Therefore, our observations suggest that innate immune cells provide a critical means of protection early in the infection by containing the bacteria within the colon and killing any that had disseminated. In support of this, delayed neutrophil recruitment three days p.i. was correlated with high bacterial loads in the colon and other tissues of MyD88$^{-/-}$ mice at later stages of infection (Figures 9A and 5C), and depletion of neutrophils in wild type mice resulted in high bacterial loads in the liver and spleen (Figure 9F). These data suggest a prominent role for the innate immune system early in the infection, though they do not preclude a requirement for antibody-mediated responses later on.

Innate immune mechanisms that provide protection by killing bacteria or limiting dissemination are not limited to A/E pathogens. In this regard, previous studies of MyD88$^{-/-}$ mice infected with lymphocytic choriomeningitis virus (LCMV) (12), *Borrelia burgdorferi* (13), *Brucella abortus* (14), or *Salmonella typhimurium (15)* have also demonstrated that MyD88 signaling is required to limit severity of disease, dissemination, and pathogen numbers. For example, following inoculation of MyD88$^{-/-}$ mice, spread of *B. abortus* to peripheral organs occurs with similar kinetics to that seen with *C. rodentium* ((14); Figure 4B). Moreover, MyD88$^{-/-}$ mice display delayed clearance of *B. burgdorferi* and *B. abortus* infections (13, 14), and strains of LCMV which are cleared in wild type mice cause chronic disease in MyD88$^{-/-}$ mice (12), indicating a sub-

optimal adaptive response in the absence of MyD88 signaling.

Our results with immunized mice provide novel information on the cross-talk between the innate and adaptive responses. Two aspects of the experiments with antibiotic treated MyD88$^{-/-}$ mice were unexpected, and may provide important information on the role of innate immune cells in bacterial clearance. First, continuous administration of an antibiotic cocktail was not sufficient to clear the pathogen in all MyD88$^{-/-}$ mice, although all wild type mice cleared the infection. It is possible that high bacterial loads might account for such a result although at the time of antibiotic administration bacterial loads in wild type and MyD88$^{-/-}$ mice were equivalent (Figure 5B). However, we cannot rule out that significantly more bacteria were present in the MyD88$^{-/-}$ mice at the time the antibiotics took effect. It is also possible that bacteria were in stationary phase and thus resistant to bactericidal effects of the antibiotics, thereby facilitating development of resistant strains (47). In this regard, preliminary experiments suggest that *C. rodentium* strains recovered after long-term antibiotic treatment were relatively resistant to the administered antibiotics (see CHAPTER IV), demonstrating that the antibiotic treatment in MyD88$^{-/-}$ mice provides selective pressure on the bacteria. These results may also suggest that an innate immune response is required for effective bacterial clearance in conjunction with an antibiotic, or for suppressing the development of resistant bacteria.

A second unexpected observation was the development of a high-titer antibody response despite undetectable levels of IL-6 in the colon (Figure 6B and C). The presence of IL-6 has been long been considered crucial for development of antibody responses (39). However, our results showing protection of μMT mice that had received

serum from immunized MyD88$^{-/-}$ mice suggest that IL-6 is not necessarily required to generate protective antibody (Figure 6B and D). Of note, the immunization protocol was not completely protective in MyD88$^{-/-}$ mice: only 73% of immunized MyD88$^{-/-}$ mice survived a challenge infection, and those mice that do survive clear the infection with delayed kinetics (Figure 6A). Thus, it remains possible that either IL-6 is required for optimal antibody responses or MyD88-dependent responses, such as phagocytosis of opsinized bacteria, are needed in conjunction with antibody to effectively clear the bacteria.

Repairing the breach.

A/E pathogens gain access to the basolateral surface by causing breakdown of the epithelial barrier using virulence factors, such as EspF, that are secreted into epithelial cells by a type III secretion system (45). Several lines of evidence indicate that epithelial hyperplasia constitutes a proliferation of crypt stem cells that repairs the breach in response to DSS, and that macrophages facilitate the repair process in a MyD88-dependent manner (32). Accordingly, infected MyD88$^{-/-}$ mice display substantial damage to the intestinal epithelium but little evidence of hyperplasia (Figure 2E and F). However, hyperplasia was evident in MyD88$^{-/-}$→WT mice comparable to that seen in wild type mice. These results suggest that MyD88 signaling on non-hematopoietic cells is sufficient for epithelial repair following infection with *C. rodentium*. Moreover, hyperplasia is evident in wild type mice by three days p.i., the same time at which neutrophils are recruited. Thus, protection may in part be mediated by wound repair of epithelial barrier breach that contains the infection within the colon and prevent dissemination to distal sites.

Repair in the intestine also involves protection from apoptosis. TLR4 and MyD88 are responsible for upregulation of Cox-2 expression, which mediates anti-apoptotic signals (34). As a result, TLR4$^{-/-}$ and MyD88$^{-/-}$ mice have increased apoptosis, reduced proliferation, and increased epithelial injury following DSS exposure (16, 34). Moreover, mutant *Salmonella* strains that do not stimulate TLR5 signaling induce greater epithelial damage due to the lack of MyD88-dependent protection from apoptosis (35). In contrast, we do not detect an increase in apoptosis in the MyD88$^{-/-}$ mice following infection with *C. rodentium*, and infected TLR4$^{-/-}$ mice actually have milder pathology than wild type (18). Together, these observations suggest that DSS colitis, *Salmonella* infection, and A/E bacterial infection each stimulate distinct protective responses in the host with different etiology. Thus, in A/E pathogen infections, MyD88 signaling facilitates clearance by inducing recruitment of neutrophils, which controls bacterial load, and repair of the epithelial barrier. In the absence of MyD88, necrosis rather than apoptosis exacerbates the infection, causing additional damage to the epithelial barrier.

A role for neutrophils in protection.

Several lines of evidence suggest that neutrophils and non-hematopoietic cells are together required for protection from *C. rodentium* infection. First, depletion of neutrophils in wild type mice results in increased dissemination of bacteria and mortality (Figure 9F). Second, neutrophil accumulation in colonic tissues is delayed in the absence of MyD88 signaling (Figure 9A and B). This delay does not appear to be a result of an intrinsic defect in neutrophil function because MyD88$^{-/-}$ neutrophils retain the capacity to migrate and to kill bacteria *in vitro* (Figure 9C and D). Notably, the delay occurs at a time when bacteria are beginning to disseminate and numbers are rapidly expanding (Figure

5B). Our data suggest that failure to restrict bacterial growth early in the infection results in loads that may be beyond the capabilities of innate or adaptive defenses to control. Although not addressed here, macrophages can also kill *C. rodentium* (data not shown), so they may act with neutrophils to restrict bacterial loads. The role of macrophages in recovery of *C. rodentium* infection is the subject of current studies.

The migration of neutrophils throughout the body is orchestrated by several chemokines, including those of the CXC class (48). It is possible that several chemokines orchestrate the recruitment of neutrophils in response to *C. rodentium*. We found at least one of these, KC, is produced in a MyD88-dependent manner (Figure 9E). Our results also demonstrate that KC is significantly reduced three days p.i. compared to wild type mice, though it is present at levels equivalent to those in wild type animals by day seven, thereby mirroring the delay in neutrophil recruitment (Figure 9A and B).

Here we demonstrate that MyD88$^{-/-}$ mice suffer from severe colonic pathology and mortality. However, because so many different aspects of the innate immune response are altered in MyD88$^{-/-}$ mice during an infection with *C. rodentium*, it is difficult to determine which aspect of the MyD88$^{-/-}$ phenotype has caused the severe pathology and ultimately death. Here three possible causes for the pathology are proposed. 1) The delayed neutrophil response caused by lowered chemokine production leads to increased pathogen load and therefore increased quantity of *C. rodentium*-induced damage (Figure 10A). 2) MyD88$^{-/-}$ mice are more susceptible to intestinal damage to other inducers, such as DSS (16, 17), and similarly the increased pathology caused by *C. rodentium* is due to a predisposition to intestinal damage (Figure 10B). 3) MyD88$^{-/-}$ mice are not capable of inducing replacement of enterocytes damaged during an infection with *C. rodentium*,

evident as lack of hyperplasia; this repair deficiency results in an accumulation of damage intestinal epithelium. Any one or combination of these models could be the cause of the increased intestinal pathology observed in MyD88$^{-/-}$ mice following infection with *C. rodentium*.

Literature Cited

1. Frankel, G., A. D. Phillips, I. Rosenshine, et al.: Enteropathogenic and enterohaemorrhagic Escherichia coli: more subversive elements. *Mol Microbiol*. 30(5), 911-921(1998).
2. Donnenberg, M. S.: Enteropathogenic Escherichia coli. In: *Infections of the gastrointestinal tract*. M. Blaser, P. Smith, J. Ravdin, H. Greenberg, and R. Guerranteds). Lippincott Williams & Wilkins, Philadelphia, PA, 595-612(2002).
3. Noel, J. M., and E. C. Boedeker: Enterohemorrhagic Escherichia coli: a family of emerging pathogens. *Dig Dis*. 15(1-2), 67-91(1997).
4. Karch, H., P. I. Tarr, and M. Bielaszewska: Enterohaemorrhagic Escherichia coli in human medicine. *Int J Med Microbiol*. 295(6-7), 405-418(2005).
5. Luperchio, S. A., and D. B. Schauer: Molecular pathogenesis of Citrobacter rodentium and transmissible murine colonic hyperplasia. *Microbes Infect*. 3(4), 333-340(2001).
6. McDaniel, T. K., and J. B. Kaper: A cloned pathogenicity island from enteropathogenic Escherichia coli confers the attaching and effacing phenotype on E. coli K-12. *Mol Microbiol*. 23(2), 399-407(1997).
7. Mundy, R., T. T. MacDonald, G. Dougan, G. Frankel, and S. Wiles: Citrobacter rodentium of mice and man. *Cell Microbiol*. 7(12), 1697-1706(2005).
8. Higgins, L. M., G. Frankel, G. Douce, G. Dougan, and T. T. MacDonald: Citrobacter rodentium infection in mice elicits a mucosal Th1 cytokine response and lesions similar to those in murine inflammatory bowel disease. *Infect Immun*. 67(6), 3031-3039.(1999).
9. Maaser, C., M. P. Housley, M. Iimura, et al.: Clearance of Citrobacter rodentium requires B cells but not secretory immunoglobulin A (IgA) or IgM antibodies. *Infect Immun*. 72(6), 3315-3324(2004).
10. Kaisho, T., and S. Akira: Pleiotropic function of Toll-like receptors. *Microbes Infect*. 6(15), 1388-1394(2004).
11. Savkovic, S. D., A. Koutsouris, and G. Hecht: Activation of NF-kappaB in intestinal epithelial cells by enteropathogenic Escherichia coli. *Am J Physiol*. 273(4 Pt 1), C1160-1167(1997).
12. Zhou, S., E. A. Kurt-Jones, L. Mandell, et al.: MyD88 is critical for the development of innate and adaptive immunity during acute lymphocytic choriomeningitis virus infection. *Eur J Immunol*. 35(3), 822-830(2005).
13. Bolz, D. D., R. S. Sundsbak, Y. Ma, et al.: MyD88 plays a unique role in host defense but not arthritis development in Lyme disease. *J Immunol*. 173(3), 2003-2010(2004).
14. Weiss, D. S., K. Takeda, S. Akira, A. Zychlinsky, and E. Moreno: MyD88, but not toll-like receptors 4 and 2, is required for efficient clearance of Brucella abortus. *Infect Immun*. 73(8), 5137-5143(2005).
15. Hapfelmeier, S., B. Stecher, M. Barthel, et al.: The Salmonella pathogenicity island (SPI)-2 and SPI-1 type III secretion systems allow Salmonella serovar typhimurium to trigger colitis via MyD88-dependent and MyD88-independent mechanisms. *J Immunol*. 174(3), 1675-1685(2005).

16. Fukata, M., K. S. Michelsen, R. Eri, et al.: Toll-like receptor-4 is required for intestinal response to epithelial injury and limiting bacterial translocation in a murine model of acute colitis. *Am J Physiol Gastrointest Liver Physiol*. 288(5), G1055-1065(2005).
17. Rakoff-Nahoum, S., J. Paglino, F. Eslami-Varzaneh, S. Edberg, and R. Medzhitov: Recognition of commensal microflora by toll-like receptors is required for intestinal homeostasis. *Cell*. 118(2), 229-241(2004).
18. Khan, M. A., C. Ma, L. A. Knodler, et al.: Toll-like receptor 4 contributes to colitis development but not to host defense during Citrobacter rodentium infection in mice. *Infect Immun*. 74(5), 2522-2536(2006).
19. Gibson, D. L., C. Ma, C. M. Rosenberger, et al.: Toll-like receptor 2 plays a critical role in maintaining mucosal integrity during Citrobacter rodentium-induced colitis. *Cell Microbiol*. 10(2), 388-403(2008).
20. Kalman, D., O. D. Weiner, D. L. Goosney, et al.: Enteropathogenic E. coli acts through WASP and Arp2/3 complex to form actin pedestals. *Nat Cell Biol*. 1(6), 389-391(1999).
21. Swimm, A., B. Bommarius, Y. Li, et al.: Enteropathogenic Escherichia coli use redundant tyrosine kinases to form actin pedestals. *Mol Biol Cell*. 15(8), 3520-3529(2004).
22. Hayashi, F., K. D. Smith, A. Ozinsky, et al.: The innate immune response to bacterial flagellin is mediated by Toll-like receptor 5. *Nature*. 410(6832), 1099-1103(2001).
23. Adachi, O., T. Kawai, K. Takeda, et al.: Targeted disruption of the MyD88 gene results in loss of IL-1- and IL-18-mediated function. *Immunity*. 9(1), 143-150(1998).
24. Horng, T., G. M. Barton, R. A. Flavell, and R. Medzhitov: The adaptor molecule TIRAP provides signalling specificity for Toll-like receptors. *Nature*. 420(6913), 329-333(2002).
25. Yang, S., N. Takahashi, T. Yamashita, et al.: Muramyl dipeptide enhances osteoclast formation induced by lipopolysaccharide, IL-1 alpha, and TNF-alpha through nucleotide-binding oligomerization domain 2-mediated signaling in osteoblasts. *J Immunol*. 175(3), 1956-1964(2005).
26. Wei, O. L., A. Hilliard, D. Kalman, and M. Sherman: Mast cells limit systemic bacterial dissemination but not colitis in response to Citrobacter rodentium. *Infect Immun*. 73(4), 1978-1985(2005).
27. Noulin, N., V. F. Quesniaux, S. Schnyder-Candrian, et al.: Both hemopoietic and resident cells are required for MyD88-dependent pulmonary inflammatory response to inhaled endotoxin. *J Immunol*. 175(10), 6861-6869(2005).
28. Taylor, R. T., A. Lugering, K. A. Newell, and I. R. Williams: Intestinal cryptopatch formation in mice requires lymphotoxin alpha and the lymphotoxin beta receptor. *J Immunol*. 173(12), 7183-7189(2004).
29. Vallance, B. A., C. Chan, M. L. Robertson, and B. B. Finlay: Enteropathogenic and enterohemorrhagic Escherichia coli infections: emerging themes in pathogenesis and prevention. *Can J Gastroenterol*. 16(11), 771-778(2002).

30. Khan, M. A., S. Bouzari, C. Ma, et al.: Flagellin-dependent and -independent inflammatory responses following infection by enteropathogenic Escherichia coli (EPEC) and Citrobacter rodentium. *Infect Immun*2008).
31. Yamamoto, M., S. Sato, H. Hemmi, et al.: Essential role for TIRAP in activation of the signalling cascade shared by TLR2 and TLR4. *Nature*. 420(6913), 324-329(2002).
32. Pull, S. L., J. M. Doherty, J. C. Mills, J. I. Gordon, and T. S. Stappenbeck: Activated macrophages are an adaptive element of the colonic epithelial progenitor niche necessary for regenerative responses to injury. *Proc Natl Acad Sci U S A*. 102(1), 99-104(2005).
33. Radtke, F., and H. Clevers: Self-renewal and cancer of the gut: two sides of a coin. *Science*. 307(5717), 1904-1909(2005).
34. Fukata, M., A. Chen, A. Klepper, et al.: Cox-2 is regulated by Toll-like receptor-4 (TLR4) signaling: Role in proliferation and apoptosis in the intestine. *Gastroenterology*. 131(3), 862-877(2006).
35. Vijay-Kumar, M., H. Wu, R. Jones, et al.: Flagellin suppresses epithelial apoptosis and limits disease during enteric infection. *Am J Pathol*. 169(5), 1686-1700(2006).
36. Wiles, S., S. Clare, J. Harker, et al.: Organ specificity, colonization and clearance dynamics in vivo following oral challenges with the murine pathogen Citrobacter rodentium. *Cell Microbiol*. 6(10), 963-972(2004).
37. Simmons, C. P., S. Clare, M. Ghaem-Maghami, et al.: Central role for B lymphocytes and CD4+ T cells in immunity to infection by the attaching and effacing pathogen Citrobacter rodentium. *Infect Immun*. 71(9), 5077-5086(2003).
38. Ehlers, M., H. Fukuyama, T. L. McGaha, A. Aderem, and J. V. Ravetch: TLR9/MyD88 signaling is required for class switching to pathogenic IgG2a and 2b autoantibodies in SLE. *J Exp Med*. 203(3), 553-561(2006).
39. Jones, S. A.: Directing transition from innate to acquired immunity: defining a role for IL-6. *J Immunol*. 175(6), 3463-3468(2005).
40. Kitamura, D., J. Roes, R. Kuhn, and K. Rajewsky: A B cell-deficient mouse by targeted disruption of the membrane exon of the immunoglobulin mu chain gene. *Nature*. 350(6317), 423-426(1991).
41. Bry, L., and M. B. Brenner: Critical role of T cell-dependent serum antibody, but not the gut-associated lymphoid tissue, for surviving acute mucosal infection with Citrobacter rodentium, an attaching and effacing pathogen. *J Immunol*. 172(1), 433-441(2004).
42. Lincoln, J. A., D. L. Lefkowitz, T. Cain, et al.: Exogenous myeloperoxidase enhances bacterial phagocytosis and intracellular killing by macrophages. *Infect Immun*. 63(8), 3042-3047(1995).
43. Kielian, T., B. Barry, and W. F. Hickey: CXC chemokine receptor-2 ligands are required for neutrophil-mediated host defense in experimental brain abscesses. *J Immunol*. 166(7), 4634-4643(2001).
44. Vallance, B. A., W. Deng, L. A. Knodler, and B. B. Finlay: Mice lacking T and B lymphocytes develop transient colitis and crypt hyperplasia yet suffer impaired bacterial clearance during Citrobacter rodentium infection. *Infect Immun*. 70(4), 2070-2081.(2002).

45. McNamara, B. P., A. Koutsouris, C. B. O'Connell, et al.: Translocated EspF protein from enteropathogenic Escherichia coli disrupts host intestinal barrier function. *J Clin Invest*. 107(5), 621-629(2001).
46. Vallance, B. A., W. Deng, K. Jacobson, and B. B. Finlay: Host susceptibility to the attaching and effacing bacterial pathogen Citrobacter rodentium. *Infect Immun*. 71(6), 3443-3453(2003).
47. Levin, B. R., and D. E. Rozen: Non-inherited antibiotic resistance. *Nat Rev Microbiol*. 4(7), 556-562(2006).
48. Kobayashi, Y.: Neutrophil infiltration and chemokines. *Crit Rev Immunol*. 26(4), 307-316(2006).

Figure Legends:

Figure 1: TLR and TLR signaling adaptor proteins localize in actin pedestals, but are not necessary for pedestal formation. (A-D) Images of 3T3 cells exposed to EPEC and stained with DAPI to identify EPEC, FITC-phalloidin to visualize actin, and α-TLR1 (A), α-TLR2 (B), α-TLR4 (C), or α-MyD88 (D). (E) Images of 3T3 cells infected with EPEC and expressing a FLAG-tagged TIRAP. Cells were stained with DAPI, FITC-phalloidin, and α-FLAG. In the merged images EPEC are pseudocolored blue, actin green, and TLRs, MyD88, or TIRAP red. (F) Images of MyD88$^{-/-}$ macrophages exposed to EPEC and stained with DAPI and FITC-phalloidin. Scale bars represent 5μm.

Figure 2: MyD88 signaling is necessary for survival and prevention of gangrenous mucosal necrosis following infection with *C. rodentium*. (A) Survival curves of 12-16 week-old MyD88$^{-/-}$ mice (n=12, grey squares) and their C57BL/6 controls (n=12, black diamonds) infected with 4 x 10^8 CFU of *C. rodentium*. MyD88$^{-/-}$ mice succumbed within 12 days, while age-matched controls survived. (B) Colons from MyD88$^{-/-}$ (upper) and C57BL/6 (lower) mice 7 days p.i. (C) H&E staining of colonic tissue from uninfected C57BL/6 mice. (D) H&E staining of colonic tissue from C57BL/6 mice seven days p.i. Colonic tissues exhibit pathology characterized by (1) loss of goblet cells, (2) edema, and (3) epithelial injury. (E) Crypt lengths of colonic tissue from uninfected C57BL/6 or MyD88$^{-/-}$ mice, or from infected C57BL/6 mice or MyD88$^{-/-}$ mice 3 or 7 days p.i. *, indicates statistical significance in comparison to MyD88$^{-/-}$ samples, $p<0.001$. The number of animals ranged from 5 to 12 for each bar. (F) H&E staining of uninfected colonic tissue from MyD88$^{-/-}$ mice. (G) H&E staining of MyD88$^{-/-}$ colonic tissue 7 days p.i. Colonic tissue exhibited gangrenous mucosal necrosis characterized by (1) visible

bacterial colonies (both with (inset 1') and without (inset 1'') neutrophil infiltration), (2) mucosal injury, (3) neutrophil infiltration (*), (4) edema, (5) apoptosis (^), (6) intramural bleeding, and (7) epithelial injury. Neutrophils, (*), can be more readily distinguished at higher magnification in the inset. Magnification for inset 3 × 800, inset 1' and 1'' × 1260, and all other histology × 400.

Figure 3: Examples of TUNEL assay scores criteria. (A) A sample receiving a score of zero, there is no intense green staining. (B) A sample receiving a score of one, there is some isolated intense green staining. (C) A sample receiving a score of two, there are several areas of intense green staining. (D) A sample receiving a score of three, most of the area has some intense green staining.

Figure 4: MyD88 signaling deficiency does not cause increased apoptosis in colonic tissue during a *C. rodentium* infection. TUNEL staining of uninfected colonic tissue from wild type mice (A) and MyD88$^{-/-}$ mice (B). TUNEL staining of colonic tissue 3 days p.i. from wild type (C) and MyD88$^{-/-}$ mice (D). TUNEL staining of colonic tissue 7 days p.i. from wild type (E) and MyD88$^{-/-}$ mice (F). Magnification × 400 for all images. (G) TUNEL scores were assessed in colonic tissue from uninfected wild type or MyD88$^{-/-}$ mice, or from infected wild type mice or MyD88$^{-/-}$ mice 3 and 7 days p.i. *, indicates statistical significance in comparison to uninfected samples, $p<0.001$.

Figure 5: MyD88$^{-/-}$ mice have higher levels of colonization of *C. rodentium*, which correlates with intramural colonic bleeding. (A) MyD88$^{-/-}$ colons were harvested 8-12 days p.i. and cut into four sections: cecum (n=10), proximal (n=10), medial (n=10), and distal (n=10). Bleeding was apparent in the distal section of each colon. Colonization was determined for each section as described in Methods. *, indicates statistical

significance in comparison with other colonic sections, $p<0.001$. Black bar indicates level of colonization in the distal colon of wild type mice 7 days p.i. (n=14). (B, C). Various tissues were harvested aseptically from MyD88$^{-/-}$ and wild type mice 3 days (B) or 7 days p.i. (C) *C. rodentium* CFU were counted as described in Methods. The number of mice ranged from 9-20 for each bar. *, indicates statistical significance in comparison to WT samples, $p<0.001$.

Figure 6: The antibody response in MyD88-/- mice is protective, but not optimal. (A) Survival curves of MyD88$^{-/-}$ mice (n=12, empty grey boxes), C57BL/6 mice (n=12, empty black diamonds), immunized MyD88$^{-/-}$ mice (n=11, filled grey circles), and immunized C57BL/6 mice (n=10, filled black diamonds). Immunized mice were infected with *C. rodentium*, and treated with antibiotics for four weeks, and then reinfected with a dose lethal to naïve MyD88$^{-/-}$ mice (4×10^8 CFU). The survival of immunized MyD88$^{-/-}$ mice is significantly higher than naïve MyD88$^{-/-}$ mice, $p<0.001$. (B) Colon supernatants from MyD88$^{-/-}$ (n=10) and C57BL/6 (n=10) were assessed for IL-6 levels via ELISA. The level of IL-6 is significantly higher in C57BL/6 mice than in MyD88$^{-/-}$ mice, $p < 0.01$. (C) Immunized MyD88$^{-/-}$ mice generate higher titers of antibodies to *C. rodentium* compared to C57BL/6 mice, likely reflecting the greater bacterial loads in these animals. (D) Survival curves of C57BL/6 (n=12, filled black diamonds), μMT mice (n=4, grey asterisks), μMT mice that received C57BL/6immune serum (n=3, empty grey triangles), and μMT mice that received MyD88$^{-/-}$ immune serum (n=5, empty grey circles). Note that serum from immunized C57BL/6 or MyD88$^{-/-}$ mice is partially protective.

Figure 7: MyD88 signaling is required on both hematopoietic and non-hematopoietic cells to prevent mortality and gangrenous mucosal necrosis. (A)

Survival curves of MyD88$^{-/-}$ mice (n=12, empty red boxes) their controls, WT (n=12, empty blue diamonds), WT→WT mice (n=9, filled blue diamonds), MyD88$^{-/-}$→MyD88$^{-/-}$ mice (n=5, filled red boxes), MyD88$^{-/-}$→WT mice (n=11, filled dark purple circles), and WT→MyD88$^{-/-}$ mice (n=9, filled light purple triangles). All mice were age matched and infected with 4 x 10^8 CFU of *C. rodentium*. (B) Colons from MyD88$^{-/-}$→WT mice (upper) and WT→WT mice (lower) nine days p.i. Note that bleeding was apparent in the medial section of colon from MyD88$^{-/-}$→WT mice. (C) H&E staining of uninfected MyD88$^{-/-}$→WT colonic tissue showed no evidence of pathology. Magnification x 400. (D,E) H&E staining of colonic tissue nine days p.i. In WT→WT mice (D), pathology of colonic tissue was characterized by (1) epithelial injury and (2) neutrophil infiltration. In MyD88$^{-/-}$→WT mice (E), colonic tissue exhibited pathology characterized by (1) mucosal injury, (2) visible bacterial colonies, (3) epithelial injury, (4) edema, and (5) neutrophil infiltration (*). Note that more severe pathology was evident in colonic tissue from MyD88$^{-/-}$→WT mice (E) than in tissue from WT→WT mice (D). Magnification × 400 (inset 2 × 1260, inset 5 × 800).

Figure 8: MyD88 signaling is required in both hematopoietic and non-hematopoietic to prevent bacteremia. (A) Crypt lengths of uninfected or infected colonic tissue from WT→MyD88$^{-/-}$ mice (days six to twelve p.i.; n=9, red bars with blue diagonal stripes) and MyD88$^{-/-}$→WT mice (days five to nine p.i.; n=6, blue bars with red diagonal stripes). *, indicates statistical significance in comparison to uninfected samples, $p<0.001$. **, indicates statistical significance between WT→MyD88$^{-/-}$ and MyD88$^{-/-}$→WT samples, $p<0.001$. (B-C) The level of colonization by *C. rodenitum* in organs was assessed. (B) Various organs were harvested from infected WT→WT mice (n=4, blue bars with blue

horizontal stripes) and MyD88$^{-/-}$→MyD88$^{-/-}$ mice (n=3, red bars with red horizontal stripes). Data shown with MyD88$^{-/-}$ (red bars) and WT (blue bars) mice is from Figure 3C. (C) Various organs were harvested from WT→MyD88$^{-/-}$ mice (n=6, red bars with blue diagonal stripes) and MyD88$^{-/-}$→WT mice (n=9, blue bars with red diagonal stripes). For comparison, colonization of WT→WT mice (blue bars with blue horizontal stripes), and MyD88$^{-/-}$→MyD88$^{-/-}$ (red bars with red horizontal stripes) are shown. CFU were counted as described in Methods.

Figure 9: Neutrophil recruitment to the colons of MyD88$^{-/-}$ mice is delayed, leading to increased bacterial colonization in the liver and spleen. (A) Neutrophil recruitment in colons was quantified by MPO assay for MyD88$^{-/-}$ (n=6-12) and wild type mice (n=7-12). *, indicates statistical significance in comparison to uninfected MyD88$^{-/-}$ samples, $p<0.01$. **, indicates statistical significance in comparison to uninfected C57BL/6 samples, $p<0.001$. (B) Manual neutrophil counts in crypts from wild type (n=6-7) and MyD88$^{-/-}$ (n=5-6) colons. *, indicates statistical significance in comparison to uninfected samples, $p<0.01$. (C) Neutrophils derived from MyD88$^{-/-}$ (n=4) and wild type (n=4) mice are able to respond the chemoattractant fNLP with equal efficacy. (D) *C. rodentium* (5 x 10^6) incubated with neutrophils (5 x 10^5) from wild type or MyD88$^{-/-}$ mice were killed with equal efficacy within 1 hour. (E) Colon supernatants from MyD88$^{-/-}$ (n=12) or wild type (n=12) mice 3 days p.i. were assessed for KC levels by ELISA. The difference between these groups was significant at $p<0.01$. (F) Treatment of wild type mice with α–GR1 antibodies rendered mice neutropenic. Significantly higher levels of *C. rodentium* colonization were evident in liver and spleen in α–GR-1-treated wild type

mice compared to PBS-treated wild type mice (n=9). Significance at the $p<0.01$ level is indicated by an *. Colonization data from MyD88$^{-/-}$ mice (grey bars) is from Figure 3C.

Figure 10: A model for showing the potential causes for the increased pathology seen in MyD88$^{-/-}$ mice. The increased intestinal pathology displayed by MyD88$^{-/-}$ mice infection with *C. rodentium* could be caused by many different phenotypes which appear to rely on MyD88 signaling including: (A) Cytokine and chemokine production following innate immune detection, leading to slower neutrophil recruitment. This delay could potentially lead to increased intestinal pathogen load, and thus, increased damage caused by *C. rodentium*. (B) Susceptibility to intestinal damage, which has previously been demonstrated to be increased in DSS administration to MyD88$^{-/-}$ animals (16, 17). (C) Repair response to damage, as measured by hyperplasia in colonic tissue. Crypt lengths do not increase in MyD88$^{-/-}$ colonic tissue, indicating that intestinal damage is not repaired potentially allowing it to accumulate. * Indicates steps where MyD88 signaling is important.

Figure 1

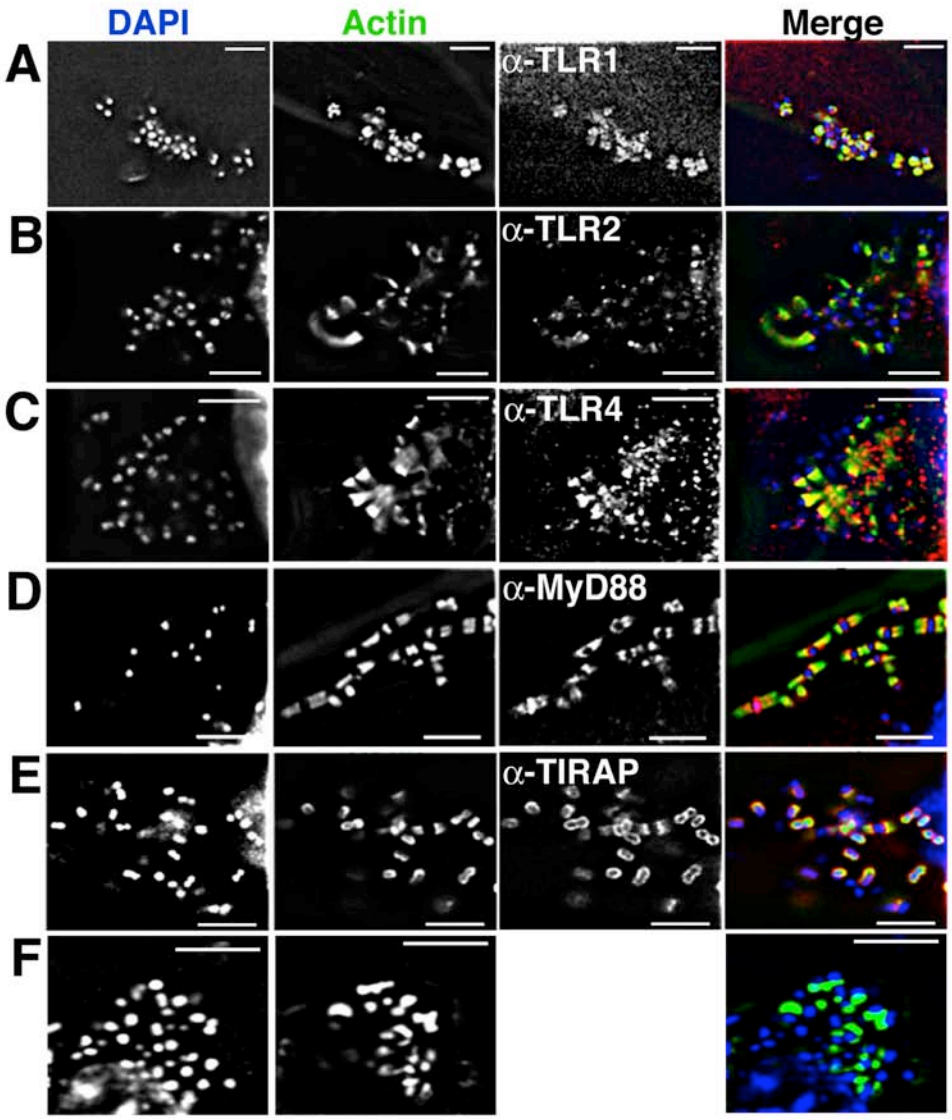

Figure 2

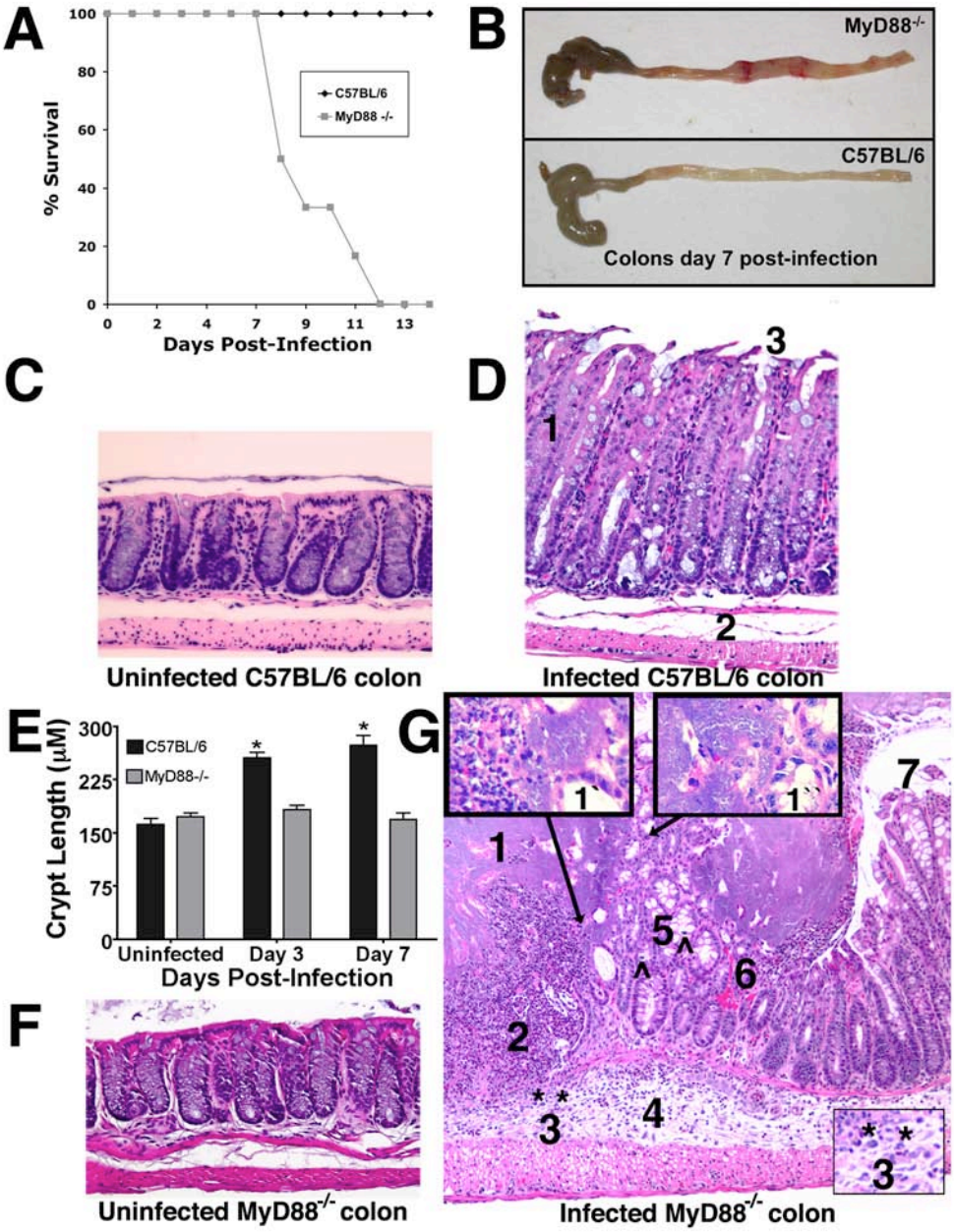
A
100
80
60
40
20
0
% Survival
C57BL/6
MyD88 -/-
0
2
4
7
9
11
13
Days Post-Infection
B
MyD88-/-
C57BL/6
Colons day 7 post-infection
C
Uninfected C57BL/6 colon
D
1
2
3
Infected C57BL/6 colon
E
300
225
150
75
0
Crypt Length (μM)
C57BL/6
MyD88-/-
*
*
Uninfected
Day 3
Day 7
Days Post-Infection
F
Uninfected MyD88-/- colon
G
1
1`
1``
2
3
4
5
6
7
Infected MyD88-/- colon

Figure 3

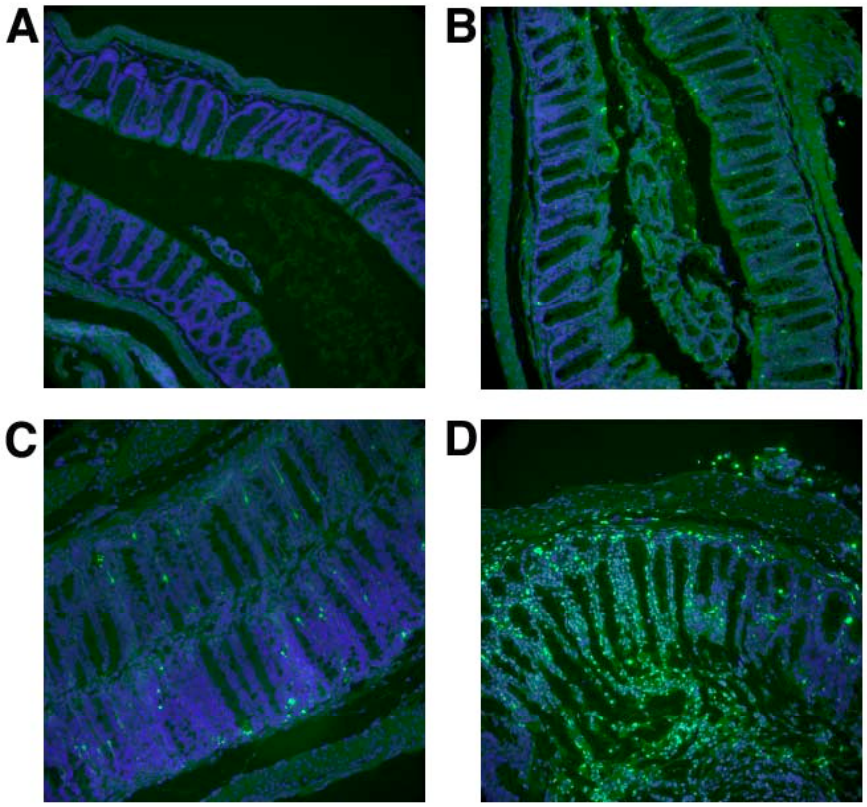

Figure 4

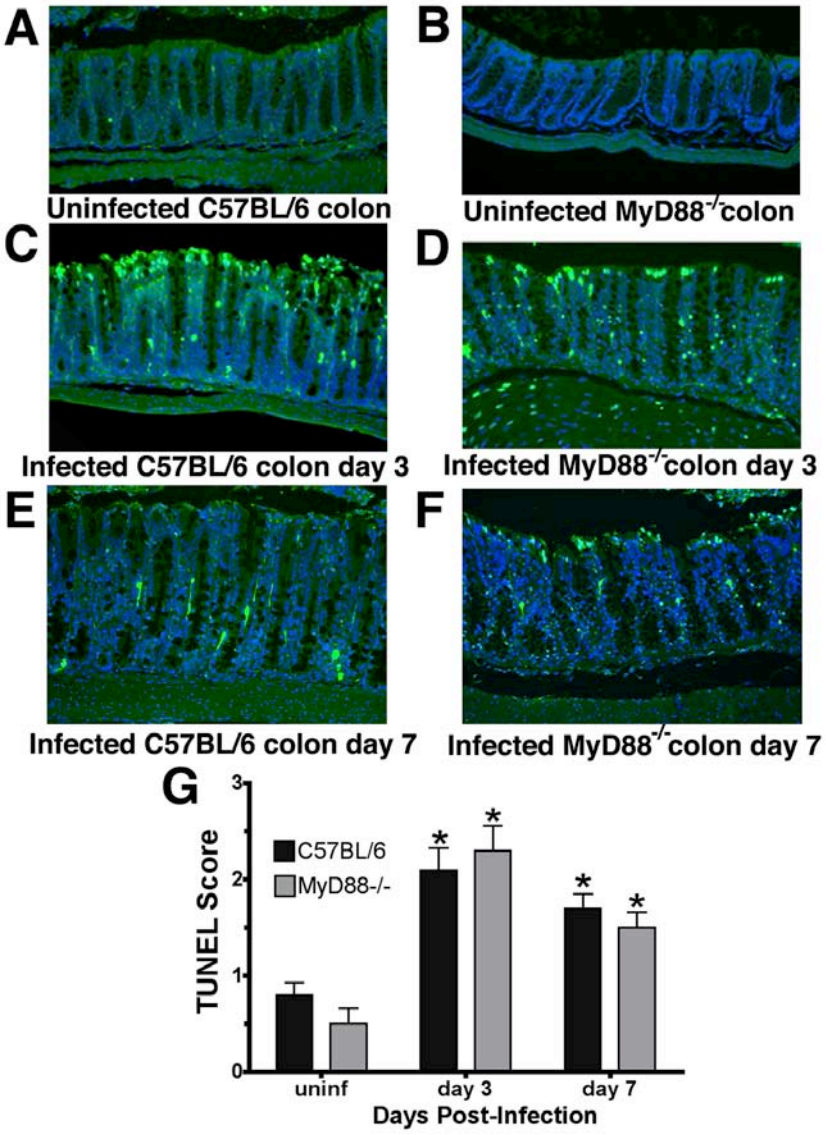
A
Uninfected C57BL/6 colon
B
Uninfected MyD88-/- colon
C
Infected C57BL/6 colon day 3
D
Infected MyD88-/- colon day 3
E
Infected C57BL/6 colon day 7
F
Infected MyD88-/- colon day 7
G
TUNEL Score
C57BL/6
MyD88-/-
0
1
2
3
uninf
day 3
day 7
Days Post-Infection

Figure 5

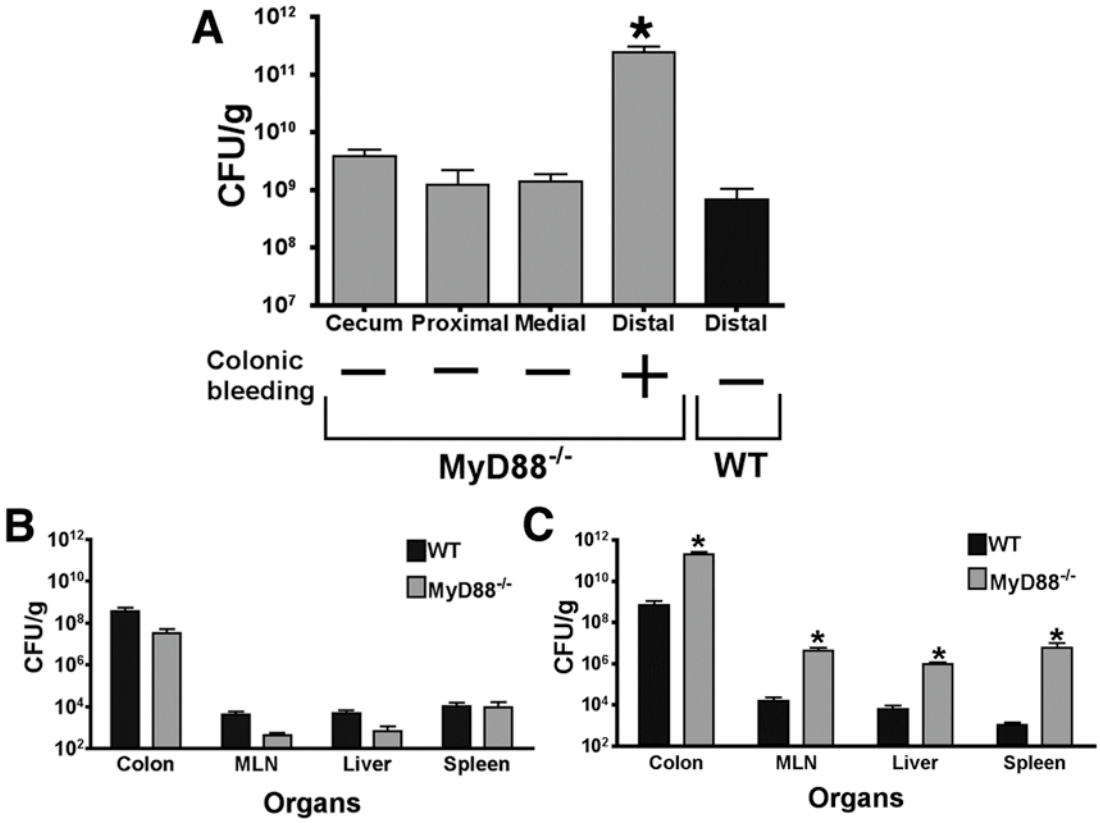
A
CFU/g
Cecum
Proximal
Medial
Distal
Distal
Colonic bleeding
MyD88-/-
WT
B
CFU/g
WT
MyD88-/-
Colon
MLN
Liver
Spleen
Organs
C
CFU/g
WT
MyD88-/-
Colon
MLN
Liver
Spleen
Organs

Figure 6

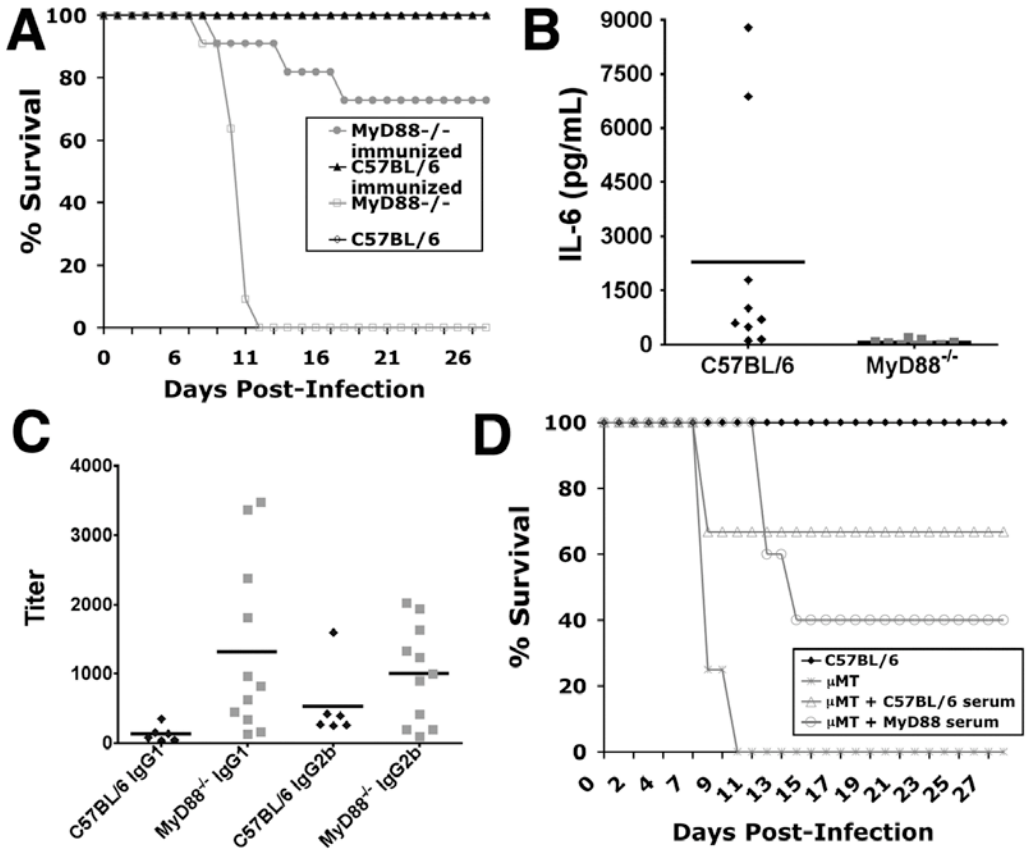
A
% Survival
Days Post-Infection
MyD88-/- immunized
C57BL/6 immunized
MyD88-/-
C57BL/6
B
IL-6 (pg/mL)
C57BL/6
MyD88-/-
C
Titer
C57BL/6 IgG1
MyD88-/- IgG1
C57BL/6 IgG2b
MyD88-/- IgG2b
D
% Survival
Days Post-Infection
C57BL/6
µMT
µMT + C57BL/6 serum
µMT + MyD88 serum

Figure 7

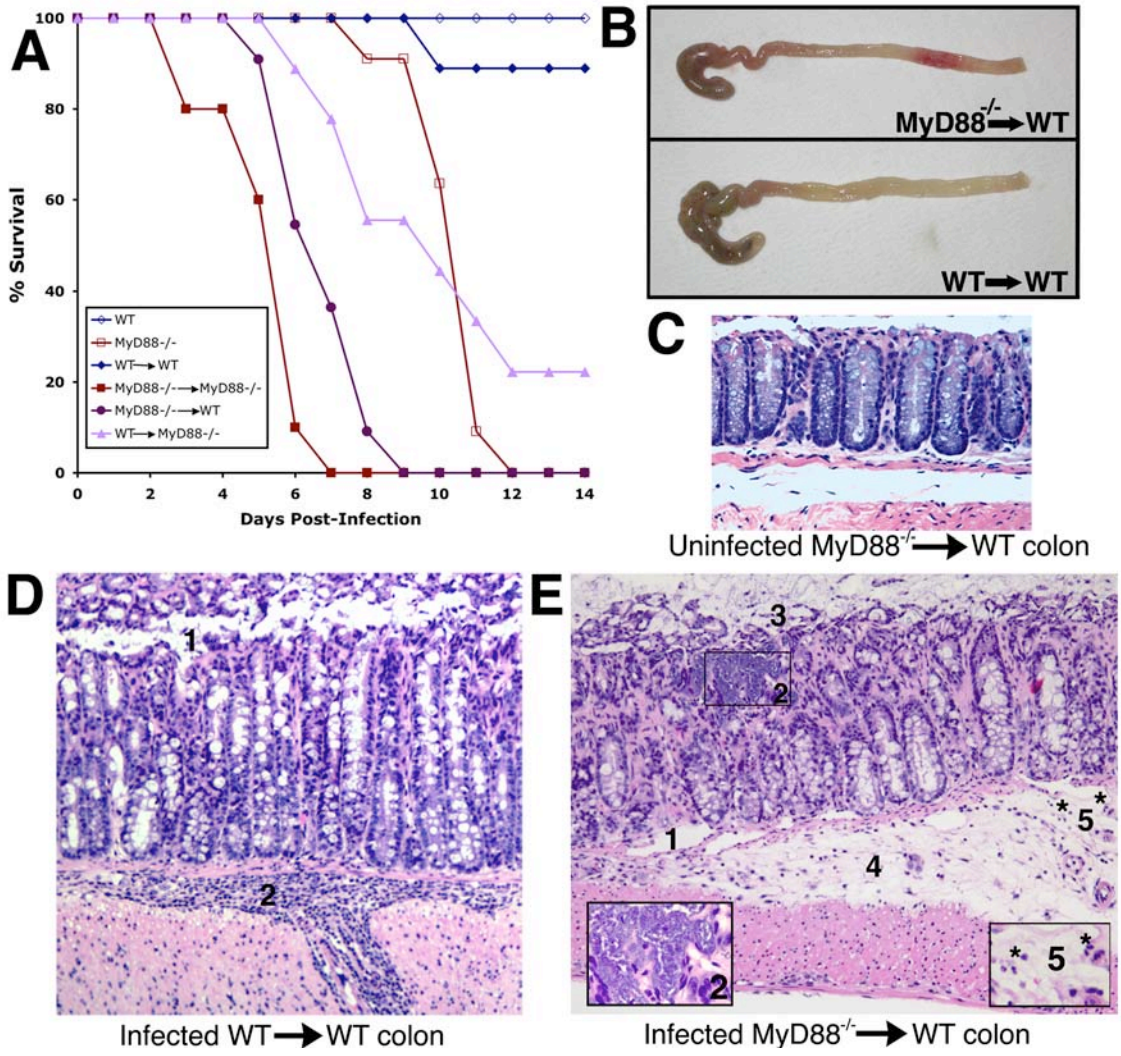
A
100
80
60
40
20
0
% Survival
0
2
4
6
8
10
12
14
Days Post-Infection
WT
MyD88-/-
WT→WT
MyD88-/-→MyD88-/-
MyD88-/-→WT
WT→MyD88-/-
B
MyD88-/-→WT
WT→WT
C
Uninfected MyD88-/-→WT colon
D
1
2
Infected WT→WT colon
E
3
2
1
4
5
5
2
Infected MyD88-/-→WT colon

Figure 8

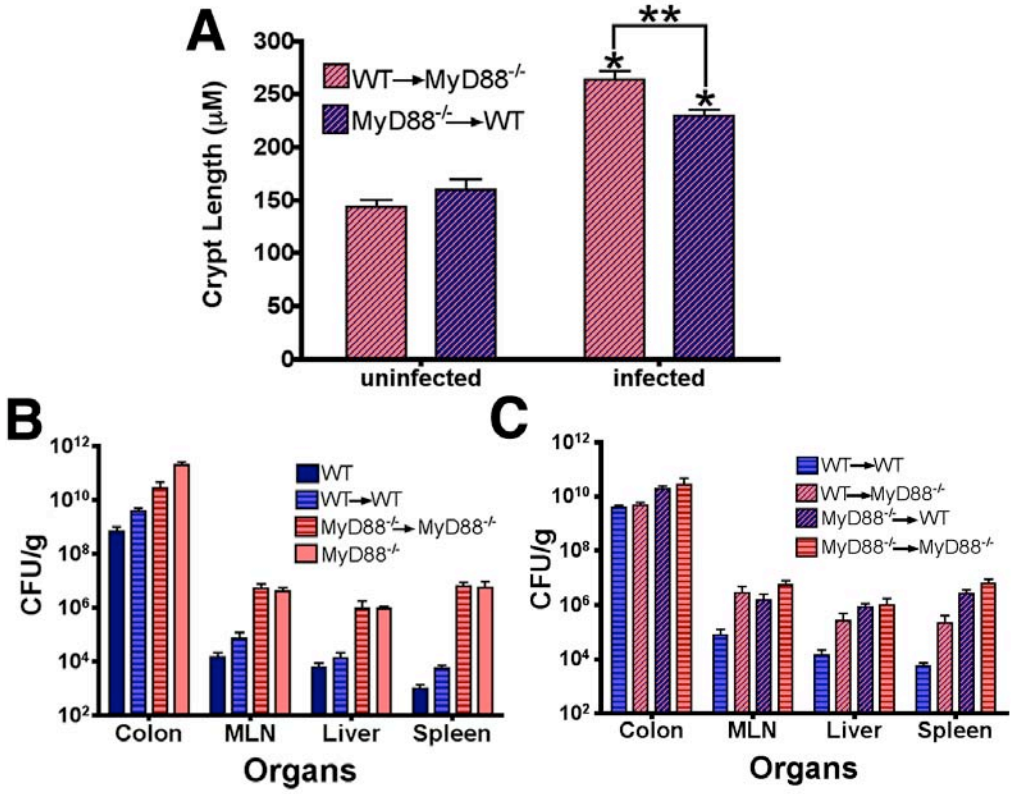
A
Crypt Length (μM)
300
250
200
150
100
50
0
WT→MyD88-/-
MyD88-/-→WT
**
*
*
uninfected
infected
B
CFU/g
10^12
10^10
10^8
10^6
10^4
10^2
WT
WT→WT
MyD88-/-→MyD88-/-
MyD88-/-
Colon
MLN
Liver
Spleen
Organs
C
CFU/g
WT→WT
WT→MyD88-/-
MyD88-/-→WT
MyD88-/-→MyD88-/-
Colon
MLN
Liver
Spleen
Organs

Figure 9

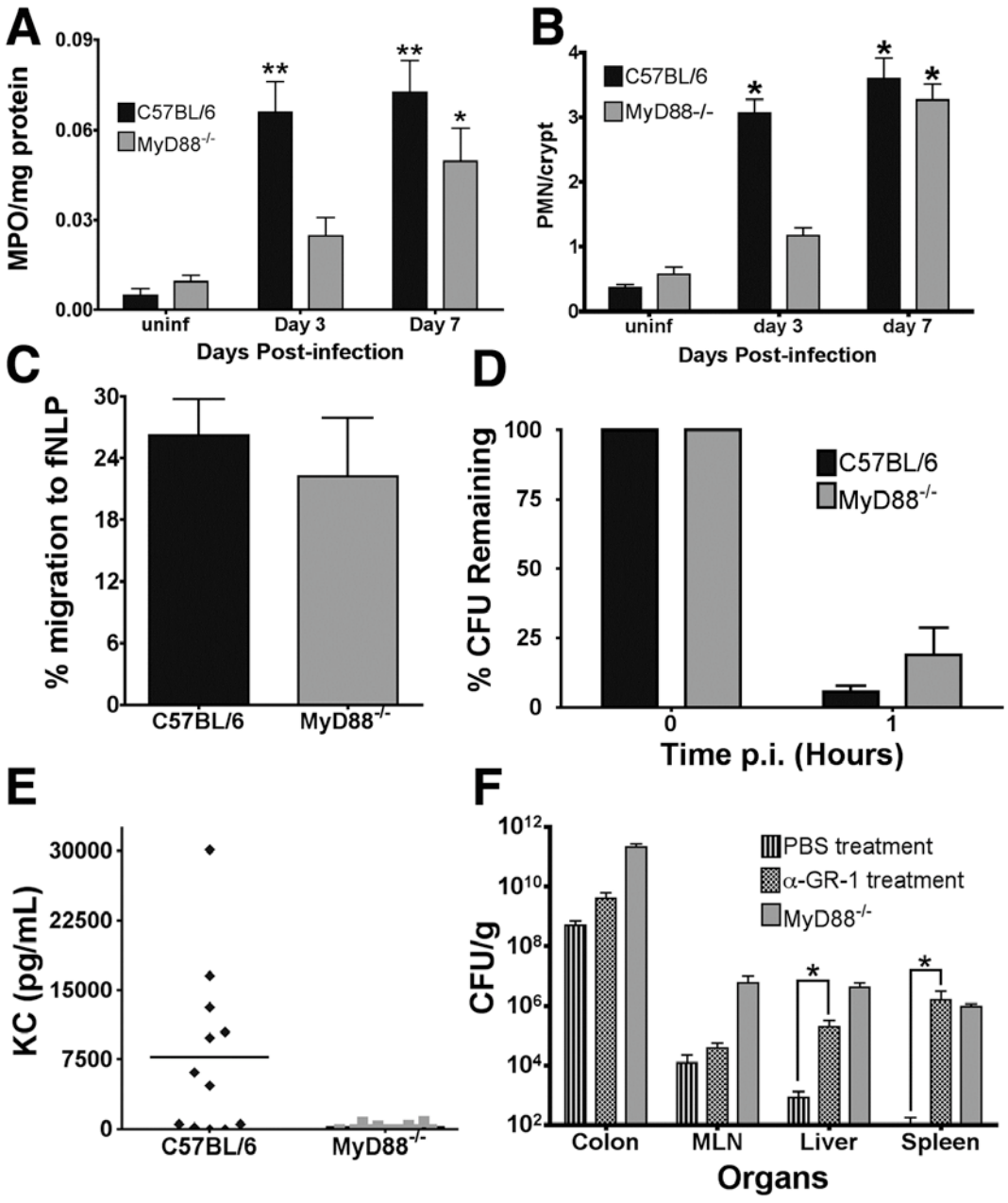
A
MPO/mg protein
0.09
0.06
0.03
0.00
C57BL/6
MyD88-/-
**
**
*
uninf
Day 3
Day 7
Days Post-infection
B
PMN/crypt
4
3
2
1
0
C57BL/6
MyD88-/-
*
*
*
uninf
day 3
day 7
Days Post-infection
C
% migration to fNLP
30
24
18
12
6
0
C57BL/6
MyD88-/-
D
% CFU Remaining
100
75
50
25
0
C57BL/6
MyD88-/-
0
1
Time p.i. (Hours)
E
KC (pg/mL)
30000
22500
15000
7500
0
C57BL/6
MyD88-/-
F
CFU/g
10^12
10^10
10^8
10^6
10^4
10^2
PBS treatment
α-GR-1 treatment
MyD88-/-
*
*
Colon
MLN
Liver
Spleen
Organs

Figure 10

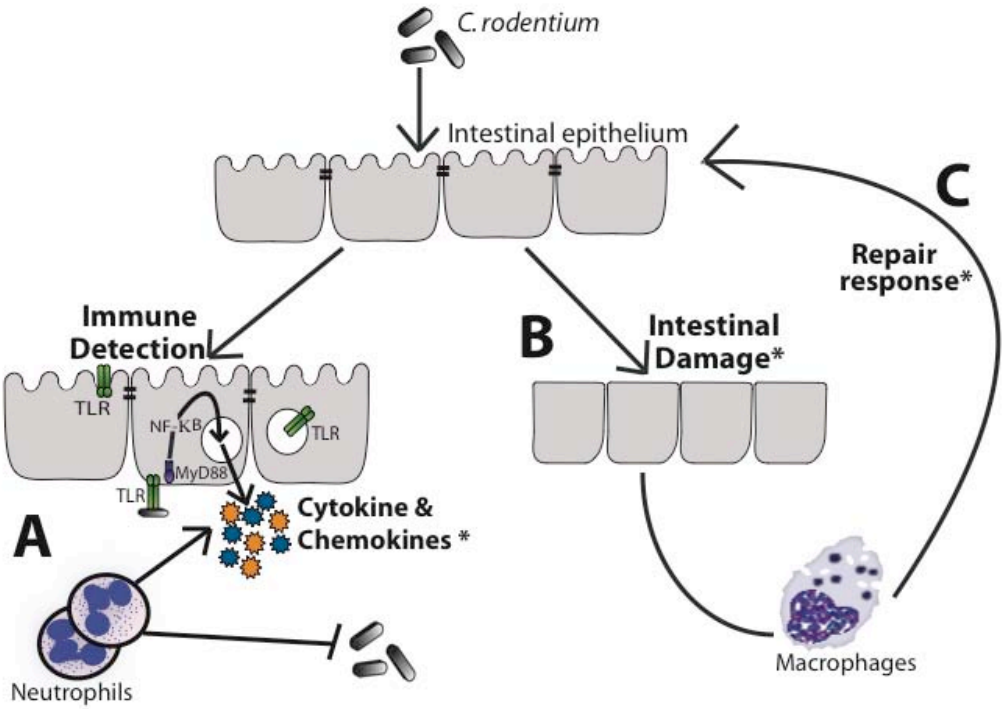
C. rodentium
Intestinal epithelium
C
Repair response*
Immune Detection
B
Intestinal Damage*
TLR
NF-KB
TLR
MyD88
TLR
Cytokine & Chemokines *
A
Neutrophils
Macrophages

CHAPTER III:

IL-1 receptor signaling protects mice from lethal intestinal damage caused by the attaching and effacing pathogen *Citrobacter rodentium*

All experiments were performed by Sarah Lebeis. The pathology and the TUNEL assay scoring was performed by Melanie Sherman.

Abstract:

Enteropathogenic *E. coli* (EPEC), enterohemorrhagic *E. coli* (EHEC), and *Citrobacter rodentium* are classified as attaching and effacing (A/E) pathogens based on their ability to adhere to intestinal epithelium via actin-filled membranous protrustions (pedestals). Infection of mice with *C. rodentium* causes breach of intestinal epithelial barrier, leading to colitis via a vigorous inflammatory response resulting in diarrhea, and a protective antibody response that ultimately clears the pathogen. Here we show that IL-1R signaling protects mice following infection of mice with *C. rodentium*. Upon infection, mice lacking the type I IL-1R (IL-1R$^{-/-}$ mice) exhibit increased mortality together with severe colitis characterized by intramural colonic bleeding and intestinal damage including gangrenous mucosal necrosis, phenotypes also evident in MyD88 deficient (MyD88$^{-/-}$) mice. However, unlike MyD88$^{-/-}$ mice, IL-1R$^{-/-}$ mice do not display increased pathogen loads, delays in recruitment of innate immune cells, such as neutrophils, or defects in the capacity to replace damaged enterocytes. Further, we demonstrate that IL-1R$^{-/-}$ mice have an increased predisposition to intestinal damage caused by *C. rodentium*, but not to that induced by chemical irritants, such as dextran sodium sulfate (DSS). Together, these data suggest that IL-1R signaling regulates susceptibility of the intestinal epithelia to damage caused by *C. rodentium*.

Introduction:

Pathogenic strains of *Escherichia coli,* including enteropathogenic *E. coli* (EPEC), are a significant public health risk especially in developing countries where they contaminate food and water supplies. Infection with EPEC causes infantile diarrhea (1), which leads to dehydration, contributing to as many as one million infant deaths per year (2). EPEC, EHEC, and the murine pathogen *Citrobacter rodentium* are classified as attaching and effacing (A/E) pathogens based on the ability of these extracellular bacteria to intimately attach to intestinal epithelium and flatten absorptive microvilli (effacement). Another hallmark feature of A/E pathogens is their ability to induce actin rearrangements that form membranous protrusions, called "pedestals," beneath the attached bacteria. Pedestal formation is associated with the development of A/E lesions, breach of the epithelial barrier, and disease (3, 4).

Upon infection, A/E pathogens displace the commensal flora and cause intestinal pathology, which includes damage characterized by cellular necrosis, disruption of the epithelium, and occasionally bleeding (5, 6). Damage induces a localized repair response characterized by hyperplasia (5), which reflects increased division of stem cells at the base of crypts to replace damaged enterocytes (7). As hyperplasia develops, goblet cells become less evident because they are not replenished as readily as enterocytes. Thus, apparent loss of goblet cells may be further evidence of repair. Additionally, infection with A/E pathogens induces recruitment of immune cells and causes edema within the lamina propria. Indeed, in addition to providing protection, immune cell types such as neutrophils may contribute to colitis and epithelial damage including formation of crypt abscesses (8). Nevertheless, an effective innate immune response allows proper

recruitment and activation of immune cell types necessary for a robust antibody response to both reduce severity of pathology upon infection (9) and to promote clearance of A/E pathogens (10).

Detection of pathogens by the innate immune system is accomplished by highly conserved families of receptors, such as Toll-like receptors (TLRs), and their respective downstream signaling cascades. Several lines of evidence suggest that signaling initiated by particular TLRs are important for protective responses to *C. rodentium*, whereas signaling by other TLRs appear unnecessary and perhaps even deleterious (11). TLRs recognize and respond to conserved structural motifs associated with microbes, which include proteins (e.g. flagellin), nucleic acids (e.g. unmethylated CpG DNA), and lipids (e.g. lipid A of lipopolysaccharide (LPS)) (12). LPS is abundant on the surface of *C. rodentium*, and is a known ligand for the TLR4 receptor complex. When LPS binds to its receptor, NF-κB becomes derepressed and, as a consequence, pro-inflammatory cytokines are expressed (13). Notably, infection of $TLR4^{-/-}$ mice with *C. rodentium* results in a slower, less severe inflammatory response and reduced mortality (11), suggesting that TLR4 signaling exacerbates disease. By contrast, TLR2 signaling appears to be required for protective responses to *C. rodentium*. Thus, following infection $TLR2^{-/-}$ mice suffer from colonic mucosal ulcerations, bleeding, increased apoptosis, and increased mortality (14). Together, these studies suggest that activation of TLRs by *C. rodentium* can cause both protective and deleterious consequences.

A variety of innate immune receptors including TLRs, the type I IL-1 receptor and IL-18 receptor utilize the signaling adaptor myeloid differentiation primary response gene 88 (MyD88) to activate NF-κB and produce an array of cytokines and chemokines

(12, 15). Following detection of *C. rodentium*, MyD88 signaling in epithelial and hematopoietic cells together provides protection from disseminating infection and mortality. Thus, MyD88 signaling facilitates epithelial repair responses, initiates recruitment of innate immune cells, limits bacterial load, and controls the amount on intestinal damage (6). We proposed that MyD88 signaling provides protection from *C. rodentium* by inducing timely recruitment of neutrophils, and thus stemming the growth of bacteria in the colon, which could exacerbate epithelial damage. MyD88 also regulates epithelial repair (16). Thus, by regulating both epithelial damage and repair, MyD88 signaling prevents bacteria from escaping the colon and reduces dissemination to peripheral organs (6). However, because MyD88 signaling contributes to several aspects of the innate immune response, it is difficult to discern whether particular phenotypes result from direct or indirect consequences of TLR signaling, or from other receptors that utilize MyD88. Such designations are important for understanding how TLRs or other receptors mediate a balanced response to a pathogen that is sufficient for containment and clearance, but limits damage due to inflammation.

Here we consider whether loss of signaling through receptors besides TLRs that also signal via MyD88 might contribute to some of phenotypes evident in MyD88$^{-/-}$ mice after *C. rodentium* infection. Using mice deficient in these signaling pathways, we reasoned that it might be possible to distinguish MyD88-dependent phenotypes that are directly controlled by TLRs or other receptors from those that are secondary consequences of MyD88-dependent signaling. We have focused in particular on IL-1 and IL-18, and their cognate receptors. IL-18 is expressed by macrophages, and was first identified as factor that induces interferon-γ (17, 18). IL-1β and the type I IL-1 receptor

(CD121a) have been implicated in protection and control against infections caused by *Staphylococcus aureus* (19). Further, IL-1β and IL-18 have both been shown to be protective against *Salmonella enterica* servovar *Typhimurium* (20) and *Shigella flexneri* (21) infections.

The type I IL-1 receptor (IL-1R) associates with an accessory protein (IL-1R-AcP) and is activated by IL-1α or IL-1β (22), molecules structurally related to IL-18. The type II IL-1 receptor is a decoy receptor, which does not lead to any cellular responses following ligand binding (22). Although IL-1α is constitutively expressed by epithelial cells, IL-1β and IL-18 precursors expression are induced by NF-κB in innate immune or epithelial cells, respectively (23, 24). Whereas IL-1α is produced in an active form, IL-1β and IL-18 are expressed as pro-peptides, and upon proteolytic cleavage, the mature forms are secreted and bind to their cognate receptors. Ligand-dependent activation of IL-1R and IL-18R in turn activates NF-κB in a MyD88-dependent fashion. This positive feedback circuit, in which IL-1β and IL-18 are both produced and signal in a MyD88-dependent fashion, has been hypothesized to amplify the NF-kB response leading to a localized inflammatory responses (23). Although IL-1β is reportedly not induced by *C. rodentium* by 6 days post-infection (p.i.) (25), this does not preclude the possibility that IL-1R signaling, perhaps activated by IL-1α or later expression of IL-1β, plays a role in infection.

Here we demonstrate that IL-1R signaling provides protection from increased mortality and pathology upon infection with *C. rodentium*, whereas IL-18 signaling does not appear to participate. Notably, mice lacking the type I IL-1R provide a means to separate the complex and interrelated phenotypes associated with inflammation. Thus, the

increased pathology evident in the absence of IL-1R signaling appears to result from an increased susceptibility to tissue damage by *C. rodentium*, and not from dysregulated immune or repair responses.

Materials and Methods:

Mouse strains and breeding: IL-1R$^{-/-}$, IL-18$^{-/-}$, and wild type control C57BL/6 mice were obtained from Jackson Laboratory (Bar Harbor, ME). Animals were kept in sterile housing and care was provided in accordance with protocols approved by the Institutional Animal Care and Use Committee of Emory University.

***In vivo* infections:** *C. rodentium* were prepared by overnight culturing (12 to 16 hours) at 37°C in Luria-Bertani broth (LB; Becton Dickinson, Franklin Lakes, NJ) without shaking to ensure that pili required for initial attachment were left intact. Cultures were harvested by centrifugation and resuspended in 20% sucrose. For infections of mice, drinking water was replaced with *C. rodentium* suspension overnight. Volume of suspension was measured before and after administration and the concentration of bacteria in the inoculum was calculated following retrospective plating. The average dosage was 1.5×10^8 CFU/mouse. Survival of infected mice and changes in body weight were monitored daily. Mice losing more than 15% of their original weight were euthanized. Clearance of *C. rodentium* was assessed by measuring the number of colonies in fecal samples.

Histology and Pathology scoring: For histology studies, colons were removed from uninfected or infected mice, fixed in 10% formalin, and embedded in paraffin. Sections (5μm) were cut and stained with hematoxylin and eosin (H&E) by the Histology Core Laboratory in the Department of Pathology at Emory University. The degree of intestinal pathology was assessed under the microscope by Melanie Sherman. The samples were coded and the observations made in a blind fashion to avoid bias in the evaluation process. Samples were scored for degree (0-3) of gangrenous mucosal necrosis (GMN), bleeding, raggedness of epithelium, hyperplasia, loss of goblet cells, edema, and

neutrophil infiltration, where a zero score represents no signs of the pathology measurement, a one score is mild pathology measurement, a two is moderate pathology measurement, and a three score is severe pathology measurement. Crypt heights were measured by micrometry using Zeiss 200M microscope, a 20× NA 1.4 lens and Slidebook software (Intelligent Imaging Innovations, Denver, CO). Well-oriented crypts were used for measurements. Two measurements were made on each image, and one image was taken per colon. The number of samples refers to the number of colons measured rather than the number of measurements.

ELISA analysis: Sandwich ELISA kits for cytokines were used according to the specifications of the manufacturer to measure levels of IL-6 (Becton Dickinson, Franklin Lakes, NJ) and KC (Biosource, Camarillo, CA) in colon supernatant, which was derived by culturing colons in DMEM with antibiotics for 48 hours before the supernatant was removed.

TUNEL assay staining and scoring: To assess the level of apoptosis in colonic tissue, sections were cut from the same paraffin blocks described above and stained using ApopTag Fluorescein In Situ Apoptosis Detection kit (S7110) (Millipore, Billerica, MA) according to the manufacturer's instructions. Briefly, the tissue was digested with terminal deoxynucleotidyl transferase (TdT) enzyme and stained with digoxigenin conjugated to fluorescein and 4, 6–diamindina-2-phenylindole. The intensity of fluorescein staining was assessed from digital images using a Nikon Eclipse 80i microscope, a 20× NA 0.75 objective and Spot software (Diagnostic Instruments, Sterling Height, MI). Longitudinal sections, which displayed the entire lengths of crypts, were used for measurements. Samples were coded and the observations made in a blind

fashion to avoid bias in the evaluation process. Samples were given a score of 0, 1, 2, or 3, where a zero score represents minimal TUNEL staining, a one score is a few apoptotic cells per field view, a two is one apoptotic cells per crypt, and a three score is multiple apoptotic cells per crypt. The number of apoptotic cells were counted in ten crypts, and the scoring scheme used was identical to that described by Gibson et al. (14).

Colony counts of *C. rodentium:* Tissue samples of colon, liver, spleen, or mesenteric lymph node (MLN) weighing ~0.1 to 0.3g were homogenized at low speed with a Tissuemizer (Fisher Scientific, Pittsburgh, PA) in 1mL of PBS. The lysate was plated on MacConkey agar plates at various dilutions, and *C. rodentium* colonies were recognized as pink with a white rim after 20 hours at 37ºC as previously described (26). Random colonies were confirmed as *C. rodentium* by PCR with Tir-specific primers (26).

Manual neutrophil counts: Crypts were observed in the slides stained with H&E as described above using a 63× NA 1.4 lens on a Zeiss 200M microscope. Neutrophils were identified by their distinctive nuclear morphology and counted in ten crypts per colon. The mean number of neutrophils per crypt was calculated for each colon observed. The number of samples (n) refers to the number of colons measured.

Neutrophil killing assays: *C. rodentium* bacteria were cultured overnight in LB broth. To isolate neutrophils, bone marrow from C57BL/6 or IL-1R$^{-/-}$ mice was removed, and red blood cells (RBCs) were lysed. As previously noted, 22-30% of cells were positive for GR-1 using this method (6). Bacteria (5×10^5) were added to 2.5×10^5 cells in 350mL of RPMI 1640 medium without antibiotics. After 1, 2, or 3 hours, the bacterium-cell culture was diluted 1:10 in water for 10 minutes to lyse neutrophils and serial

dilutions in PBS were plated of MacConkey agar to determine the number of bacterial colonies remaining. Assays were conducted in triplicate.

DSS administration: For DSS treatment, drinking water was replaced with 2% DSS dissolved in sterile distilled water for 7 days followed by 7 days of regular drinking water. Volume of suspension was measured before and after administration to ensure that mice in different cages drank the same amount of water. Survival of treatment mice and changes in body weight were monitored daily.

Statistical analysis: For mortality curves, a two-sided Fisher's exact test determined statistical significance of data. For all other experiments, level of statistical significance was determined by a Mann-Whitney rank-sum test. Results were considered significant if the p value was <0.02.

Results

IL-18 is not required to protect against infection with *C. rodentium.*

IL-18 acts via MyD88 to induce IFN-γ, which has previously been shown to participate in the immune response to *C. rodentium* (27). To determine whether IL-18 itself plays a role in the immune response to *C. rodentium*, we infected mice deficient in IL-18 (IL-$18^{-/-}$ mice). IL-$18^{-/-}$ mice survived infection with *C. rodentium* to nearly the same extent as wild type mice (Figure 1A). Pathology scores for IL-$18^{-/-}$ mice were only marginally higher than those for wild type mice, and were not statistically significant ($p>0.05$; Figure 1B). The main determinant of the change was a slight increase in neutrophil recruitment (Figure 1C). Notably, IL-$18^{-/-}$ mice also suffer from intermittent bleeding in the cecum by seven days p.i. (data not shown). In all other respects, including bacterial load (Figure 1D), the profile of IL-$18^{-/-}$ and wild type mice were nearly identical. Notably, increased immune cell infiltration, and in particular neutrophils, does not alone exacerbate damage or facilitate repair responses. Together, these data indicate that IL-18 plays a limited role in the response to *C. rodentium* infection.

IL-1R signaling protects mice following infection with *C. rodentium.*

To determine whether IL-1R signaling participates in the immune response to *C. rodentium*, we assessed morbidity and mortality in mice deficient in the type I IL-1 receptor (IL-$1R^{-/-}$ mice). Following infection, 78.8% of IL-$1R^{-/-}$ mice died between one and two weeks p.i. (Figure 2A). By contrast, the control strain, C57BL/6 mice, all survived (Figure 2A). Interestingly, the IL-$1R^{-/-}$ mice that survived the infection cleared the pathogen by 4 weeks p.i., a rate similar to that observed in wild type mice (data not shown). Therefore IL-1R signaling is required to protect mice from mortality.

IL-1R$^{-/-}$ mice suffer from increased colonic pathology.

The increased mortality seen in IL-1R$^{-/-}$ mice is associated with increased macroscopic and microscopic intestinal pathology. When colons were removed, it was revealed that most IL-1R$^{-/-}$ mice exhibited severe intramural colonic bleeding by seven days p.i. (Figure 2B), reminiscent of that seen in colons of MyD88$^{-/-}$ mice infected with *C. rodentium* (CHAPTER II)(6). This bleeding was not evident in colons of uninfected wild type or IL-1R$^{-/-}$ animals (data not shown) or in colons from infected wild type animals (Figure 2B). Further, at seven days p.i., the overall pathology score of colonic tissue from IL-1R$^{-/-}$ mice was significantly higher that that seen in wild type colonic tissue (Figure 2C). However, prior to that time point little pathology was evident in colonic tissue from either wild type or IL-1R$^{-/-}$ mice (Figure 2C). Together, these data suggest that the increased pathology following *C. rodentium* infection of IL-1R$^{-/-}$ mice may contribute to increased mortality.

IL-1R signaling contributes to IL-6 induction.

To determine whether additional immune defects might account for the increased pathology evident in IL-1R$^{-/-}$ mice, we next assessed levels of IL-6 in colonic tissue of infected animals. Notably, by three days p.i., the production of IL-6 increased over uninfected levels by two and a half fold in colon supernatants from wild type animals (Figure 2D). By contrast, no such increase was detectable in colonic tissue from infected IL-1R$^{-/-}$ mice (Figure 2D), indicating that IL-1R signaling was required to induce IL-6 in response to *C. rodentium*. This is very similar to production pattern to that seen in MyD88$^{-/-}$ mice in response to *C. rodentium* (6) and to the chemical irritant dextran sodium sulfate (DSS) (28). Notably, mice deficient in IL-6 are more likely suffer from

mucosal ulceration following infection with *C. rodentium* (29). Moreover, IL-6 has been identified as a factor important for protection from intestinal injury induced by chemical irritants such as DSS (28).

These data raised the possibility that the lowered induction of IL-6 in the absence IL-1R signaling might increase the susceptibility of the epithelium to damage by *C. rodentium*. To test this possibility, we next assessed the contribution to the overall pathology of specific determinants. The overall pathology score is comprised of 1) measurements of damage that include bleeding, epithelial barrier disruption or "raggedness," which includes loss of epithelial cells, and gangrenous mucosal necrosis (GMN); 2) measurements of repair response which include presence of hyperplasia and decreased evidence of goblet cells; and 3) measurements of immune cell recruitment including neutrophil infiltration and edema. Notably, infiltration of neutrophils into the crypts, and the accumulation of fluid and immune cells in the lamina propria (edema), comprises an inflammatory response or colitis. However, here we seek to define possible causes of damage as inflammatory or bacterial. As such we distinguish measures of damage (pathology category 1) from possible causes, which include changes in the repair response (pathology category 2), or immune cell infiltration (pathology category 3), or bacterial load. We next set out to more rigorously characterize elements within each of these categories so as to determine which contributed most to the overall pathology.

IL-1R$^{-/-}$ mice have increased levels of colonic damage.

To characterize the histological pathology associated with *C. rodentium* infection in IL-1R$^{-/-}$ mice, longitudinal sections of colonic tissue were stained with H&E and observed under the microscope for evidence of intestinal damage. Inspection revealed

that both IL-1R$^{-/-}$ and wild type mice suffer from microscopic bleeding between crypts and epithelial injury by seven days p.i. (compare Figures 3B and 3E). However, incidence of bleeding and the extent of damage to the epithelium (raggedness) were significantly higher in IL-1R$^{-/-}$ mice compared to their wild type counterparts ($p<0.001$ and $p<0.01$; Figure 3C). In addition, colonic tissue from IL-1R$^{-/-}$ mice also displayed pathology consistent with GMN, a pathological feature characterized by foci of mucosal necrosis associated with large colonies of bacteria (Figure 3E). GMN was not evident in colonic tissue from uninfected mice of either strain (Figure 3A and 3D), or in colons of wild type mice infected with *C. rodentium* (Figure 3B). Therefore, the increased morbidity and mortality evident in IL-1R$^{-/-}$ colonic tissue appears to be at least in part due to increased damage to the epithelium.

To determine if the increased damage in colonic tissue from IL-1R$^{-/-}$ mice was caused by an increase in apoptosis of epithelial cells, TdT dUTP nick end labeling (TUNEL) assays were performed. TUNEL staining revealed no difference in the staining of apoptotic cells in the colons of IL-1R$^{-/-}$ mice compared to those in wild type mice at any point during the infection (data not shown). Together, these data suggest that the increased damage in colonic tissue of infected IL-1R$^{-/-}$ mice results from necrosis rather than apoptosis.

Increased colonic pathology in IL-1R$^{-/-}$ mice is not caused by increased bacterial load or delayed neutrophil infiltration.

To determine if the increased damage in IL-1R$^{-/-}$ colonic tissue was caused by increased bacterial load, *C. rodentium* colonization was measured in several organs. As shown in Figure 4A, no differences in colonization were evident between the colons

taken from wild type or IL-1R$^{-/-}$ mice seven days p.i. (Figure 4A). By contrast, levels of bacteria were two to three logs higher in colons of MyD88$^{-/-}$ mice at this time (6). However, we did find significant increases (0.5 to 1 log) in colonization of the liver and the spleen seven days p.i. (Figure 4A). Together, these data suggest that increases in bacterial load in colon cannot account for increased colonic damage seen in IL-1R$^{-/-}$ mice.

Interestingly, increased load of *C. rodentium* in only livers and spleens has previously been associated with lack of neutrophils following depletion by treatment with a neutralizing α-GR1 antibody in wild type mice (6). When colonic tissue from IL-1R$^{-/-}$ mice or wild type mice was scored for neutrophil infiltration and edema, an increase in both parameters was evident in colons from IL-1R$^{-/-}$ mice ($p<0.01$ and $p<0.01$; Figure 4B). Because pathology scoring of neutrophil infiltration is a rather imprecise measure and subject to inaccuracy, we next quantitated the recruitment of neutrophils by performing manual counts of neutrophils per crypt (Figure 4C). These data suggest that there was no significant difference in neutrophil recruitment to the colon between IL-1R$^{-/-}$ and wild type animals at any point during the infection (Figure 4C). Further, we could find no difference in the capacity of neutrophils taken from IL-1R$^{-/-}$ and wild type animals to kill *C. rodentium in vitro* (Figure 4D), suggesting that the neutrophils from IL-1R$^{-/-}$ mice have no intrinsic defects. Together these data suggest that IL-1R signaling regulates susceptibility of the epithelia to damage upon infection with *C. rodentium* although damage cannot be attributed to increased bacterial load in the colon, or to the effects of neutrophil recruitment. However, the extensive damage to the colonic epithelia likely contributes to increased bacterial load in the spleens and livers of infected IL-1R$^{-/-}$ mice.

IL-1R$^{-/-}$ mice exhibit hyperplasia comparable to that seen in wild type mice.

To measure the capacity of IL-1R$^{-/-}$ mice to repair their increased colonic damage, degree of hyperplasia and goblet cell loss were measured. Hyperplasia occurs when stem cells present at the base of intestinal crypts differentiate into enterocytes, divide, and migrate along the crypts to the site of damage (7). Such hyperplasia, measured as an increase in crypt length, is also a hallmark feature of A/E pathogen infections (5, 30) and is indicative of restoration of damaged intestinal epithelium. In this process, stem cells are no longer available to differentiate into other cell types, such as goblet cells; thus, reduced evidence of goblet cells is an indirect measure of hyperplasia. When colonic tissue was scored for the presence of hyperplasia, we could detect no differences between the two strains of mice (Figure 5A). Likewise, the loss of goblet cells was determined to be higher in IL-1R$^{-/-}$ colonic tissue although it was only at the 10% significance level ($p>0.02$; data not shown). To directly quantify the extent of hyperplasia, crypt lengths were measured in colonic tissue from both strains of mice. We observed that crypts of both wild type and IL-1R$^{-/-}$ mice were nearly twice as long seven days p.i (Figure 5B). Moreover, we found no evidence for a proportional increase of crypt lengths in colonic tissue from IL-1R$^{-/-}$ despite the increased level of damage. Together, these data suggest that IL-1R signaling is not required for either sensing *C. rodentium* or for the development of hyperplasia initiated upon damage to the epithelia.

DSS causes an increased colitis in IL-1R$^{-/-}$ mice.

Our data suggest that IL-1R signaling increases susceptibility to damage following *C. rodentium* infection but without concomitant increases in bacterial load, reduction in enterocytes replacement capacity, or reduced neutrophil recruitment. We

hypothesized that hyperplasia and recruitment of immune cells would also be evident in colonic tissue from IL-1R$^{-/-}$ mice in response to chemical injury. Intestinal damage induced by DSS has been reported to induce a repair mechanism that replenishes epithelial cells and restores the integrity of the intestinal barrier in a TLR4 and MyD88-dependent manner (28, 31). Following oral administration of DSS, IL-1R$^{-/-}$ mice suffer from significantly increased levels of pathology after 14 days post-treatment (Figure 6A), though, as with wild type mice, pathology was not as severe as that induced upon infection with *C. rodentium* (Figure 4C). Pathology scores indicative of hyperplasia and infiltration were equal or higher in colonic tissue from IL-1R$^{-/-}$ mice compared to those in wild type animals (Figure 6B). Accordingly, following DSS treatment, crypt lengths in both strains significantly increased, indicating that aspects of a repair process were unperturbed in these two strains (Figure 6C). However, by 14 days post-treatment, the crypt lengths seen in IL-1R$^{-/-}$ colonic tissue were significantly longer than those seen in wild type mice ($p<0.001$) (Figure 6C), accounting for much of the increased overall pathology score (Figure 6B). Together, these data suggest that IL-1R does not mediate development of hyperplasia or infiltration of immune cells in response to damage induced by either pathogens or chemicals.

Discussion:

In the present study, we describe the protective role for the IL-1R signaling against infections caused by *C. rodentium*. By separating pathology scores into components, we have distinguished pathology caused by the bacteria from that caused by the host. Specifically, we demonstrate that IL-1R signaling controls susceptibility to damage by *C. rodentium* at a given bacterial load. As a consequence IL-1R signaling restricts the infection to the colon and controls dissemination of the bacteria to other organs.

Utilizing innate immune receptor knockout mice to assign cause of pathological phenotypes.

Following infection with *C. rodentium,* MyD88$^{-/-}$ mice exhibit a wide variety of phenotypes including mortality, delayed neutrophil recruitment, higher bacterial loads, and severe colonic pathology. It is problematic to assign these diverse phenotypes to specific causes for two reasons. First, MyD88 is used to mediate the signaling from many TLRs and other innate immune receptors activated by *C. rodentium* (15). Second, the phenotypes and the signaling pathways that regulate them may be interrelated and codependent. Thus, reduced neutrophil infiltration may result in higher bacterial loads. However, it may still be possible to assign pathologies to particular signaling pathways because phenotypes displayed in animals lacking a single TLR are more restricted than those seen in MyD88$^{-/-}$ animals. For example, like MyD88$^{-/-}$ mice, TLR2$^{-/-}$ animals display increased mortality and pathology, but do not have concomitant increases in pathogen load or delayed neutrophil infiltration. These data suggest that MyD88 signaling activated by TLR2 plays an important role in preventing pathology and

mortality. These data point to the utility of comparing pathology of animals deficient in particular innate immune signaling pathways with those deficient in signaling intermediaries that act pleiotropically, to define the molecular basis for complex phenotypes.

IL-1 but not IL-18 signaling mediates host protection against *C. rodentium* infection.

The advances presented here utilize mice deficient in signaling by various cytokines to distinguish the contributions of various pathologies to the overall disease. In contrast to disease in mice lacking MyD88 or TLR2, the disease in mice deficient in IL-18 was only marginally different from that observed in wild type mice. Although slightly increased pathology was evident in IL-$18^{-/-}$ mice (Figure 1B), it did not appear to negatively impact host defenses against *C. rodentium*, as these mice exhibit mortality comparable to that seen in the control strain (Figure 1A). The major determinant to the increased overall pathology score in IL-$18^{-/-}$ mice was neutrophil infiltration rather than damage characterized by bleeding, ragged epithelium, and GMN (Figure 1C). These data suggest that increased neutrophil infiltration in response to *C. rodentium* alone is not sufficient to cause increased epithelial damage, and is consistent with a protective role for this cell type.

IL-1 is a potent pro-inflammatory cytokine, and is found in elevated levels in individuals suffering from Inflammatory Bowel Disease (IBD) (32). Oral administration of the chemical irritant DSS in mice induces many of the symptoms of ulcerative colitis in mice (33). IL-1 appears to mediate development of DSS-induced colitis because administration of neutralizing IL-1β antibodies reduced colitis (34). Thus, it has been hypothesized that inhibitors of IL-1R signaling may be useful in treating IBD patients.

However, this cytokine also to plays a protective role in host defense against pathogens. For example, IL-1α enhances resistance to *Listeria monocytogenes* in mice (35). Further, a protective role for IL-1β has been demonstrated in response to infections by *S. aureus* (19), *S. typhimurium* (20) and *S. flexneri* (21). However, in all these studies, the molecular basis for the protective effect has not been established.

Here we demonstrate that IL-1R signaling is likewise a mediator of protection during an infection with *C. rodentium*. Unlike the phenotype seen in MyD88$^{-/-}$ mice, which is multi-faceted, IL-1R$^{-/-}$ mice display a more restricted pathology, which is confined to intestinal damage. Thus, the knockout mice allow us to assess how IL-1R signaling contributes to protection from such damage, and more importantly how damage alone without attendant effects on bacterial load, immune cell infiltration and hyperplasia development, contributes to disease. Previously, we demonstrated that GMN are present following *C. rodentium* infection of MyD88$^{-/-}$ mice (6). We hypothesized that this pathology was the result of several interdependent phenotypes, the most important of which appeared to be an increased pathogen load in the colon. However, here we demonstrate that, given equivalent degree of colonization in the colon (Figure 4A), IL-1R$^{-/-}$ mice exhibit GMN as well as other manifestations of damage (Figure 3). Thus, IL-1R$^{-/-}$ mice appear more susceptible to intestinal damage caused by *C. rodentium* than wild type mice. In this respect, the phenotype of IL-1R$^{-/-}$ mice infected with *C. rodentium* is very similar to that seen in TLR2$^{-/-}$ mice, which also suffer from lethal colitis without an attendant increase in pathogen load (14). However, unlike the intestinal damage seen in IL-1R$^{-/-}$ and MyD88$^{-/-}$ mice, the intestinal damage seen in TLR2$^{-/-}$ mice is associated with an increased level of epithelial apoptosis (14). Because both of these receptors appear to

be necessary during an infection with *C. rodentium*, and both require MyD88 as a signaling mediator, the severity of the MyD88$^{-/-}$ phenotype compared to either of the receptor knockout mice, suggests that protection from *C. rodentium* derives from the combination of signaling by multiple innate immune receptors.

Damage and neutrophil recruitment regulate the extent of pathogen dissemination.

The increased damage measurements evident in IL-1R$^{-/-}$ mice following *C. rodentium* infection was not recapitulated upon administration of DSS, indicating that IL-1R$^{-/-}$ mice are only more susceptible to *C. rodentium*-induced damage. Interestingly, the increased damage results from necrosis, but not apoptosis, because no increase in TUNEL staining was evident in colons of IL-1R$^{-/-}$ mice (data not shown). The difference between susceptibility to DSS and *C. rodentium* may in part be explained by the observation that DSS induces colitis by increasing the expression of pro-inflammatory cytokines, which in turn cause increased apoptosis and intestinal barrier disruption (36). Thus, IL-1R signaling appears to mediate protection from pathogen-induced necrosis, whereas other pro-inflammatory cytokines may mediate apoptosis. In support of this idea, increased necrosis in IL-1R$^{-/-}$ mice has also been demonstrated in a periodontal disease model (37). Notably, increased necrotic damage evident in IL-1R$^{-/-}$ mice compared to their wild type animals is associated with higher pathogen loads in the connective tissue in the periodontal model, and in liver and spleen in the *C. rodentium* model (Figure 4A). Moreover, bacterial dissemination occurred in both models without concomitant differences from wild type mice in neutrophil infiltration (37) (Figure 4A and 4B,C). Thus, necrotic damage rather than a lack of neutrophil infiltration appears to contribute to increased dissemination in IL-1R$^{-/-}$ mice, perhaps by creating routes of entry that allow

bacteria to penetrate into the lamina propria. However, our previous data with wild type mice depleted of neutrophils suggest that this cell type nevertheless plays a crucial role in limiting pathogen dissemination (6). The resolution to this apparent paradox is that increased intestinal damage and decreased neutrophil infiltration may contribute to dissemination together. Thus, the bacterial load in livers and spleens in MyD88$^{-/-}$ mice, which have both increased colonic damage and decreased neutrophil infiltration, is 2-4 logs higher than wild type mice (6). By contrast, increases of only a log or less are evident in livers and spleens of IL-1R$^{-/-}$ mice, which have increased damage but intact neutrophil infiltration (Figure 4A).

A defect in epithelial repair is another hypothesized factor contributing to GMN and therefore dissemination. However, GMN is observed although there is evidence of damage enterocyte replacement, suggesting that lack of repair does not contribute to GMN formation (Figures 2B and 5B). Notably, IL-1R$^{-/-}$ mice exhibit hyperplasia equivalent to those seen in colons of wild type animals, despite increased damage. These data suggest that development of hyperplasia may already be at a maximal level, and increases may be limited by such factors as the rate at which stem cells differentiate and migrate to replenish damaged enterocytes.

IL-1R signaling and protection from pathogen-induced damage.

Previous reports indicate that *C. rodentium*, unlike many other pathogens, does not induce production of IL-1β by six days p.i. (25). These data, together with our results suggest that IL-1R signaling may instead be mediated by IL-1α. IL-1α is constitutively produced by epithelial cells (38), and reportedly enhances antibacterial activities of the innate immune system against *Listeria monocytogenes* (35). Further, LPS, which is

present on the surface of *C. rodentium*, induces IL-1α expression in a MyD88-dependent manner *in vitro* (39). *In vivo* studies will be required to determine whether MyD88 signaling induces IL-1α in the intestinal epithelia upon infection with *C. rodentium*. Previous work also suggests that activation of MyD88 results in increased production of cytokines, such as IL-6 (12). IL-6 leads to increased protective acute phase responses elicited following tissue damage or infection (40). Our data suggests that IL-1R$^{-/-}$ mice fail to induce IL-6 production above uninfected levels, whereas wild type mice exhibit a 2.5 fold increase upon infection with *C. rodentium* (Figure 2D). Moreover, IL-6 appears to play a critical role in protecting mice from mucosal ulceration during an infection with *C. rodentium* (29). However, unlike the IL-1R$^{-/-}$ mice, most of the IL-6$^{-/-}$ mice survive the infection (29), so IL-6 alone cannot completely account for the increased susceptibility to *C. rodentium*-induced damage in IL-1R$^{-/-}$ mice.

IL-1R signaling in chemical and pathogen-induced colitis.

While it has been previously demonstrated that MyD88 mediates protection against both *C. rodentium* and DSS induced intestinal damage (6, 25, 28), our data suggest that lack of IL-1R signaling only increases the susceptibility to intestinal damage induced by *C. rodentium*. These data may have important therapeutic implications. Previous results suggest that DSS induces colitis in mice that closely resembles that seen in human patients with IBD (33). Based on evidence showing that IL-1R signaling induces pro-inflammatory cytokines, it has been suggested that therapeutics directed against IL-1R signaling might prove beneficial in IBD patients (34). However, our data indicate that such therapeutics may cause increased susceptibility to pathogenic strains of *E. coli*, which have been isolated from patients with IBD (41). Further, our data suggest

that key features of DSS-induced colitis including neutrophil infiltration, which contributes to inflammation, and hyperplasia, which contributes to tumor progression, are unperturbed in the absence of IL-1R signaling. Together these data suggest that therapeutics directed against IL-1R signaling may not be optimal for inhibiting IBD symptoms, and indeed may even prove detrimental.

Literature Cited:

1. Frankel, G., A. D. Phillips, I. Rosenshine, et al.: Enteropathogenic and enterohaemorrhagic Escherichia coli: more subversive elements. *Mol Microbiol*. 30(5), 911-921(1998).
2. Mead, P. S., L. Slutsker, V. Dietz, et al.: Food-related illness and death in the United States. *Emerg Infect Dis*. 5(5), 607-625(1999).
3. McDaniel, T. K., and J. B. Kaper: A cloned pathogenicity island from enteropathogenic Escherichia coli confers the attaching and effacing phenotype on E. coli K-12. *Mol Microbiol*. 23(2), 399-407(1997).
4. Mundy, R., T. T. MacDonald, G. Dougan, G. Frankel, and S. Wiles: Citrobacter rodentium of mice and man. *Cell Microbiol*. 7(12), 1697-1706(2005).
5. Luperchio, S. A., and D. B. Schauer: Molecular pathogenesis of Citrobacter rodentium and transmissible murine colonic hyperplasia. *Microbes Infect*. 3(4), 333-340(2001).
6. Lebeis, S. L., B. Bommarius, C. A. Parkos, M. A. Sherman, and D. Kalman: TLR signaling mediated by MyD88 is required for a protective innate immune response by neutrophils to Citrobacter rodentium. *J Immunol*. 179(1), 566-577(2007).
7. Radtke, F., and H. Clevers: Self-renewal and cancer of the gut: two sides of a coin. *Science*. 307(5717), 1904-1909(2005).
8. Higgins, L. M., G. Frankel, G. Douce, G. Dougan, and T. T. MacDonald: Citrobacter rodentium infection in mice elicits a mucosal Th1 cytokine response and lesions similar to those in murine inflammatory bowel disease. *Infect Immun*. 67(6), 3031-3039.(1999).
9. Donnenberg, M. S., C. O. Tacket, G. Losonsky, et al.: Effect of prior experimental human enteropathogenic Escherichia coli infection on illness following homologous and heterologous rechallenge. *Infect Immun*. 66(1), 52-58(1998).
10. Maaser, C., M. P. Housley, M. Iimura, et al.: Clearance of Citrobacter rodentium requires B cells but not secretory immunoglobulin A (IgA) or IgM antibodies. *Infect Immun*. 72(6), 3315-3324(2004).
11. Khan, M. A., C. Ma, L. A. Knodler, et al.: Toll-like receptor 4 contributes to colitis development but not to host defense during Citrobacter rodentium infection in mice. *Infect Immun*. 74(5), 2522-2536(2006).
12. Kaisho, T., and S. Akira: Pleiotropic function of Toll-like receptors. *Microbes Infect*. 6(15), 1388-1394(2004).
13. Fitzgerald, K. A., D. C. Rowe, and D. T. Golenbock: Endotoxin recognition and signal transduction by the TLR4/MD2-complex. *Microbes Infect*. 6(15), 1361-1367(2004).
14. Gibson, D. L., C. Ma, C. M. Rosenberger, et al.: Toll-like receptor 2 plays a critical role in maintaining mucosal integrity during Citrobacter rodentium-induced colitis. *Cell Microbiol*. 10(2), 388-403(2008).
15. Adachi, O., T. Kawai, K. Takeda, et al.: Targeted disruption of the MyD88 gene results in loss of IL-1- and IL-18-mediated function. *Immunity*. 9(1), 143-150(1998).

16. Pull, S. L., J. M. Doherty, J. C. Mills, J. I. Gordon, and T. S. Stappenbeck: Activated macrophages are an adaptive element of the colonic epithelial progenitor niche necessary for regenerative responses to injury. *Proc Natl Acad Sci U S A*. 102(1), 99-104(2005).
17. Okamura, H., H. Tsutsui, S. Kashiwamura, T. Yoshimoto, and K. Nakanishi: Interleukin-18: a novel cytokine that augments both innate and acquired immunity. *Adv Immunol*. 70(281-312(1998).
18. Okamura, H., K. Nagata, T. Komatsu, et al.: A novel costimulatory factor for gamma interferon induction found in the livers of mice causes endotoxic shock. *Infect Immun*. 63(10), 3966-3972(1995).
19. Miller, L. S., E. M. Pietras, L. H. Uricchio, et al.: Inflammasome-mediated production of IL-1beta is required for neutrophil recruitment against Staphylococcus aureus in vivo. *J Immunol*. 179(10), 6933-6942(2007).
20. Raupach, B., S. K. Peuschel, D. M. Monack, and A. Zychlinsky: Caspase-1-mediated activation of interleukin-1beta (IL-1beta) and IL-18 contributes to innate immune defenses against Salmonella enterica serovar Typhimurium infection. *Infect Immun*. 74(8), 4922-4926(2006).
21. Sansonetti, P. J., A. Phalipon, J. Arondel, et al.: Caspase-1 activation of IL-1beta and IL-18 are essential for Shigella flexneri-induced inflammation. *Immunity*. 12(5), 581-590(2000).
22. Dinarello, C. A.: Biologic basis for interleukin-1 in disease. *Blood*. 87(6), 2095-2147(1996).
23. Barnes, P. J., and M. Karin: Nuclear factor-kappaB: a pivotal transcription factor in chronic inflammatory diseases. *N Engl J Med*. 336(15), 1066-1071(1997).
24. Grandjean-Laquerriere, A., F. Antonicelli, S. C. Gangloff, M. Guenounou, and R. Le Naour: UVB-induced IL-18 production in human keratinocyte cell line NCTC 2544 through NF-kappaB activation. *Cytokine*. 37(1), 76-83(2007).
25. Gibson, D. L., C. Ma, K. S. Bergstrom, et al.: MyD88 signalling plays a critical role in host defence by controlling pathogen burden and promoting epithelial cell homeostasis during Citrobacter rodentium-induced colitis. *Cell Microbiol*. 10(3), 618-631(2008).
26. Wei, O. L., A. Hilliard, D. Kalman, and M. Sherman: Mast cells limit systemic bacterial dissemination but not colitis in response to Citrobacter rodentium. *Infect Immun*. 73(4), 1978-1985(2005).
27. Simmons, C. P., N. S. Goncalves, M. Ghaem-Maghami, et al.: Impaired resistance and enhanced pathology during infection with a noninvasive, attaching-effacing enteric bacterial pathogen, Citrobacter rodentium, in mice lacking IL-12 or IFN-gamma. *J Immunol*. 168(4), 1804-1812.(2002).
28. Rakoff-Nahoum, S., J. Paglino, F. Eslami-Varzaneh, S. Edberg, and R. Medzhitov: Recognition of commensal microflora by toll-like receptors is required for intestinal homeostasis. *Cell*. 118(2), 229-241(2004).
29. Dann, S. M., M. E. Spehlmann, D. C. Hammond, et al.: IL-6-dependent mucosal protection prevents establishment of a microbial niche for attaching/effacing lesion-forming enteric bacterial pathogens. *J Immunol*. 180(10), 6816-6826(2008).

30. Borenshtein, D., M. E. McBee, and D. B. Schauer: Utility of the Citrobacter rodentium infection model in laboratory mice. *Curr Opin Gastroenterol*. 24(1), 32-37(2008).
31. Fukata, M., K. S. Michelsen, R. Eri, et al.: Toll-like receptor-4 is required for intestinal response to epithelial injury and limiting bacterial translocation in a murine model of acute colitis. *Am J Physiol Gastrointest Liver Physiol*. 288(5), G1055-1065(2005).
32. Dinarello, C. A.: Inflammatory cytokines: interleukin-1 and tumor necrosis factor as effector molecules in autoimmune diseases. *Curr Opin Immunol*. 3(6), 941-948(1991).
33. Okayasu, I., S. Hatakeyama, M. Yamada, et al.: A novel method in the induction of reliable experimental acute and chronic ulcerative colitis in mice. *Gastroenterology*. 98(3), 694-702(1990).
34. Arai, Y., H. Takanashi, H. Kitagawa, and I. Okayasu: Involvement of interleukin-1 in the development of ulcerative colitis induced by dextran sulfate sodium in mice. *Cytokine*. 10(11), 890-896(1998).
35. Czuprynski, C. J., and J. F. Brown: Recombinant murine interleukin-1 alpha enhancement of nonspecific antibacterial resistance. *Infect Immun*. 55(9), 2061-2065(1987).
36. Edelblum, K. L., M. K. Washington, T. Koyama, et al.: Raf Protects Against Colitis by Promoting Mouse Colon Epithelial Cell Survival Through NF-kappaB. *Gastroenterology*2008).
37. Chen, C. P., M. Hertzberg, Y. Jiang, and D. T. Graves: Interleukin-1 and tumor necrosis factor receptor signaling is not required for bacteria-induced osteoclastogenesis and bone loss but is essential for protecting the host from a mixed anaerobic infection. *Am J Pathol*. 155(6), 2145-2152(1999).
38. Murphy, J. E., C. Robert, and T. S. Kupper: Interleukin-1 and cutaneous inflammation: a crucial link between innate and acquired immunity. *J Invest Dermatol*. 114(3), 602-608(2000).
39. Hawn, T. R., A. Ozinsky, D. M. Underhill, et al.: Leishmania major activates IL-1 alpha expression in macrophages through a MyD88-dependent pathway. *Microbes Infect*. 4(8), 763-771(2002).
40. Kopf, M., H. Baumann, G. Freer, et al.: Impaired immune and acute-phase responses in interleukin-6-deficient mice. *Nature*. 368(6469), 339-342(1994).
41. Sasaki, M., S. V. Sitaraman, B. A. Babbin, et al.: Invasive Escherichia coli are a feature of Crohn's disease. *Lab Invest*. 87(10), 1042-1054(2007).

Figure Legends:

Figure 1: IL-18 signaling does not play a critical role in host defense against *C. rodentium*. (A) Survival curves of 6-10 week old IL-$18^{-/-}$ mice (n=6, grey circles) and their C57BL/6 controls (n=12, black diamonds) infected with 1.5 x10^8 CFU of *C. rodentium*. (B) Pathology scores were assessed in colonic tissue from uninfected C57BL/6 or IL-$18^{-/-}$ mice, or from infected C57BL/6 or IL-$18^{-/-}$ mice 3 or 7 days p.i. The number of mice for each group ranged from 8-12 for C57BL/6 and 5-7 for IL-$18^{-/-}$. (C) Pathology scores for 7 days p.i. are shown in each category assessed including bleeding, ragged epithelium, gangrenous mucosal necrosis (GMN), hyperplasia, goblet cell loss, edema, and neutrophil infiltration for C57BL/6 (n=12) and IL-$18^{-/-}$ (n=7) mice. (D) Various tissues were harvested aseptically from C57BL/6 (n=12) and IL-$18^{-/-}$ (n=7) 7 days p.i. *C. rodentium* CFU were quantitated as described in *Material and Methods*.

Figure 2: IL-1R signaling is required to protect mice from increased mortality and pathology. (A) Survival curves of 6-10 week old IL-$1R^{-/-}$ (n=9, grey circles) and their C57BL/6 controls (n=12, black diamonds) infected with 1.5 x10^8 CFU of *C. rodentium*. (B) Colons from IL-$1R^{-/-}$ (upper) and C57BL/6 (lower) mice 7 days p.i. (C) Pathology scores were assessed in colonic tissue from uninfected C57BL/6 or IL-$1R^{-/-}$ mice, or from infected C57BL/6 or IL-$1R^{-/-}$ mice 3 or 7 days p.i. The number of mice ranged from 8-12 for C57BL/6 and 8-13 IL-$1R^{-/-}$ for each group. *, indicates statistical significance in comparison to uninfected C57BL/6 samples, $p<0.01$.; **, indicates statistical significance in comparison to uninfected IL-$1R^{-/-}$ samples, $p<0.001$; # indicates statistical significance between C57BL/6 and IL-$1R^{-/-}$ samples, $p<0.001$). (D) Colon supernatants from uninfected C57BL/6 mice (n=9), C57BL/6 mice 3 days p.i. (n=9) and C57BL/6 mice 7

days p.i. (n=12) were assessed for IL-6 levels by ELISA. Colon supernatants from uninfected IL-1R$^{-/-}$ mice (n=8), IL-1R$^{-/-}$ mice 3 days p.i. (n=7) and IL-1R$^{-/-}$ mice 7 days p.i. (n=15) were assessed also for IL-6 levels by ELISA. The difference between these groups 3 days p.i. was significant at $p<0.02$.

Figure 3: Increased intestinal damage is a major determinant of the pathology seen in IL-1R$^{-/-}$ colonic tissue. (A) H&E staining of colonic tissue from uninfected C57BL/6 mice. (B) H&E staining of colonic tissue from C57BL/6 7 days p.i. (C) Pathology scores of the damage measurements including bleeding, ragged epithelium, and GMN were assessed in colonic tissue from C57BL/6 (n=12) or IL-1R$^{-/-}$ (n=13) mice 7 days p.i. (*, indicates statistical significance in comparison to C57BL/6 samples, $p<0.001$.; **, indicates statistical significance in comparison to C57BL/6 samples, $p<0.01$.). (D) H&E staining of uninfected colonic tissue from IL-1R$^{-/-}$ mice. (E) H&E staining of IL-1R$^{-/-}$ colonic tissue 7 days p.i. (F) Pathology scores were assessed in colonic tissue from IL-1R$^{-/-}$ mice at various time points during an infection with *C. rodentium* including uninfected (n=11), 3 days p.i. (n=8), 7 days p.i. (n=13), and at the time of death (n=7). By 7 days p.i., colonic tissue from IL-1R$^{-/-}$ mice displayed maximal damage. Magnification, X 400 for all H&E images.

Figure 4: Neither increased bacterial load nor decreased neutrophil infiltration contributed to increased pathology in IL-1R$^{-/-}$ mice. (A) Various tissues were harvested aseptically from C57BL/6 (n=12) and IL-1R$^{-/-}$ (n=9) 7 days p.i. *C. rodentium* CFU were quantitated as described in *Material and Methods*. (B) Pathology scores for recruitment measurements including edema and neutrophil infiltration were assessed in colonic tissue from C57BL/6 (n=12) or IL-1R$^{-/-}$ (n=13) mice 7 days p.i. *, indicates

statistical significance in comparison to C57BL/6 samples, $p<0.01$. (C) Manual neutrophil counts in crypts from C57BL/6 (n=5-15) and IL-1R$^{-/-}$ (n=7-15) colons *, indicates statistical significance in comparison to uninfected C57BL/6 samples, $p<0.01$.; **, indicates statistical significance in comparison to uninfected IL-1R$^{-/-}$ samples, $p<0.02$; #, indicates statistical significance in comparison to uninfected samples, $p<0.001$. (D) *C. rodentium* (5×10^5) incubated with neutrophils (2.5×10^5) from C57BL/6 or IL-1R$^{-/-}$ mice were killed with equal efficacy. Representative experiment repeated three times in triplicate.

Figure 5: IL-1R$^{-/-}$ mice are capable of a normal hyperplasia response in the colon. IL-1R$^{-/-}$ mice have equal levels of hyperplasia following infection with *C. rodentium*. (A) Pathology score was assessed for degree of hyperplasia in colonic tissue taken from IL-1R$^{-/-}$ (n=13) and C57BL/6 (n=12) mice. (B) Crypt lengths of colonic tissue from uninfected C57BL/6 or IL-1R$^{-/-}$ mice, or from C57BL/6 or IL-1R$^{-/-}$ mice 3 or 7 days p.i. were measured. *, indicates statistical significance in comparison to uninfected samples, $p<0.001$.

Figure 6: IL-1R$^{-/-}$ mice are more susceptible to DSS-induced colitis. (A) Pathology scores were assessed in colonic tissue from untreated C57BL/6 or IL-1R$^{-/-}$ mice, or from treated C57BL/6 or IL-1R$^{-/-}$ mice 7 or 14 days post-treatment. The numbers ranged from 6-10 C57BL/6 mice and 9-12 IL-1R$^{-/-}$ mice for each bar. *, indicates statistical significance in comparison to C57BL/6 14 days post-treatment samples, $p<0.01$. (B) Pathology scores for each category were assessed in colonic tissue from treated C57BL/6 or IL-1R$^{-/-}$ mice 14 days post-treatment (C) Crypt lengths of colonic tissue from untreated C57BL/6 or IL-1R$^{-/-}$ mice, or from C57BL/6 or IL-1R$^{-/-}$ mice 7 or 14 days post-treatment

were measured. *, indicates statistical significance in comparison to uninfected samples, $p<0.01$; **, indicates statistical in comparison to uninfected samples, $p<0.001$; #, indicates statistical significance between C57BL/6 and IL-1R$^{-/-}$ samples, $p<0.02$; ^, indicates statistical significance between C57BL/6 and IL-1R$^{-/-}$ samples, $p<0.01$.

Figure 1

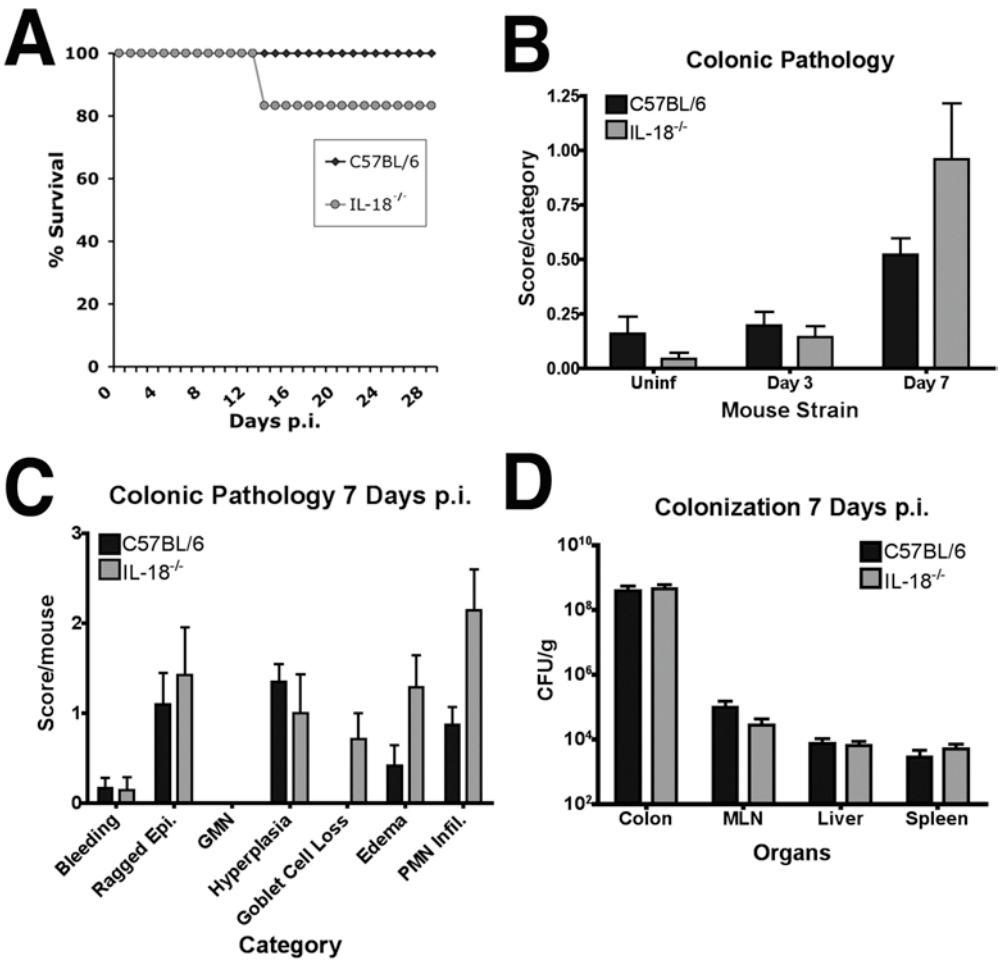
A
100
80
60
40
20
0
% Survival
C57BL/6
IL-18-/-
0
4
8
12
16
20
24
28
Days p.i.
B
Colonic Pathology
C57BL/6
IL-18-/-
1.25
1.00
0.75
0.50
0.25
0.00
Score/category
Uninf
Day 3
Day 7
Mouse Strain
C
Colonic Pathology 7 Days p.i.
C57BL/6
IL-18-/-
3
2
1
0
Score/mouse
Bleeding
Ragged Epi.
GMN
Hyperplasia
Goblet Cell Loss
Edema
PMN Infil.
Category
D
Colonization 7 Days p.i.
C57BL/6
IL-18-/-
10^10
10^8
10^6
10^4
10^2
CFU/g
Colon
MLN
Liver
Spleen
Organs

Figure 2

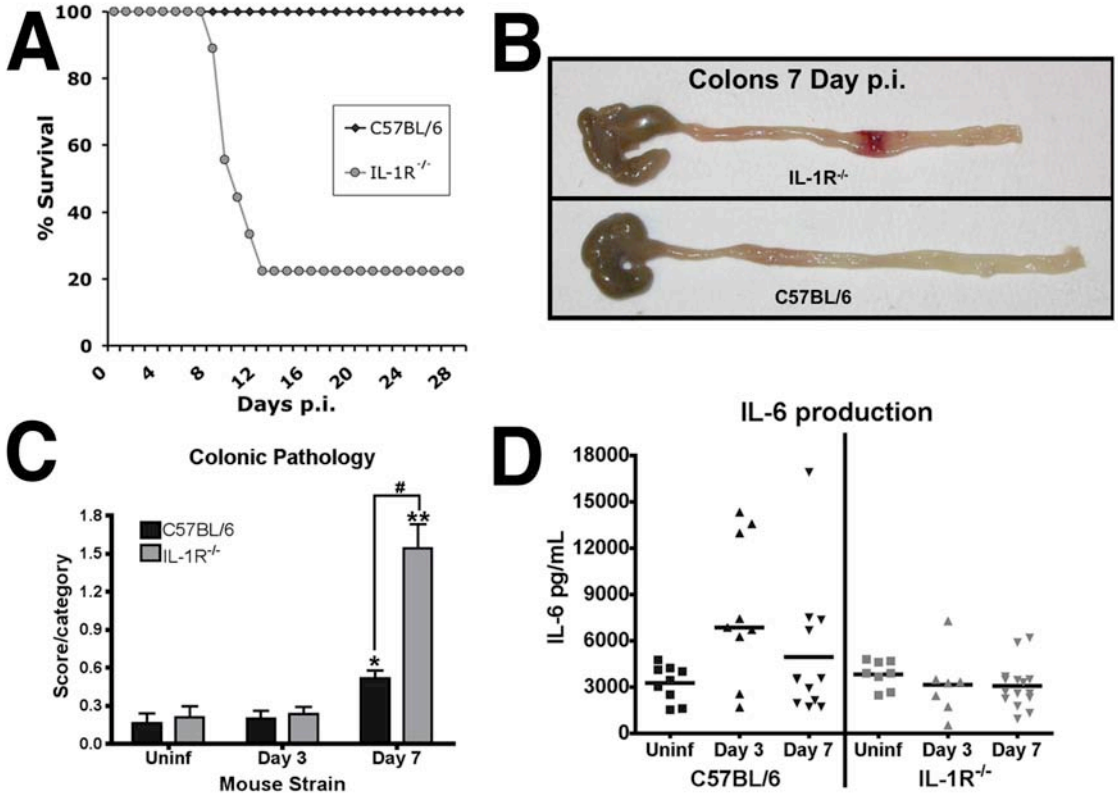
A
100
80
60
40
20
0
% Survival
C57BL/6
IL-1R -/-
0
4
8
12
16
20
24
28
Days p.i.
B
Colons 7 Day p.i.
IL-1R-/-
C57BL/6
C
Colonic Pathology
C57BL/6
IL-1R-/-
Score/category
1.8
1.5
1.2
0.9
0.6
0.3
0.0
*
#
**
Uninf
Day 3
Day 7
Mouse Strain
D
IL-6 production
IL-6 pg/mL
18000
15000
12000
9000
6000
3000
0
Uninf
Day 3
Day 7
Uninf
Day 3
Day 7
C57BL/6
IL-1R-/-

Figure 3

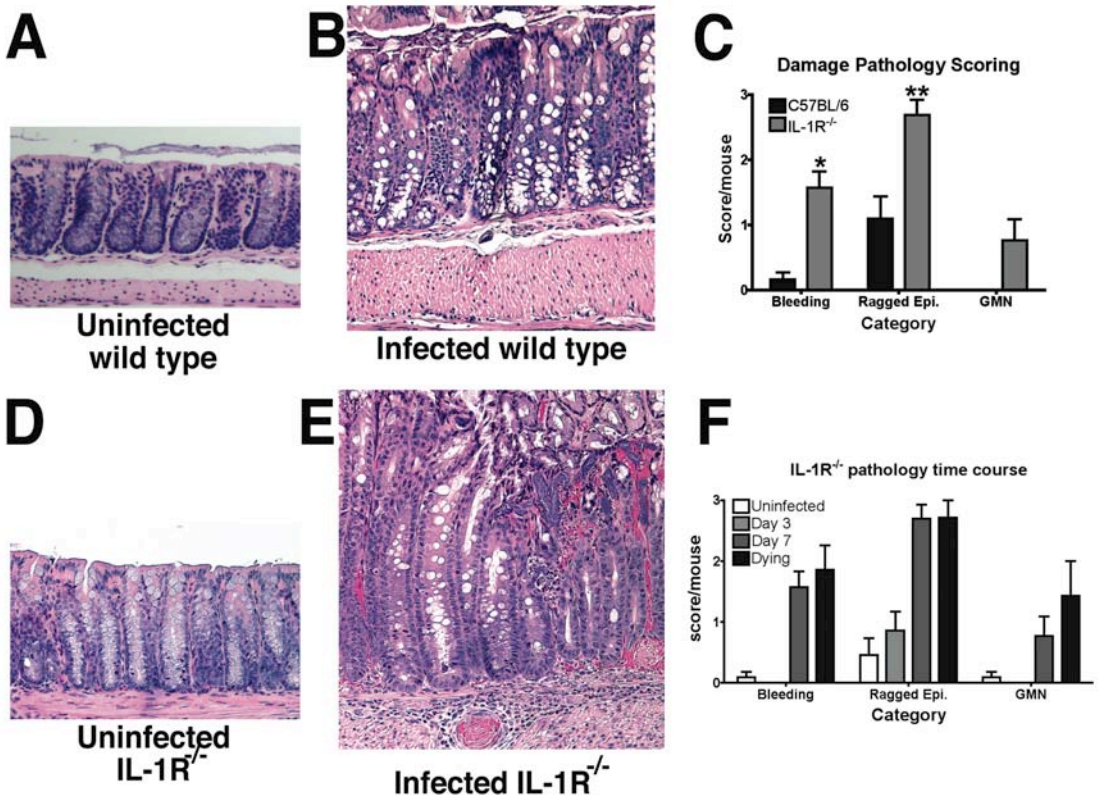
A
B
C
Damage Pathology Scoring
C57BL/6
IL-1R-/-
Score/mouse
Bleeding
Ragged Epi.
GMN
Category
Uninfected wild type
Infected wild type
D
E
F
IL-1R-/- pathology time course
Uninfected
Day 3
Day 7
Dying
score/mouse
Bleeding
Ragged Epi.
GMN
Category
Uninfected IL-1R-/-
Infected IL-1R-/-

Figure 4

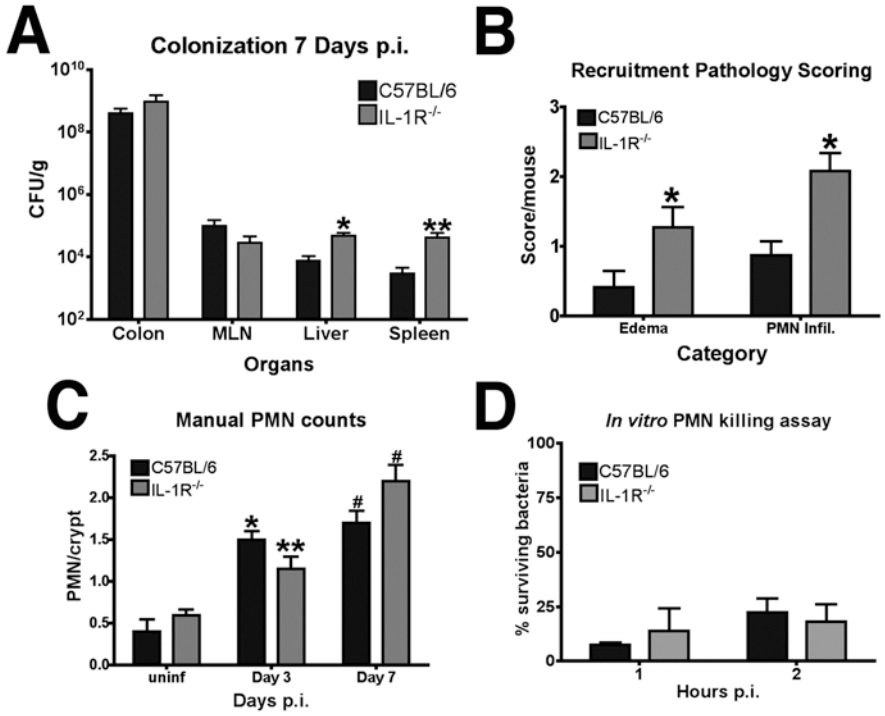
A
Colonization 7 Days p.i.
C57BL/6
IL-1R-/-
CFU/g
Colon
MLN
Liver
Spleen
Organs
B
Recruitment Pathology Scoring
Score/mouse
Edema
PMN Infil.
Category
C
Manual PMN counts
PMN/crypt
uninf
Day 3
Day 7
Days p.i.
D
In vitro PMN killing assay
% surviving bacteria
Hours p.i.

Figure 5

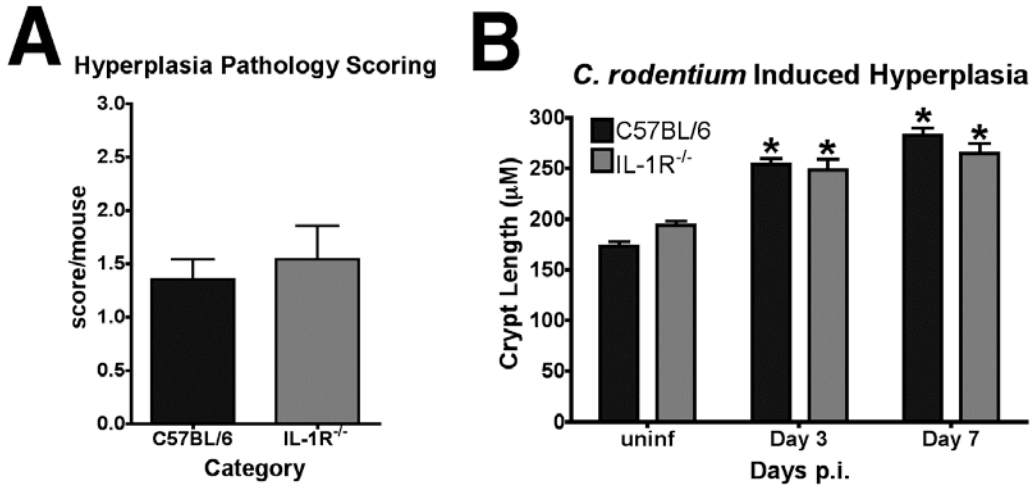
A
Hyperplasia Pathology Scoring
score/mouse
3.0
2.5
2.0
1.5
1.0
0.5
0.0
C57BL/6
IL-1R-/-
Category
B
C. rodentium Induced Hyperplasia
Crypt Length (μM)
300
250
200
150
100
50
0
C57BL/6
IL-1R-/-
*
*
*
*
uninf
Day 3
Day 7
Days p.i.

Figure 6

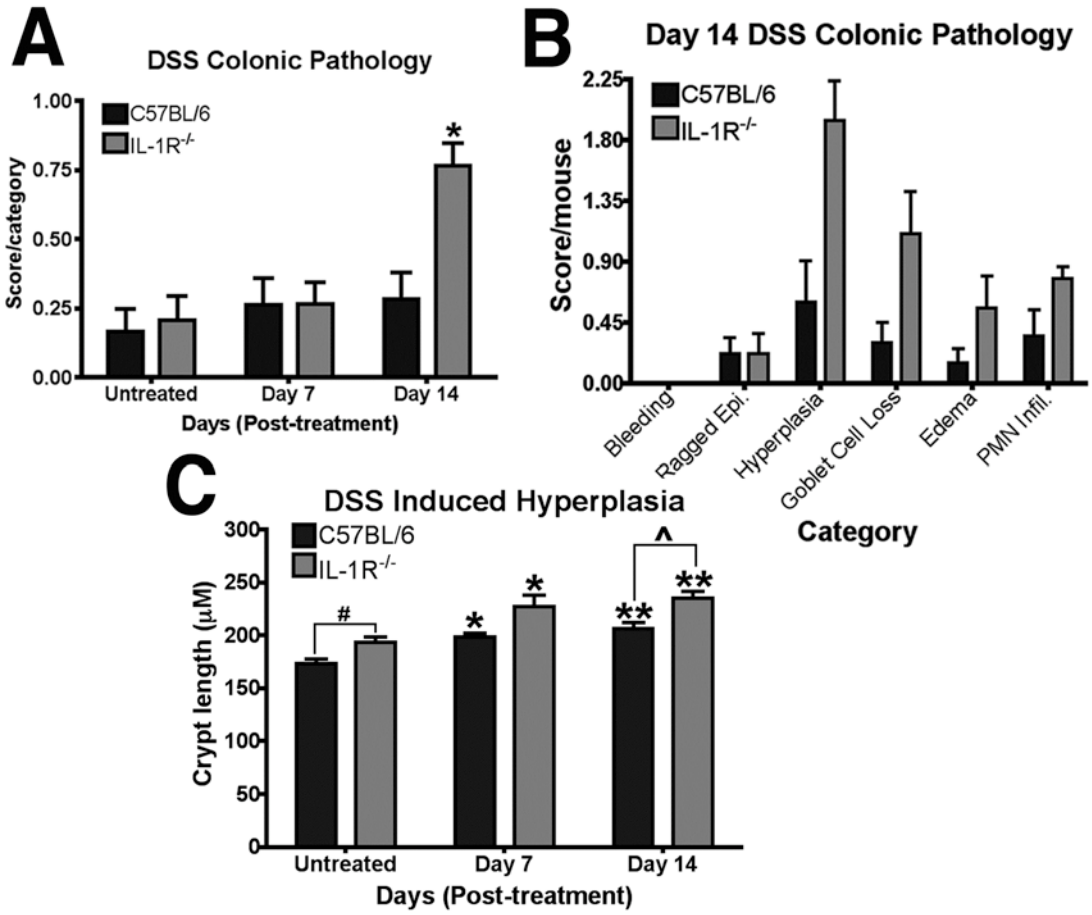
A
DSS Colonic Pathology
C57BL/6
IL-1R-/-
Score/category
1.00
0.75
0.50
0.25
0.00
*
Untreated
Day 7
Day 14
Days (Post-treatment)
B
Day 14 DSS Colonic Pathology
C57BL/6
IL-1R-/-
Score/mouse
2.25
1.80
1.35
0.90
0.45
0.00
Bleeding
Ragged Epi.
Hyperplasia
Goblet Cell Loss
Edema
PMN Infil.
Category
C
DSS Induced Hyperplasia
C57BL/6
IL-1R-/-
Crypt length (μM)
300
250
200
150
100
50
0
#
*
*
**
^
**
Untreated
Day 7
Day 14
Days (Post-treatment)

CHAPTER IV:

The generation of small colony variants (SCV) reveals the importance of growth rate in causing pathology during an infection with *Citrobacter rodentium*

All experiments were performed by Sarah Lebeis. Pathology scoring was performed by Melanie Sherman.

Abstract:

Although introduced bacterial pathogens must overcome several obstacles in order to cause disease, the most important task for the bacteria is to maintain growth by acquisition of essential nutrient. A small colony variant (SCV) of the mouse A/E pathogen *Citrobacter rodentium* was isolated from persistently infected mice deficient in the innate immune signaling adaptor protein MyD88 (MyD88$^{-/-}$ mice). It was determined that SCV *C. rodentium* had a severe growth defect, low level resistance to aminoglycosides, decreased virulence in mice, and appeared to be auxotrophic for Fe^{3+}. Thus, addition of excess $Fe(III)Cl_3$ rescued the slow growth rate displayed by SCV in liquid culture *in vitro*. Further, the decreased colonization rate of SCV *C. rodentium in vivo* subsequently led to dramatically decreased pathology following infection of mice. In fact, wild type and MyD88$^{-/-}$ mice have equivalent pathology scores seven days p.i. when they are infected with SCV *C. rodentium.* These data implicate the capacity of *C. rodentium* to grow as a major contributing factor to the development of bleeding, epithelium damage, and gangrenous mucosal necrosis in colonic tissue of infected MyD88$^{-/-}$ mice. Notably, in each persistently SCV *C. rodentium* infected mouse another variant of *C.* rodentium which had normal colony size was isolated. This variant was defined as a standard-growth variant (StV), and induced an antibody response in fewer infected mice through an unknown mechanism. Together these studies demonstrate that passage of *C. rodentium* through MyD88$^{-/-}$ mice provide enough selective pressure to generate multiple variants of the pathogen, which may identify critical targets for therapeutic intervention.

Introduction:

The exposure of a host to pathogenic microbes does not always lead to disease (1). To establish an infection, the pathogen must accomplish multiple tasks in the host including: successful colonization of mucosal surfaces, transit across mucosal barriers, proliferation inside the host, induction of damage to host tissues, and often participation in immune evasion and/or immunomodulation (2). For all of these tasks, a pathogen must maintain its ability to grow. During the course of an infection, pathogenic bacteria encounter multiple environments during dissemination from one organ to another, inflammation, and tissue breakdown in the host (2). In addition to environmental changes, bacterial pathogens must also maintain growth in the face of an onslaught of host defenses. The protective measures taken against bacterial pathogens includes, but are not limited to, a community of commensal organisms that deplete essential nutrients from microbial niches, antimicrobial peptides produced by epithelial cells, infiltration of phagocytes, which ingest and kill bacteria, and finally a protective antibody response specifically directed against the pathogen. When antibiotics are administered to combat the infection, additional selective pressure is placed on bacteria. Together these represent some of the obstacles that pathogenic bacteria must circumvent to survive within the host.

When specific immunity or antibiotic treatments fail to clear the infection, bacteria are given the opportunity to mutate, potentially allowing some variants to cause persistent infections. A common bacterial phenotype associated with persistent, relapsed, or antibiotic resistant infections are small colony variants (SCV). In *Staphylococcus* infections, SCV were reported by the early part of the 20th century (3). While SCV are most commonly characterized in clinical isolates of *Staphylococcus* species, they have

also been documented in *Listeria monocytogenes* (4), *Salmonella enterica* (5), and *Escherichia coli* (6). In *L. monocytogenes*, SCV result from a mutation in *perR*, a metal regulatory protein, required for both metal ion and H_2O_2 regulation (7). Thus, *perR* mutants are more sensitive to reactive oxygen species and different zinc and iron ion homeostasis. Iron is critical for bacterial pathogens, as evident by the large genomic investment in its acquisition and storage (8). These mutations lead to defects in electron transport chain and therefore decreased growth rate under aerobic conditions (5). SCV are often associated with auxotrophy (e.g. hemin, menadine, and thiamine), decreased respiration, the ability to revert to normal growth, and decreased uptake of aminoglycosides, rendering the bacteria resistant to these antibiotics (3, 5). Interestingly, it has been proposed that SCV can be induced following administration of suboptimal concentrations of antimicrobial agents (5), linking selective pressure to generation of pathogen variants. In general, SCV pathogens cause milder infections than the wild type strains (5). Therefore, although SCV variants sacrifice some of their pathogenicity, a lowered growth rate enables pathogen variants to survive many of the selective pressures that wild type pathogens cannot.

Due to their short generation time and ability to transfer genetic element horizontally, bacteria are capable of acquiring elements that render them more pathogenic. Thus, in contrast to the reduced virulence seen in SCV, passage through a host can also make pathogens more virulent. For A/E pathogens, it has been hypothesized that the conservation of the intact LEE pathogenicity island, an element found in all A/E pathogens, is consistent with horizontal gene transfer between unrelated bacteria (9). However, there are other transient modifications that may also render pathogens, such as

Vibrio cholera (9) temporarily more virulent. Interestingly, *C. rodentium* passage through mice induces a "hyperinfectious" state, in which *C. rodentium* transferred from mouse to mouse is more virulent than that grown in Luria-Bertani (LB) broth from a laboratory stock (10). *C. rodentium* in its hyperinfectious state is able to directly colonize the intestine, without first having to colonize the cecum. Further, these bacteria were capable of disseminating to peripheral organs more readily, and lead to increased hyperplasia response in mice (10). It has been suggested that colonization of the cecum allows *C. rodentium* to acclimate to the environment of the intestine, possibly altering its gene expression and protein production (10). However, when the *C. rodentium* from one mouse directly infects a naïve mouse, the bacteria is "primed" to infect the next host. In fact, Wiles and colleagues hypothesize that since this is more akin to the natural infection these variants are not hyperinfectious, but rather that bacteria grown up in the laboratory are hypoinfectious (10). Further, when hyperinfectious *C. rodentium* was cultured in LB overnight the increased virulence was lost, again indicating that the changes in this bacteria are transient (10) and not permanent due to mutations.

The work here describes a method to create stable variants of *C. rodentium* via passage through MyD88$^{-/-}$ mice. Rather than being transiently hypervirulent, these variants grew more slowly and were thus less virulent upon subsequent infection of mice. Notably, apparent standard-growth variants (StV) were also isolated, which behaved similarly to wild type *C. rodentium* in every manner except that StV *C. rodentium* stimulates an antibody response in fewer mice than wild type of SCV *C. rodentium* infected mice. Finally, addition of Fe^{3+} to SCV *C. rodentium* compensates for the growth

defects *in vitro*, suggesting that, as with numerous other pathogens, iron acquisition is crucial for *C. rodentium* pathogenesis.

Material and Methods:

Mouse strains and breeding: MyD88$^{-/-}$ mice on a C57BL/6 background were the generous gift of David Underhill, and were originally generated in the laboratory of Shizuo Akira (11). These mice were bred at Emory University. C57BL/6 mice were used as the control strain for MyD88$^{-/-}$ mice and were obtained from Jackson Laboratory (Bar Harbor, ME). Animals were kept in sterile housing and care was provided in accordance with protocols approved by the Institutional Animal Care and Use Committee of Emory University.

***In vivo* infections:** *C. rodentium* cultures were prepared by overnight culturing (12 to 16 hours) at 37ºC in Luria-Bertani (LB) broth (Becton Dickinson, Franklin Lakes, NJ) without shaking for optimal virulence factor expression. Cultures were harvested by centrifugation and resuspended in 20% sucrose. For infections of mice, drinking water was replaced with *C. rodentium* suspension overnight. The volume of suspension was measured before and after administration and the concentration of bacteria in the inoculum was calculated following retrospective plating. The average dosage was 4×10^8 CFU/mouse. Survival of infected mice and changes in body weight were monitored daily. Mice losing more than 15% of their original weight were euthanized. Clearance of *C. rodentium* was assessed by culturing the bacteria found in fecal samples.

Generation of SCV *C. rodentium*: MyD88$^{-/-}$ mice were infected with laboratory strain *C. rodentium*. On the third day of the infection, mice were treated with a low dose of antibiotics consisting of neomycin (0.5 mg/mL; Sigma-Aldrich, St. Louis, MO) and polymyxin B (2000U/mL; Sigma-Aldrich). Most MyD88$^{-/-}$ mice were then capable of surviving the infection. After four weeks of antibiotic treatment, animals were sacrificed

and bacterial contents of the intestine were assessed. 33.33% of animals had colonies resembling *C. rodentium* species colonizing their distal colon. Colonies were confirmed as *C. rodentium* by PCR with Tir-specific primers (forward primer 5'-GCGCGAATTCA TGCCTATTGGTAATCTTGGTAATAATAAT-3' and reverse primer 5'-GCGCCCCG GGTTAGACGAAACGTTCAACTCCCGGTGTTGT-3'). Reactions were conducted using the Peltier Thermal Cycler-200 from MJ Research (Bio-Rad, Waltham, MA) under the following conditions: 94^{o}C for 3 minutes; 35 cycles of 94^{o}C for 30 seconds, 65^{o}C for 1 minute and 72^{o}C for 1 minute; and 72^{o}C for 2 minutes.

Analysis of secreted proteins: The secreted proteins of the *C. rodentium* variants were determined by diluting an overnight culture of each variant 1:100 into DMEM and grown at 37^{o}C in 5% CO_2 to an optical density of 0.5-0.7 hours. Bacteria were pelleted and supernatant was collected. Trichloroacetic acid (TCA, Sigma-Aldrich) in a final concentration of 10% was added to the supernatant to precipitate the proteins and mixture incubated overnight at -20^{o}C. Proteins were pelleted by spinning 13,000 rpm at 4^{o}C for 10 minutes and washed twice with 1mL of acetone. The pellet was resuspended in 15µL of 1.0 M Tris and an equal volume of sodium dodecyl sulfate (SDS) sample buffer (2×) was added. Samples were heated to 95^{o}C for 5-8 minutes and separated on a 12% SDS-polyacrylamide gel by electrophoresis. Proteins were visualized following Coomassie G250 (Sigma-Aldrich) staining of the gels.

Growth Curves: The growth of each *C. rodentium* variant was measured in liquid cultures of 25mL of LB broth without shaking to match the growth conditions of cultures used for *in vivo* infection. The starting OD for each culture was 0.001. The turbidity of each culture was measured using a Klett-Summerson photoelectric colorimeter (Arthur

H. Thomas Company, Philadelphia, PA) reader in the laboratory of Dr. Bernard Weiss. Measurements were taken every hour during lag and stationary phase and every half an hour during exponential growth phase. To rescue the growth defect in SCV *C. rodentium*, 0.5 μg/mL of $FeCl_3$ was added to LB liquid broth in which cultures were grown. Curves were measured three independent times.

Identification and sequencing of *entCEBA* genes in *C. rodentium*: The sequences of *entC, entE, entB,* and *entA* genes of *Citrobacter koseri* were aligned against the *C. rodentium* genome using 2 sequence BLAST (12) at the NCBI website. Potential homologs were found for each gene, and the putative operon was found to be structured the same as the *ent* operon of *C. koseri*. Primers were then generated against the *C. rodentium* sequences for *entC* (2 sets of primers, forward 1 5'-GGTTAGCGCCGAAATATAAAT-3', reverse 1 5'-CGCCATCCTGCAACGACACA-3', forward 2 5'-CATGTGTCGTTGCAGGATG G-3' and reverse 2 5'-GCTCATCATCACTCCTTAATGC-3'), *entE* (2 sets of primers, forward 1 5'-CGTCTTTGGATTGCATTAAGGAG-3', reverse 1 5'-AATCAGCGGGA AGCACAGCG-3', forward 2 5'-GCTGTGCTTCCCGCTGATTG-3', and reverse 2 5'-GGATTGCCATCGTATATTCTCC-3'), *entB* (forward 5'-CCGGCCTGAAGGAGAAT ATACG-3' and reverse 5'-GTGACCCACACCGTTTTA CCG-3'), and *entA* (forward 5'-GATTGACGGCTGGTGGAAAC-3' and reverse 5'-GCTCTGCAAGCGTTAACACTG C-3'). PCR reactions were conducted using the FailSafe™ PCR PreMix Selection Kit (EPICENTRE, Madison, WI) buffer F was found to work the best. PCR products were purified using the DNA Clean & Concentrator™-5 (Zymo, Orange, CA) and sequenced (MWG Biotech, High Point, NC).

Neutrophil killing assays: *C. rodentium* and its isolated variants were cultured overnight in LB broth. To isolate neutrophils, bone marrow from C57BL/6 or MyD88$^{-/-}$ mice was removed, and red blood cells (RBCs) were lysed. As previously noted, 22-30% of cells were positive for GR-1 using this method (13). Bacteria (5×10^5) were added to 2.5×10^5 cells in 350mL of RPMI 1640 medium without antibiotics. After 1, 2, or 3 hours, the bacterium-cell culture was diluted 1:10 in water for 10 minutes to lyse neutrophils and serial dilutions in PBS were plated of MacConkey agar to determine the number of bacterial colonies remaining. Assays were conducted in triplicate.

Colony counts of *C. rodentium:* Tissue samples of colon, liver, spleen, or mesenteric lymph node (MLN) weighing ~0.1 to 0.3g were homogenized at low speed with a Tissuemizer (Fisher Scientific, Pittsburgh, PA) in 1 mL of phosphate buffered saline (PBS). The lysate was plated on MacConkey agar plates at various dilutions, and *C. rodentium* colonies were recognized as pink with a white rim after 20 hours at 37ºC as previously described (14). Random colonies were confirmed as *C. rodentium* by PCR with Tir-specific primers as described above and previously (14).

Histology and Pathology scoring: For histology studies, colons were removed from uninfected or infected mice, fixed in 10% formalin, and embedded in paraffin. Sections (5μm) were cut and stained with hematoxylin and eosin (H&E) by the Histology Core Laboratory in the Department of Pathology at Emory University. The degree of intestinal pathology was assessed under the microscope by Melanie Sherman. The samples were coded and the observations made in a blind fashion to avoid bias in the evaluation process. Samples were scored for degree (0-3) of gangrenous mucosal necrosis (GMN), bleeding, raggedness of epithelium, hyperplasia, loss of goblet cells, edema, and

neutrophil infiltration, where a zero score represents no signs of pathology measurement, a one score is mild pathology measurement, a two is moderate pathology measurement, and a three score is severe pathology measurement. Crypt heights were measured by micrometry using Zeiss 200M microscope, a 20× NA 1.4 lens and Slidebook software (Intelligent Imaging Innovations, Denver, CO). Well-oriented crypts were used for measurements. Two measurements were made on each image, and one image was taken per colon. The number of samples refers to the number of colons measured rather than the number of measurements.

ELISA for C. *rodentium*-specific antibody: For antibody isotype analysis, antibody titers in sera were determined by enzyme-linked immunosorbent assay (ELISA). Three sets of plates were made with each set made from the lysate of either wild type, SCV or StV overnight cultures. Plates were coated with 100µl of 10µg of C. *rodentium* lysate per ml in 0.1 M carbonate buffer and incubated overnight at 4°C. The plates were washed with 0.05% polyoxyethylenesorbitan monolaurate (Tween® 20, Sigma-Aldrich) in phosphate buffered saline (PBS, 50mM K_2HPO_4, 50mM KH_2PO_4, pH 6.0, Sigma-Aldrich) and then blocked with blocking solution (0.2% bovine serum albumin (BSA; Sigma-Aldrich) and 0.05% Tween® 20 in PBS) at room temperature for 2 hours. Dilutions of serum starting at 1:20 were made with blocking solution, and 100µl of each dilution was added to coated plates. After incubation at 37°C for 2 hours, the coated plates were washed with Tween® 20 in PBS and bound immunoglobulin (Ig) was detected with horseradish peroxidase -conjugated goat anti-mouse IgG1 and IgG2b (Roche, Basel, Switzerland) at 37°C for 2 hours. The plates were then washed with Tween 20 in PBS. After incubation, color was developed with tetramethylbenzidine

(Promega, Madison, WI), stopped with 0.18 N sulfuric acid, and measured by determination of optical density at 450 nm on a microplate reader (Biotek, Winooski, VT). The antibody titer was defined as the dilution required to reduce a positive signal to threefold above the background.

Quantitative biofilm assays: To measure biofilm formation, fresh LB or DMEM was inoculated from an overnight of each *C. rodentium* variant at approximately an OD of 0.01. Cultures were grown for either 4, 8, 24, or 36 hours. All experiments were performed in 96-well plate with 100μL/well in 6 replicates per condition. Prior to staining, the optical density at 600nm was measured for each well was measured. At the end of the incubation time, plates were washed by immersion in dH_20 three times. Enough crystal violet was added to cover the bottom of each well (1-2 drops). Plates were against washed by immersion three times, and dried. To quantify the amount of biofilm formed, 100μL of 33% acetic acid was added to each well, and plates were read at an optical density of 630nm.

Statistical analysis: For antibody studies, a two-sided Fisher's exact test determined statistical significance of data. Results were considered significant if the *p* value was <0.01.

Results:

Selection of SCV *C. rodentium* in mice.

To generate novel variants, *C. rodentium* was passaged through MyD88$^{-/-}$ mice, which have an increased pathogen load, and therefore a higher chance being colonized with a variant capable of surviving selective pressure. Moreover, because MyD88$^{-/-}$ mice control the infection to a lesser degree, we presumed some bacterial variants could be isolated from these mice that could not survive in wild type mice. Three days after infection, when *C. rodentium* had out-competed most of the resident commensal bacterial species (15), low doses of antibiotics were administered, allowing most MyD88$^{-/-}$ mice to survive the infection. A combination of neomycin and polymyxin B added to the drinking water of these animals were used to provide selective pressure on *C. rodentium* (Figure 1A). It has previously been demonstrated that wild type *C. rodentium* is susceptible to this antibiotic cocktail (data not shown). After 4 weeks of treatment, small colony variants (SCV) of *C. rodentium* were isolated from several mice (Figure 1B), and were found to be resistant to antibiotic water on agar plates. Notably, a standard-growth variant (StV) *C. rodentium* was also isolated from every mouse with a SCV variant (Figure 1B). For all subsequent experiments a SCV that could be re-cultured and maintain its small colony phenotype as well as resistance to antibiotic water was used.

The stable SCV was confirmed to be *C. rodentium* by several methods including: appearance on several media, confirmed presence of the virulence factor Tir by PCR, and a secreted protein profile identical to that seen in a laboratory *C. rodentium* strain (Figure 1C). Notably, SCV *C. rodentium* grows more slowly in liquid culture (Figure 1D). The StV *C. rodentium* was also confirmed to be *C. rodentium* by these assays (Figure 1C) and

grew with the exact same kinetics as wild type *C. rodentium* (data not shown). Together these data indicate that a stable SCV can be isolated following passage of *C. rodentium* through mice treated with a low-dose of antibiotic treatment in MyD88$^{-/-}$ mice.

Phenotypic analysis of *C. rodentium* SCV.

To further characterize the drug resistance properties of SCV *C. rodentium*, the minimum inhibitory concentration (MIC) of various antibiotics was determined. As shown in Figure 2A, SCV *C. rodentium* had low level resistance to multiple aminoglycosides including neomycin, kanamycin, and streptomycin. Further, it was determined that SCV *C. rodentium* was not resistant to killing with tetracycline, ampicillin, or chloramphenicol (data not shown). By contrast, the MIC for each of the antibiotics against StV *C. rodentium* isolate was equivalent to that seen in wild type *C. rodentium.* Together, these studies establish that SCV *C. rodentium* is specifically resistant to aminoglycosides, a phenotype previously seen with SCV mutants in other pathogens (3, 5).

To determine the cause of the SCV *C. rodentium* growth defect, it was plated on several different agar plates. Wild type *C. rodentium* was grown on the same plates as a control for colony size. When they were grown on minimal media with various carbon sources, including glucose, lactose, glycerol, and succinate, both wild type and SCV *C. rodentium* formed small colonies of equivalent size (Figure 2B). Further, when a mixture of amino acids was added to minimal media supplemented with glucose, wild type and SCV *C. rodentium* colony size remained small (Figure 2B). Interestingly, wild type and SCV *C. rodentium* grew equally well on Brain-Heart Infused (BHI) agar. In fact, MacConkey, eosin methylene blue agar (EMB), and LB agar plates were the only media

types that showed a difference between the colony size of the two strains (Figure 2B). These studies indicate that the difference between the growth rate of SCV and wild type *C. rodentium* is only evident when bacteria are cultured on rich media, and that the difference can be compensated for by some component within BHI agar.

Previous work is other pathogens suggests that decreased iron transport could result in smaller colony size (4). To investigate this possibility, we next assessed of a role for various forms of iron during growth of *C. rodentium*. First, gradient of concentrations of hemin or Fe^{2+} was added to MacConkey plates, but did not increase the colony size of SCV *C. rodentium* (data not shown). Notably, high concentrations of hemin or Fe^{2+} inhibited growth of both types of *C. rodentium* (data not shown). Finally, it was determined that 0.25-1μg/mL $Fe(III)Cl_3$ added to MacConkey media rescued the small colony phenotype of SCV *C. rodentium*. To quantify the growth rate of SCV *C. rodentium* in media supplemented with $Fe(III)Cl_3$, growth curves were performed. As shown in Figure 2C, SCV *C. rodentium* grew at the same rate as wild type *C. rodentium*. Additionally, the increased iron present in the media did not increase the rate at which wild type *C. rodentium* grew. In every test of growth or growth rate the StV *C. rodentium* had the same phenotype as wild type *C. rodentium*.

Identification of the siderophore operon in *C. rodentium*.

Because iron is an essential nutrient for all bacteria growth, microbes have developed several strategies for iron acquisition and storage. One such mechanism utilizes siderophores, iron chelators, which are secreted, bind iron, and are taken up by bacteria through specialized cell-surface protein receptors (8, 16). Siderophores are capable of binding up to six Fe^{3+} ions, which are generally unavailable for cells to use

because they are fairly insoluble in aqueous solutions (17). Once the siderophore-bound Fe^{3+} is inside the bacteria, the iron is liberated for use by the bacteria (8). Bacteria often produce many siderophores, one the most effective of which is enterobactin (18), a cyclic triester of 2,3-dihydroxy-*N*-benzoyl-L-serine (DHBS) (19). Enterobactin is produced in a multi-step process that converts chorismic acid into the three DHB residues required for enterobactin (20). There are clustered genes required for synthesis of enterobactin, *entA-F* in *E. coli* (21). More specifically, *entC* encodes an isochorismate synthase, which converts chorismate into isochorismate (21). Next, *entB*, encoding for isochorismate lyase that catalyzes the conversion of isochorismate into 2, 3-dihydro-2, 3-dihydroxybenzoic acid (21). Finally, EntA utilizes this molecule as a substrate, forming DHB (21). In addition to EntB, EntE and EntF are also multiple domained non-ribosomal peptide synthetases that generate enterobactin from three serines and three DHB molecules (22). Finally, EntD is a phosphopantetheinyl transferase which adds the required cofactors to EntB and EntF (23). A mutation in any of the *ent* genes would alter the production of enterobactin and may cause the decreased growth rate by hindering binding of iron and therefore iron acquisition of the SCV *C. rodentium.* This hypothesis also correspond with the ability of excess iron to compensate for the decreased growth rate observed in SCV *C. rodentium*, possibly by iron binding to a less effective siderophore.

Although the *C. rodentium* genome has been sequenced, it remains to be annotated. However, utilizing the sequence of the *entC, entE, entB,* and *entA* genes of *Citrobacter koseri* and sequence alignment tools we identified a putative analog of the *entC, entE, entB,* and *entA* genes in *C. rodentium*. Further, this region of the *C. rodentium*

genome contains sequence homology for all of the genes found in the *entC, entE, entB,* and *entA* genes of *C. koseri* with 80-85% identity, and the downstream genes encoding the transport machinery for the siderophore also appear to be conserved between the two *Citrobacter* strains. When each of the genes in the putative *C. rodentium ent* operon was sequenced, it was revealed that there were no sequence differences present between the genome of wild type and SCV *C. rodentium*. Together, these data indicate that the decreased growth rate is not caused by a mutation in *entA, entE, entB,* or *entA* of SCV *C. rodentium* although we cannot rule out the possibility that the regulation of these genes may be altered in SCV *C. rodentium*.

SCV *C. rodentium* is not more susceptible to neutrophil killing *in vitro*.

Notably, a mutation in *perR* in *L. monocytogenes* causes a SCV phenotype and increased susceptibility to reactive oxygen species (4). This is relevant to host defense because reactive oxygen bursts are commonly used by phagocytic innate immune cells to kill bacteria (24). To determine if this were the case for SCV *C. rodentium*, susceptibility to neutrophil killing *in vitro* was assayed. When the resistance of wild type and SCV *C. rodentium* to neutrophil killing was assessed *in vitro*, it was discovered that there was no increased susceptibility in SCV *C. rodentium* to the bactericidal capacities of these cells (Figure 2D). However, further studies are required to determine the susceptibility of SCV *C. rodentium* to reactive species of oxygen. Thus, preliminary data indicate that a mutation in *perR* or the peroxide pathway does not play a role in the SCV *C. rodentium* small colony phenotype.

Small *C. rodentium* variants are less virulent in mice.

To determine if SCV *C. rodentium* was less virulent *in vivo*, naïve MyD88$^{-/-}$ mice were infected and mortality was measured. As seen in Figure 3A, while all MyD88$^{-/-}$ mice infected with SCV *C. rodentium* do succumb to the infection, it is with delayed kinetics. This delay correlates with the slower growth rate *in vitro* (Figure 1D). To further examine the growth of both types of *C. rodentium* during the infection of mice, degree of colonization was measured in various organs at three and seven days p.i. (Figure 3B and 3C). At both time points, the level of SCV *C. rodentium* colonization was lower in each organ sampled. These data demonstrate that SCV *C. rodentium* has a decreased rate of colonization during *in vivo* infection, matching the decreased growth rate *in vitro*. Further, when C57BL/6 mice were infected with wild type or SCV *C. rodentium* a similar pattern of results was observed (Figure 3D), with the exception that no mortality occurred in infected C57BL/6 mice (data not shown). Together these data demonstrate that the decreased growth rate of SCV *C. rodentium* impacts the ability of this pathogen to cause mortality.

To determine if SCV *C. rodentium* caused less severe disease in mice, colonic pathology was assessed. Upon observation, it was revealed that colonic tissue from C57BL/6 and MyD88$^{-/-}$ mice both displayed less pathology following infection with SCV *C. rodentium* than those mice that had been infected with wild type *C. rodentium* seven days p.i. (Figure 4A). Interestingly, C57BL/6 and MyD88$^{-/-}$ mice infected with SCV *C. rodentium* suffer from the same degree of pathology seven days p.i. (Figure 4A) although MyD88$^{-/-}$ mice begin dying by ten days p.i. (Figure 3A). When the overall pathology was split into groups measuring damage, repair, or immune cell recruitment, it was further

discovered that the difference in overall scores was mostly caused by a decrease in damage measurement (Figure 4B-D). These data indicate that the induction of bleeding, epithelial raggedness, and gangrenous mucosal necrosis (GMN) is accomplished by *C. rodentium* and not the host immune response. Together these studies indicate that the decreased morbidity and mortality seen in mice infected with SCV *C. rodentium* is most likely caused by the slower growth rate of this variant.

Fewer mice infected with StV *C. rodentium* generate an antibody response.

When the SCV *C. rodentium* was isolated from MyD88$^{-/-}$ mice, a StV was always present. Normal-sized SCV 'revertants' are often isolated in mice infected with SCV and could be the result the selective pressure of decreased SCV fitness leading to a secondary suppressor mutation, allowing the bacteria to grow at a normal rate. However, StV *C. rodentium* is not resistant to any antibiotics, suggesting that it may simply be wild type *C. rodentium* that survived the low dose treatment of antibiotics. Therefore it is unclear from the *in vitro* characterization if StV is wild type *C. rodentium*, a size reversion of SCV, or a novel variant.

To assess pathogenicity of StV *in vivo* wild type and MyD88$^{-/-}$ mice were infected with the StV *C. rodentium*. In most categories, StV *C. rodentium* leads to identical phenotypes as those seen in mice infected with wild type *C. rodentium* (data not shown). However, the antibody response was slightly altered in mice infected with the StV *C. rodentium* isolate. To determine cross-reactivity of the three variants of *C. rodentium*, serum was harvested from three groups of mice infected with either wild type, SCV, or StV *C. rodentium* and tested for its ability to bind to the three lysates made from overnight cultures of each different type of *C. rodentium*. For example, serum was

harvested from mice infected with StV *C. rodentium* and tested for its ability to bind to lysate made from either a wild type, StV, or SCV *C. rodentium* overnight. Although the overall antibody titer response was similar between all of the groups of mice (Figure 5A-C), there were differences in the number of reactive serum samples between the groups. Hence, although there were similar numbers of mice infected with each *C. rodentium* type, less mice infected with StV *C. rodentium* generated a positive serum response to antigen present in the lysates made from each *C. rodentium* (Figure 5A-C). As seen in Figure 5A, more mice infected with wild type or SCV *C. rodentium* generate anti-wild type *C. rodentium* serum than mice infected StV *C. rodentium* (76.47% and 88.24% compared to 56.25%, respectively). Interestingly, even when serum taken from mice infected with StV *C. rodentium* was tested against StV lysate, significantly fewer mice were found to generate antibodies than the other two groups of mice (wild type vs. StV, $p<0.006$; SCV vs. StV, $p<0.007$; Figure 5B). Together, these data suggest that infection with StV *C. rodentium* less often induces an antibody response in mice, perhaps explaining in part why it has not been cleared from mice four week p.i.

It is possible that StV *C. rodentium* could be hiding from the immune system in complex bacterial structures, such as biofilms. When formation of biofilms from each variant was quantitated, it was revealed that there was no significant difference between the two types of *C. rodentium* (Figure 5D). The amount of biofilm formation did increase over time, but was much lower than levels seen in *E. coli* (25). Together these studies reveal that StV *C. rodentium* induces an antibody response in fewer mice during infection through an unknown mechanism. Further, these data indicate the StV *C. rodentium* is not wild type *C. rodentium*, but instead a novel variant of the pathogen.

Discussion:

Here a method for producing SCV of *C. rodentium* has been defined using low dose treatment of antibiotics in MyD88$^{-/-}$ mice. These SCV isolates display many of the phenotypes associated with SCV in other pathogens including: decreased growth rate, auxotrophy, resistance to aminoglycosides, and possibly the ability to revert to normal growth (3). The aminoglycoside resistance is at low levels and could be caused by decreased growth rate or decreased aminoglycoside uptake, it remains unclear which is the case. The auxotrophy appears to be related to iron uptake and may account for the decreased growth rate, since excess Fe(III)Cl_3 is able to rescue the decreased growth rate *in vitro*.

Damage measurements of pathology during a *C. rodentium* infection only occur when the bacteria are growing normally.

Previously, it was determined that the increased intestinal damage seen in MyD88$^{-/-}$ and IL-1R$^{-/-}$ mice was *C. rodentium*-induced and not host-induced (CHAPTER III). It has been further demonstrated here that growth rate does affect ability to cause disease. These data indicate that perhaps a minimal number of *C. rodentium* are required to cause damage to the intestinal epithelium. Alternatively, the slower growth rate of SCV *C. rodentium* may change the expression pattern of virulence factors *in vivo* although, when grown *in vitro* to equivalent optical density SCV *C. rodentium* the secreted proteins visible were identical. Regardless, these data indicate that slow-growing *C. rodentium* causes a minimal pathology.

Iron appears to facilitate pathogen growth and induce of pathology during a *C. rodentium* infection.

The role of iron uncovered here may raise the possibility of altering iron in the diet of individuals infected with A/E pathogens by limiting the access of iron to the bacteria as part of a treatment strategy to improve outcomes. Previously, it has been demonstrated that an iron-reduced diet is more effective at reducing bacterial growth than injection of iron chelators in mice (8). Notably, there appears to be a relatively narrow range of iron concentration in the host for optimal immune system function. Thus iron deficiency in individuals leads to lowered function of several immune cells, and therefore decreased defense against invading pathogens (8). Conversely, in excess of iron the host may increase pathogen's access to iron and impaired immune cell function (8).

Although there were no mutations found in the putative *entC, entE, entB,* or *entA* genes of SCV *C. rodentium*, it is still possible that enterobactin function is suboptimal in SCV *C. rodentium*. Additionally, the *entD* and *entF* genes still need to be sequenced. Alternatively, because bacteria generally produce more than one siderophore, an increased concentration of Fe^{3+} could potentially allow another, less efficient siderophore to import the required iron for bacterial growth. Further, it has been demonstrated with *E. coli* that siderophores made by other bacteria can be imported as a mechanism to scavenger iron (16). This evidence indicates that bacteria possess many mechanisms to compensate for a mutation in enterobactin production and therefore may not result in a dramatic phenotype. The possibility that the internalization machinery may have altered function also exists, and the phenotypes displayed by the SCV are consistent with a possible mutation in the siderophore importing machinery.

StV *C. rodentium* may be immunoevasive during infection of mice.

Unlike the temporary hyperinfectious or natural infection previously seen in *C. rodentium* infections, here a new variant of *C. rodentium* has been documented. StV *C. rodentium* was isolated from mice that had been treated with neomycin and polymyxin B for four weeks. The SCV *C. rodentium* also isolated from mice at this time are resistant to multiple aminoglycoside, including neomycin, suggesting that the antibiotic treatment was sufficient to engender resistance. Interestingly, StV is not resistant to any antibiotics, including aminoglycosides. This leaves two hypotheses for why StV is present: it is either a size revertant of SCV or it is subverting an antibody response by the host. It is worth noting that neomycin and polymyxin B are used topically in humans, and it has been shown that neomycin is poorly absorbed by the intestinal tract (26). Therefore, if StV *C. rodentium* was present on the basolateral side of the epithelium, it would be sequestered from antibiotic treatment without being resistant. Unfortunately, initial studies to assess location of StV *C. rodentium* by immunofluorescence staining of colonic tissue were unsuccessful; therefore no conclusion could be made regarding this hypothesis.

The antibody cross-reactive experiments produced unexpected results. While some mice infected with StV *C. rodentium* were capable of generating a wild type level antibody response against all lysates types, many were not. In fact, on average >30% fewer animals infected with StV *C. rodentium* generated specific antibody, compared to those animals infected with either wild type or SCV *C. rodentium*. The lowered antibody response is presumably not caused by an intrinsic problem with the main antigenic protein, intimin (27), because serum taken from mice infected with wild type or the SCV responded equally well to StV lysate (Figure 5B) as they did to the lysate made from wild

type *C. rodentium*. Further, the secreted protein profiles indicate that StV *C. rodentium* is capable of producing and secreting virulence factors to same degree as wild type *C. rodentium* (Figure 1C) although the expression patterns may be quite different *in vivo* than they are *in vitro*. Notably, StV is presumably not sequestered in increased biofilm production, because it does not produce increased biofilm formation *in vitro*. Alternatively, StV could induce increased mucus production in infected mice and be hiding in an extra thick layer of mucus. Initial staining with Periodic acid-Schiff (PAS) did not reveal a dramatic difference between wild type and StV *C. rodentium* infected colons, but further studies are required for a definitive answer.

Together these studies demonstrate that the variants generated by passage of *C. rodentium* through MyD88$^{-/-}$ mice may reveal previously undiscovered crucial aspects of infection of mice by *C. rodentium* required for causing disease. For example, the reduced damage measurements pathology observed in colonic tissue following infection with SCV *C. rodentium* cement the role of pathogen growth as the cause of bleeding, epithelium raggedness, and GMN, rather than the host response. These results indicate the importance of controlling A/E pathogen growth to reduce disease symptoms. Therefore, the newly discovered mechanisms by which *C. rodentium* causes disease represent novel targets for therapeutic interventions.

Literature Cited:

1. Casadevall, A., and L. A. Pirofski: Host-pathogen interactions: basic concepts of microbial commensalism, colonization, infection, and disease. *Infect Immun*. 68(12), 6511-6518(2000).
2. Smith, H.: Questions about the behaviour of bacterial pathogens in vivo. *Philos Trans R Soc Lond B Biol Sci*. 355(1397), 551-564(2000).
3. von Eiff, C., G. Peters, and K. Becker: The small colony variant (SCV) concept -- the role of staphylococcal SCVs in persistent infections. *Injury*. 37 Suppl 2(S26-33(2006).
4. Rea, R., C. Hill, and C. G. Gahan: Listeria monocytogenes PerR mutants display a small-colony phenotype, increased sensitivity to hydrogen peroxide, and significantly reduced murine virulence. *Appl Environ Microbiol*. 71(12), 8314-8322(2005).
5. Cano, D. A., M. G. Pucciarelli, M. Martinez-Moya, J. Casadesus, and F. Garcia-del Portillo: Selection of small-colony variants of Salmonella enterica serovar typhimurium in nonphagocytic eucaryotic cells. *Infect Immun*. 71(7), 3690-3698(2003).
6. Colwell, C. A.: Small Colony Variants of Escherichia coli. *J Bacteriol*. 52(4), 417-422(1946).
7. Bsat, N., A. Herbig, L. Casillas-Martinez, P. Setlow, and J. D. Helmann: Bacillus subtilis contains multiple Fur homologues: identification of the iron uptake (Fur) and peroxide regulon (PerR) repressors. *Mol Microbiol*. 29(1), 189-198(1998).
8. McDermid, J. M., and A. M. Prentice: Iron and infection: effects of host iron status and the iron-regulatory genes haptoglobin and NRAMP1 (SLC11A1) on host-pathogen interactions in tuberculosis and HIV. *Clin Sci (Lond)*. 110(5), 503-524(2006).
9. McDaniel, T. K., K. G. Jarvis, M. S. Donnenberg, and J. B. Kaper: A genetic locus of enterocyte effacement conserved among diverse enterobacterial pathogens. *Proc Natl Acad Sci U S A*. 92(5), 1664-1668(1995).
10. Wiles, S., G. Dougan, and G. Frankel: Emergence of a 'hyperinfectious' bacterial state after passage of Citrobacter rodentium through the host gastrointestinal tract. *Cell Microbiol*. 7(8), 1163-1172(2005).
11. Adachi, O., T. Kawai, K. Takeda, et al.: Targeted disruption of the MyD88 gene results in loss of IL-1- and IL-18-mediated function. *Immunity*. 9(1), 143-150(1998).
12. Tatusova, T. A., and T. L. Madden: BLAST 2 Sequences, a new tool for comparing protein and nucleotide sequences. *FEMS Microbiol Lett*. 174(2), 247-250(1999).
13. Lebeis, S. L., B. Bommarius, C. A. Parkos, M. A. Sherman, and D. Kalman: TLR signaling mediated by MyD88 is required for a protective innate immune response by neutrophils to Citrobacter rodentium. *J Immunol*. 179(1), 566-577(2007).
14. Wei, O. L., A. Hilliard, D. Kalman, and M. Sherman: Mast cells limit systemic bacterial dissemination but not colitis in response to Citrobacter rodentium. *Infect Immun*. 73(4), 1978-1985(2005).

15. Luperchio, S. A., and D. B. Schauer: Molecular pathogenesis of Citrobacter rodentium and transmissible murine colonic hyperplasia. *Microbes Infect*. 3(4), 333-340(2001).
16. Grass, G.: Iron transport in Escherichia coli: all has not been said and done. *Biometals*. 19(2), 159-172(2006).
17. Neilands, J. B.: Iron absorption and transport in microorganisms. *Annu Rev Nutr*. 1(27-46(1981).
18. Pollack, J. R., and J. B. Neilands: Enterobactin, an iron transport compound from Salmonella typhimurium. *Biochem Biophys Res Commun*. 38(5), 989-992(1970).
19. Raymond, K. N., E. A. Dertz, and S. S. Kim: Enterobactin: an archetype for microbial iron transport. *Proc Natl Acad Sci U S A*. 100(7), 3584-3588(2003).
20. Liu, J., K. Duncan, and C. T. Walsh: Nucleotide sequence of a cluster of Escherichia coli enterobactin biosynthesis genes: identification of entA and purification of its product 2,3-dihydro-2,3-dihydroxybenzoate dehydrogenase. *J Bacteriol*. 171(2), 791-798(1989).
21. Sundlov, J. A., J. A. Garringer, J. M. Carney, et al.: Determination of the crystal structure of EntA, a 2,3-dihydro-2,3-dihydroxybenzoic acid dehydrogenase from Escherichia coli. *Acta Crystallogr D Biol Crystallogr*. 62(Pt 7), 734-740(2006).
22. Drake, E. J., D. A. Nicolai, and A. M. Gulick: Structure of the EntB multidomain nonribosomal peptide synthetase and functional analysis of its interaction with the EntE adenylation domain. *Chem Biol*. 13(4), 409-419(2006).
23. Gehring, A. M., K. A. Bradley, and C. T. Walsh: Enterobactin biosynthesis in Escherichia coli: isochorismate lyase (EntB) is a bifunctional enzyme that is phosphopantetheinylated by EntD and then acylated by EntE using ATP and 2,3-dihydroxybenzoate. *Biochemistry*. 36(28), 8495-8503(1997).
24. Clifford, D. P., and J. E. Repine: Hydrogen peroxide mediated killing of bacteria. *Mol Cell Biochem*. 49(3), 143-149(1982).
25. Goller, C., X. Wang, Y. Itoh, and T. Romeo: The cation-responsive protein NhaR of Escherichia coli activates pgaABCD transcription, required for production of the biofilm adhesin poly-beta-1,6-N-acetyl-D-glucosamine. *J Bacteriol*. 188(23), 8022-8032(2006).
26. Brewer, N. S.: Antimicrobial agents--Part II. The aminoglycosides: streptomycin, kanamycin, gentamicin, tobramycin, amikacin, neomycin. *Mayo Clin Proc*. 52(11), 675-679(1977).
27. Ghaem-Maghami, M., C. P. Simmons, S. Daniell, et al.: Intimin-specific immune responses prevent bacterial colonization by the attaching-effacing pathogen Citrobacter rodentium. *Infect Immun*. 69(9), 5597-5605.(2001).

Figure Legends:

Figure 1: The generation of a SCV *C. rodentium* from persistently infected mice. (A) A schematic of the protocol used to generate variants of *C. rodentium* in MyD88$^{-/-}$ mice. (B) Two morphologies of *C. rodentium* were isolated from persistently infected mice a small colony variant (SCV) and a standard-growth variant (StV). (C) The secreted protein profiles for wild type (WT), StV, and SCV *C. rodentium* were identical. Proteins the same size as EspA, EspB, and EspD were observed. (D) Growth curves of WT and SCV *C. rodentium* in standing liquid culture. Curves were repeated in triplicate; a representative curve has been shown.

Figure 2: Characterization of SCV *C. rodentium*. (A) The minimum inhibitory concentration (MIC) was determined for neomycin, kanamycin, streptomycin, and polymyxin B by adding various concentration of each antibiotic to MacConkey agar plates. (B) Colony size was assessed on several different types of media, including minimal media with various carbon sources. (C) Growth curves were repeated in liquid cultures grown without (WT *C. rodentium* dark blue diamonds and SCV *C. rodentium* light green squares) and with Fe(III)Cl_3 supplemented in the LB media (WT *C. rodentium* light blue diamonds and SCV *C. rodentium* dark green squares). (D) WT or SCV *C. rodentium* (5×10^5) incubated with neutrophils (2.5×10^5) from C57BL/6 mice was killed with equal efficacy. Representative experiment repeated three times in triplicate.

Figure 3: SCV *C. rodentium* colonizes mice and causes mortality more slowly than WT *C. rodentium*. (A) Survival curves of 6-10 week old MyD88$^{-/-}$ infected with 4×10^8 CFU of either WT (n=6, red diamonds) or SCV (n=7, orange squares) *C. rodentium*. Various tissues were harvested aseptically from MyD88$^{-/-}$ mice infected with either WT

or SCV *C. rodentium.* CFU were quantitated 3 days p.i. (B, WT n=4 and SCV n=7) and 7 days p.i. (C, WT n=4-6 and SCV n=6). (D) C57BL/6 mice were infected with either WT (n=4) or SCV *C. rodentium* (n=6) various tissues were harvested aseptically 7 days p.i. *C. rodentium* CFU were quantitated as described in *Material and Methods*.

Figure 4: The decreased pathology seen in SCV infected colonic tissue is mostly caused by decreased damage measurements. (A) Pathology scores were assessed in colonic tissue from C57BL/6 (n=4) or MyD88$^{-/-}$ mice (n=6) 7 days p.i. (B) Pathology scores of the damage measurements including bleeding, ragged epithelium, and GMN were assessed in colonic tissue from C57BL/6 (n=4) and MyD88$^{-/-}$ (n=6) mice 7 days p.i. (C) Pathology score was assessed for degree of hyperplasia and goblet cell loss in colonic tissue taken from C57BL/6 (n=4) and MyD88$^{-/-}$ (n=6) mice 7 days p.i. (D) Pathology scores for recruitment measurements including edema and neutrophil infiltration were assessed in colonic tissue from C57BL/6 (n=4) or MyD88$^{-/-}$ (n=6) mice 7 days p.i.

Figure 5: Fewer mice infected with StV *C. rodentium* generate an antibody response. **(**A) The antibody response of serum taken from mice infected with either WT (n=17), StV (n=16), or SCV (n=17) against WT *C. rodentium* lysate was measured. (B) The antibody response of serum taken from mice infected with either WT (n=16), StV (n=13), or SCV (n=17) against StV *C. rodentium* lysate was measured. (C) The antibody response of serum taken from mice infected with either WT (n=17), StV (n=15), or SCV (n=17) against SCV *C. rodentium* lysate was measured. (D) Biofilm formation in 96-well plates was quantitated by degree of crystal violet staining and absorbance reading at 630 nm for WT and StV *C. rodentium* after 4, 8, 24, and 36 incubation times. *, indicates

Statistically lower in comparison to mice infected with either WT or SCV *C. rodentium*, at a significance level $p < 0.01$.

Figure 1

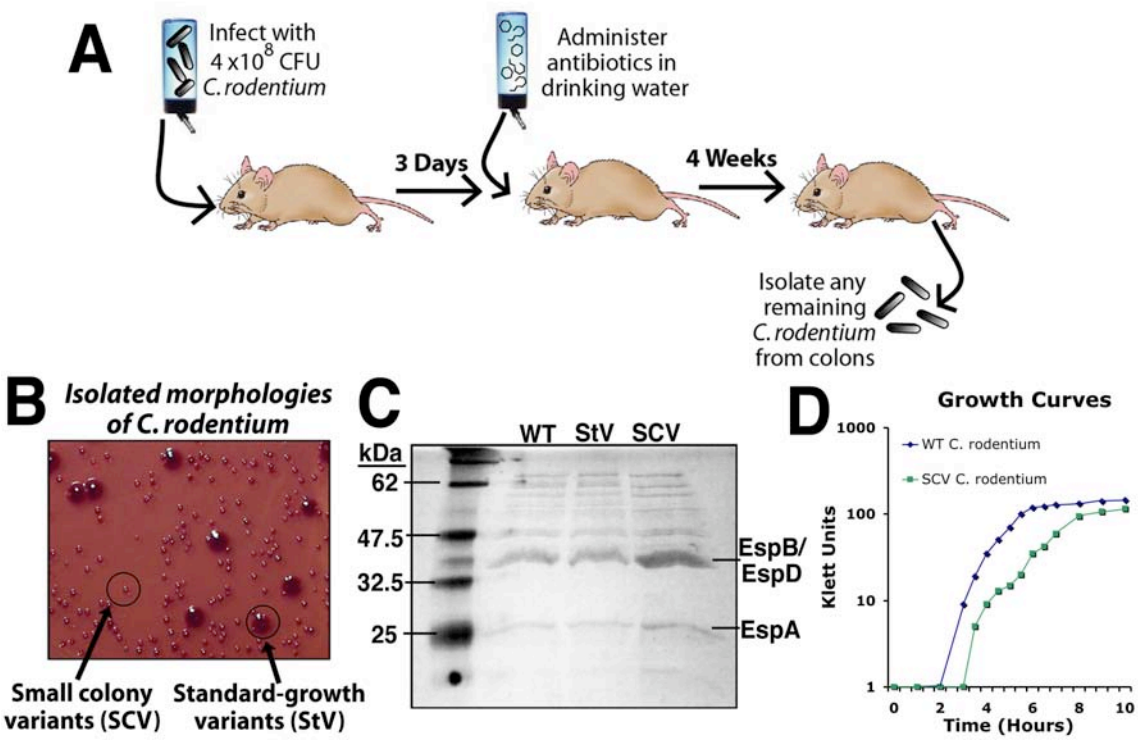
A
Infect with
4 x10^8 CFU
C. rodentium
Administer
antibiotics in
drinking water
3 Days
4 Weeks
Isolate any
remaining
C. rodentium
from colons
B
Isolated morphologies
of C. rodentium
Small colony
variants (SCV)
Standard-growth
variants (StV)
C
WT StV SCV
kDa
62
47.5
32.5
25
EspB/
EspD
EspA
D
Growth Curves
WT C. rodentium
SCV C. rodentium
Klett Units
1000
100
10
1
0 2 4 6 8 10
Time (Hours)

Figure 2

A

MIC for various antibiotics

Neomycin	MIC (μg/mL)
WT *C. rodentium*	5
SCV *C. rodentium*	50
Kanamycin	**MIC (μg/mL)**
WT *C. rodentium*	3
SCV *C. rodentium*	30
Streptomycin	**MIC (μg/mL)**
WT *C. rodentium*	5
SCV *C. rodentium*	15

B

***C. rodentium* growth on various medias**

Media	WT *C. rodentium*	SCV *C. rodentium*
MacConkey agar	Large	Small
LB agar	Large	Small
EMB agar	Large	Small
Minimal media		
+ glucose	Small	Small
+ lactose	Small	Small
+ glycerol	Small	Small
+ succinate	Small	Small
+ glucose & His	Small	Small
+ glucose & Trp	Small	Small
+ glucose, His, & Trp	Small	Small
+ glucose & essential amino acids	Small	Small
BHI agar	Large	Large

C

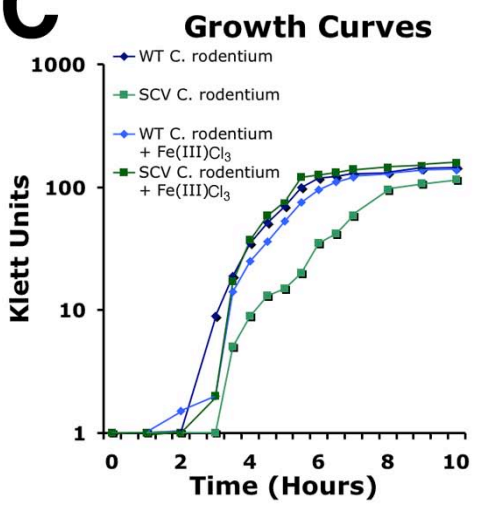

D

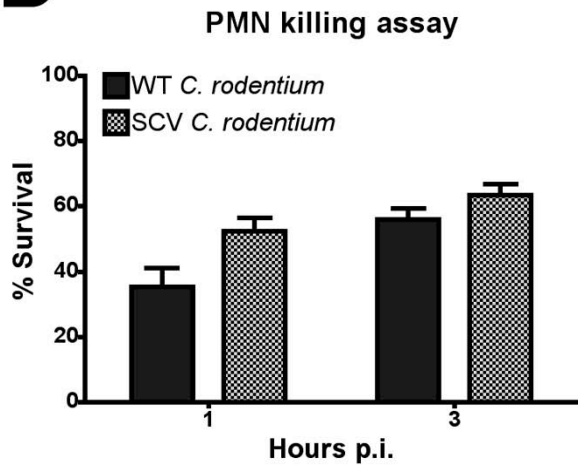

Figure 3

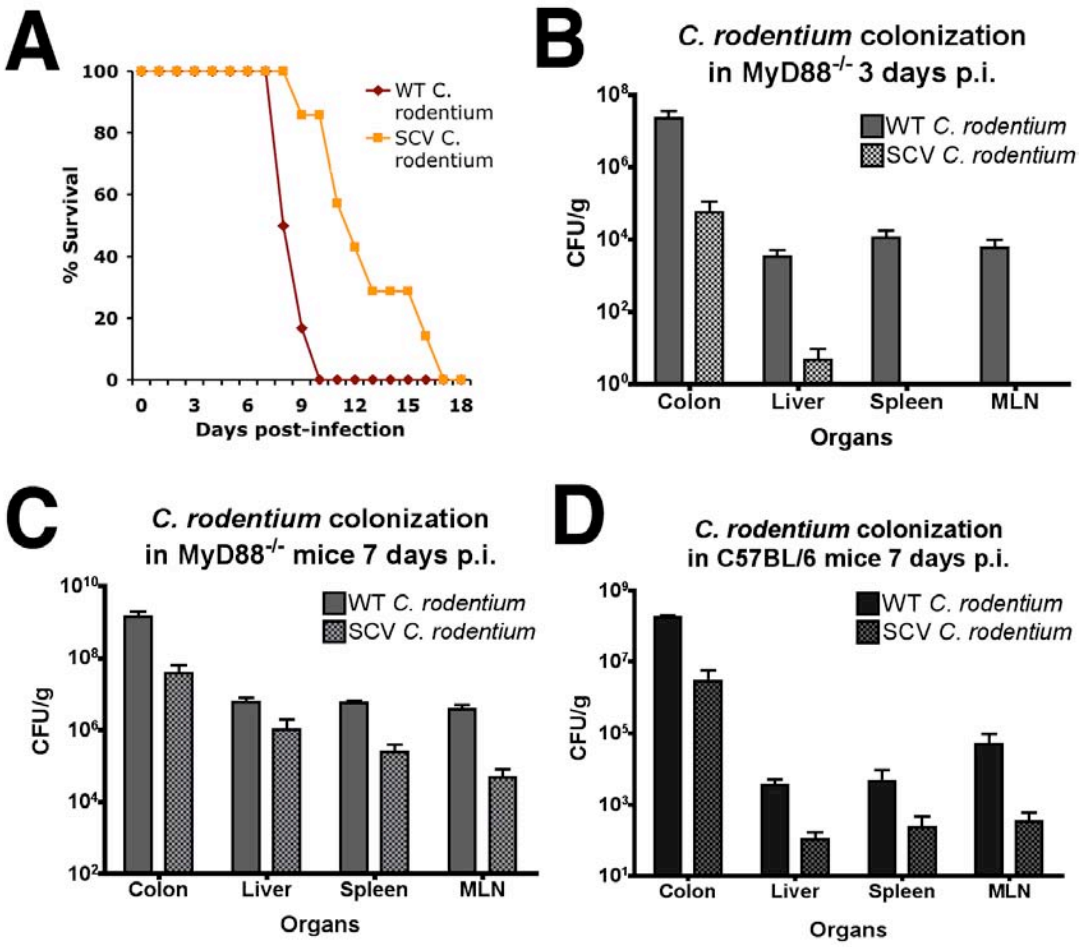
A
100
80
60
40
20
0
% Survival
0
3
6
9
12
15
18
Days post-infection
WT C. rodentium
SCV C. rodentium
B
C. rodentium colonization in MyD88-/- 3 days p.i.
CFU/g
Colon
Liver
Spleen
MLN
Organs
WT C. rodentium
SCV C. rodentium
C
C. rodentium colonization in MyD88-/- mice 7 days p.i.
CFU/g
Colon
Liver
Spleen
MLN
Organs
WT C. rodentium
SCV C. rodentium
D
C. rodentium colonization in C57BL/6 mice 7 days p.i.
CFU/g
Colon
Liver
Spleen
MLN
Organs
WT C. rodentium
SCV C. rodentium

Figure 4

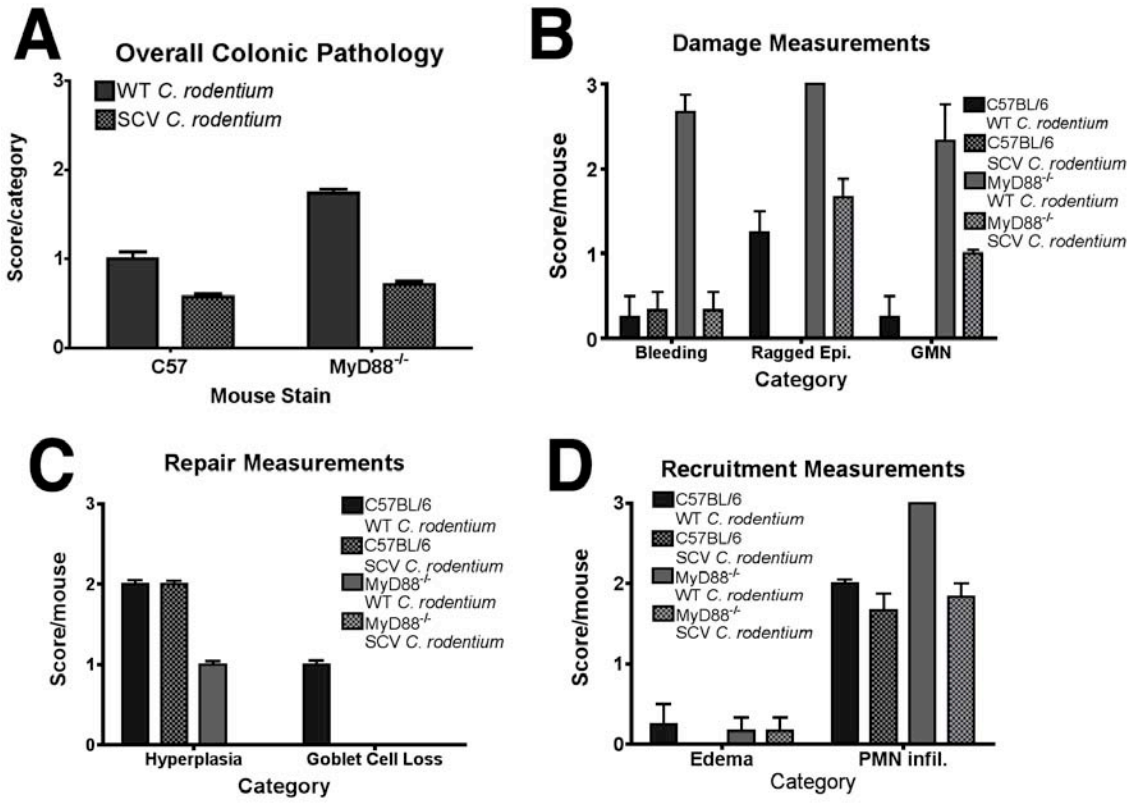
A
Overall Colonic Pathology
WT C. rodentium
SCV C. rodentium
Score/category
C57
MyD88-/-
Mouse Stain
B
Damage Measurements
C57BL/6 WT C. rodentium
C57BL/6 SCV C. rodentium
MyD88-/- WT C. rodentium
MyD88-/- SCV C. rodentium
Score/mouse
Bleeding
Ragged Epi.
GMN
Category
C
Repair Measurements
Hyperplasia
Goblet Cell Loss
D
Recruitment Measurements
Edema
PMN infil.

Figure 5

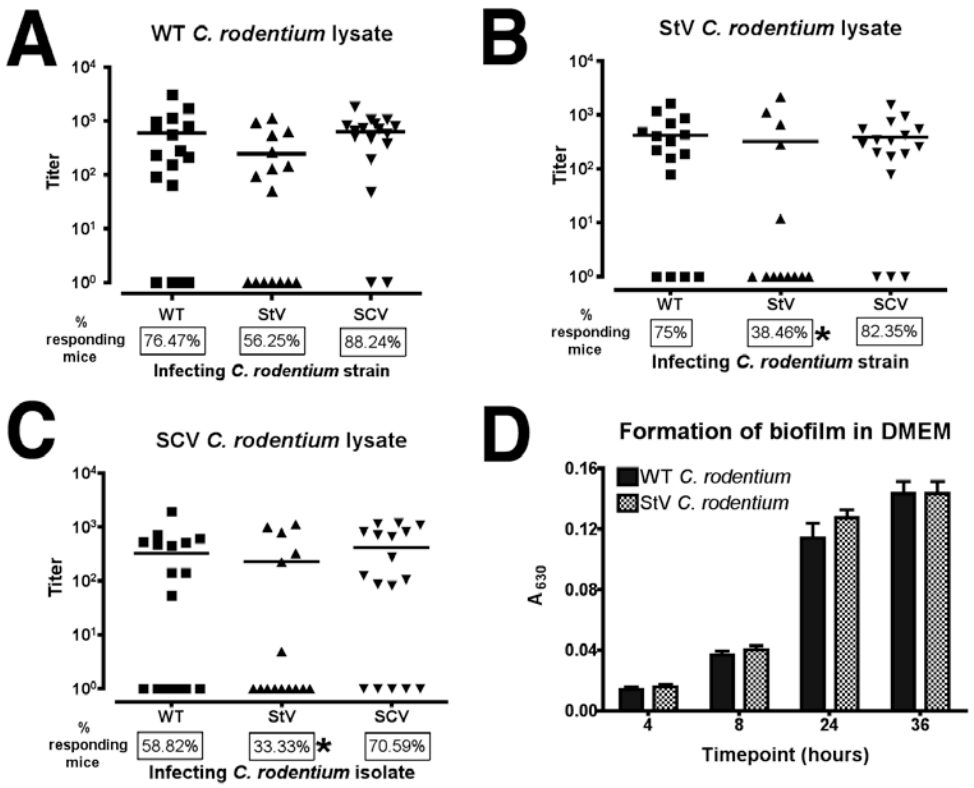
A
WT C. rodentium lysate
Titer
WT
StV
SCV
% responding mice
76.47%
56.25%
88.24%
Infecting C. rodentium strain
B
StV C. rodentium lysate
Titer
WT
StV
SCV
% responding mice
75%
38.46%
*
82.35%
Infecting C. rodentium strain
C
SCV C. rodentium lysate
Titer
WT
StV
SCV
% responding mice
58.82%
33.33%
*
70.59%
Infecting C. rodentium isolate
D
Formation of biofilm in DMEM
WT C. rodentium
StV C. rodentium
A630
Timepoint (hours)

CHAPTER V:

DISCUSSION

Discussion:

Prior to the work described here, the innate immune response to *C. rodentium* in mice was poorly understood. In fact, there was evidence suggesting that aspects of the innate immune response are detrimental during an infection with an A/E pathogen (1, 2). However, the studies presented in this dissertation prove that innate immunity grants protection on multiple levels against *C. rodentium*. More specifically, my research has demonstrated that the intestinal damage including bleeding, epithelial injury, and gangrenous mucosal necrosis (GMN) observed during *C. rodentium* infection is pathogen-induced and not caused by the host response. Thus, these studies represent a significant change in our understanding of the roles played by innate immunity in response to an infection with A/E pathogens. The information gathered here may contribute to the development of improved therapeutic approaches utilized to treat A/E infections.

Protective roles innate immune responses play during infection with *C. rodentium.*

The data presented in this dissertation suggests that MyD88 signaling by both hematopoietic and non-hematopoietic cells is required at multiple levels to protect the host from disseminated bacterial infection (Figure 1) including production of chemokines (e.g. KC) in a MyD88-dependent manner (step 1b) leading to recruitment of neutrophils, which contain the infection by killing bacteria (step 1c). Concurrently, recruitment of macrophages facilitate repairs to the damage to the epithelial barrier in a MyD88-dependent fashion (3) (step 1g). Notably, MyD88 signaling contributes to the quality of the antibody response and facilitates clearance of *C. rodentium* in a timely fashion (step 5). In the absence of MyD88 signaling, neutrophil recruitment is delayed resulting in

expansion of pathogen load in colonic tissue, and transit of additional bacteria from the lumen due to increased intestinal damage. Bacterial dissemination to liver and spleen (step 3) is greatly increased if neutrophil function is inhibited (CHAPTER II) or if the intestine has incurred significant damage, as with MyD88$^{-/-}$ and IL-1R$^{-/-}$ mice (CHAPTERS II and III), and overwhelms the animal before an effective adaptive response can be mounted. In summary, our results provide a crucial role for MyD88 and IL-1R signaling in host responses that confer protection from lethal colitis. In addition, we demonstrate that lethal colitis occurs in IL-1R$^{-/-}$ mice despite normal levels of neutrophil recruitment, damage epithelium enterocyte replacement, and *C. rodentium* load control, indicating that these mice have increased predisposition to intestinal damage. Further, these data indicate that it is more important to control damage than to improve neutrophil recruitment or increase hyperplasia responses. Finally, we show that the key to inhibiting the ability of *C. rodentium* to cause disease in mice may be to simply inhibit its growth *in vivo*, reminding us of the utility of antibiotic treatments against A/E pathogens.

Addressing the focal nature of *C. rodentium* colonization

Interestingly, the presence of bacterial surface adherence fimbriae allows EPEC to form small aggregates or "microcolonies" on epithelial cells *in vitro* and is suggested to be part of the initial attachment phase during A/E infection *in vivo* (4). Indeed, anecdotal evidence suggests that *C. rodentium* colonizes and causes disease in isolated pockets throughout the colon (S.L.L. unpublished observations). The development of GMN following infection with *C. rodentium* in the intestine of predisposed animals, such as MyD88$^{-/-}$ and IL-1R$^{-/-}$ mice, may merely be an exaggeration of this phenomenon.

Interestingly, bleeding between crypts is often in close proximity to GMN formation, suggesting that the blood may provide necessary nutrients that allow microcolonies to develop into GMN. Indeed it has previously been demonstrated that heme, which is present in red blood cells (RBCs), is a major source of iron for microbes (5). In fact, many pathogens including *Yersinia enterocolitica* (6) and *Shigella dysenteriae* (7) actually possess receptors on their surface to bind and internalize heme as an iron source. Further, it has been recently noted that the addition of mouse blood to *C. rodentium* liquid LB cultures causes an increased growth rate (8). Thus, the blood could lead to focal overgrowth of *C. rodentium* one of the hallmark features of GMN.

When Dann and colleagues separated out the components of the blood, it was discovered that the RBC lysate only allowed a mild growth increase and that serum components lead to a greater increase in growth rate, indicating that any increase caused by the iron components of blood do not cause the majority of the increased growth rate of *C. rodentium*. This data correlates with the lack of increased growth in wild type *C. rodentium* when excess $Fe(III)Cl_3$ iron was added (CHAPTER IV). Dann et al. further demonstrated that the serum component promoting growth of *C. rodentium* is a low molecular weight, heat stable factor, which lead them to investigate the effect of various amino acids to the growth of *C. rodentium*. Indeed, a mixture of nonessential amino acids to LB did increase the growth rate of *C. rodentium in vitro*. However, the investigation performed in CHAPTER IV demonstrates that a mixture of amino acids on minimal media did not lead to overgrowth by the pathogen, indicating that this phenomenon only occurs when bacteria are grown in a rich media, such as LB. Together these data indicate that blood may be an important source of nutrients during infection of mice with *C.*

rodentium. Thus, our data suggest a molecular strategy of *C. rodentium* of to induce bleeding; thus, gaining access to iron and amino acids which potentially aids the ability of A/E pathogens to colonize host organisms.

The implications of these studies to development of therapeutics

We have reached an exciting point in the quest to understand the role of innate immunity during infection with A/E pathogens. The *C. rodentium* model has uncovered both protective and deleterious innate immune responses. Such findings remain to be validated with other A/E pathogens using small animal models. Such data for EHEC and EPEC are of particular interest, because invasive strains of *E. coli* are commonly present in patients with IBD (9), an inflammatory disease that affects 1.4 million people in the United States alone. An understanding of the innate immune response is crucial for the design of therapeutics that mitigates destructive responses without disrupting protective ones. For example, previous studies have suggested that therapeutics directed against IL-1R signaling might be beneficial to lower the symptoms of IBD patients (10). However, our data indicate that such therapeutics may cause increased susceptibility to pathogenic *E. coli* strains and would not dampen key aspects of inflammation, including neutrophil recruitment or development of hyperplasia. Another seemingly obvious target for intervention is the TLR4 signaling pathway (2). However, putative inhibitors would need to distinguish the amount of TLR4 signaling that is deleterious from the amount of TLR4 signaling that is necessary for the repair of damaged intestinal epithelia (11). Nevertheless, novel and exciting alternative approaches are on the horizon. For example, antimicrobial peptides (AMPs) have dual functions as antimicrobials and immunomodulators (12), and their therapeutic potential in treating inflammatory disease

is currently under investigation. Furthermore, systems biology approaches can be used as a means to both understand the complexity of the innate immune response, and in the simultaneous development of therapeutics that target key aspects of the response (13). Ultimately, multiple therapeutic strategies, including highly tuned anti-inflammatory agents, antibiotics, probiotics and restorative measures such as fluid replacement, may together prove successful in the treatment of the complex inflammatory disease caused by A/E pathogens.

Literature Cited:

1. Higgins, L. M., G. Frankel, G. Douce, G. Dougan, and T. T. MacDonald: Citrobacter rodentium infection in mice elicits a mucosal Th1 cytokine response and lesions similar to those in murine inflammatory bowel disease. *Infect Immun*. 67(6), 3031-3039.(1999).
2. Khan, M. A., C. Ma, L. A. Knodler, et al.: Toll-like receptor 4 contributes to colitis development but not to host defense during Citrobacter rodentium infection in mice. *Infect Immun*. 74(5), 2522-2536(2006).
3. Pull, S. L., J. M. Doherty, J. C. Mills, J. I. Gordon, and T. S. Stappenbeck: Activated macrophages are an adaptive element of the colonic epithelial progenitor niche necessary for regenerative responses to injury. *Proc Natl Acad Sci U S A*. 102(1), 99-104(2005).
4. Nataro, J. P., and J. B. Kaper: Diarrheagenic Escherichia coli. *Clin Microbiol Rev*. 11(1), 142-201.(1998).
5. Letoffe, S., P. Delepelaire, and C. Wandersman: Functional differences between heme permeases: Serratia marcescens HemTUV permease exhibits a narrower substrate specificity (restricted to heme) than the Escherichia coli DppABCDF peptide-heme permease. *J Bacteriol*. 190(6), 1866-1870(2008).
6. Stojiljkovic, I., and K. Hantke: Transport of haemin across the cytoplasmic membrane through a haemin-specific periplasmic binding-protein-dependent transport system in Yersinia enterocolitica. *Mol Microbiol*. 13(4), 719-732(1994).
7. Wyckoff, E. E., D. Duncan, A. G. Torres, et al.: Structure of the Shigella dysenteriae haem transport locus and its phylogenetic distribution in enteric bacteria. *Mol Microbiol*. 28(6), 1139-1152(1998).
8. Dann, S. M., M. E. Spehlmann, D. C. Hammond, et al.: IL-6-dependent mucosal protection prevents establishment of a microbial niche for attaching/effacing lesion-forming enteric bacterial pathogens. *J Immunol*. 180(10), 6816-6826(2008).
9. Sasaki, M., S. V. Sitaraman, B. A. Babbin, et al.: Invasive Escherichia coli are a feature of Crohn's disease. *Lab Invest*. 87(10), 1042-1054(2007).
10. Arai, Y., H. Takanashi, H. Kitagawa, and I. Okayasu: Involvement of interleukin-1 in the development of ulcerative colitis induced by dextran sulfate sodium in mice. *Cytokine*. 10(11), 890-896(1998).
11. Fukata, M., K. S. Michelsen, R. Eri, et al.: Toll-like receptor-4 is required for intestinal response to epithelial injury and limiting bacterial translocation in a murine model of acute colitis. *Am J Physiol Gastrointest Liver Physiol*. 288(5), G1055-1065(2005).
12. Hancock, R. E., and H. G. Sahl: Antimicrobial and host-defense peptides as new anti-infective therapeutic strategies. *Nat Biotechnol*. 24(12), 1551-1557(2006).
13. Brown, K. L., C. Cosseau, J. L. Gardy, and R. E. Hancock: Complexities of targeting innate immunity to treat infection. *Trends Immunol*. 28(6), 260-266(2007).

Figure Legends:

Figure 1: Model for C. rodentium infection and dissemination. Upon infection, A/E pathogens cause breach of the epithelial barrier and entry of bacteria into the lamina propria (step 1a) and subsequent innate immune detection by TLRs leads to NF-?B activation and production of cytokines and chemokines (step 1b). Neutrophils and macrophages are then recruited to the site of infection (step 1c). A/E pathogens gain further access to intestinal tissues following nonspecific damage by neutrophils (step 1d) However, neutrophils and macrophages kill A/E pathogens (step 1e); in response, bacteria inhibit phagocytosis by macrophages (step 1f). Macrophages also induce the repair response in intestinal crypts (step 1g). Resident mast cells induce vasodilatation; thus inducing further destructive inflammation (step 1h). Importantly, mast cells also secrete factor(s) that kill bacteria (step 1i). Dendritic cells sample luminal antigens via dendrites that extend across the epithelial barrier (step 1j), and then migrate to draining lymphoid tissue where they present antigens to naïve T cells. Disruption of the epithelial barrier allows dissemination of the bacteria to the mesenteric lymph nodes (MLN; Step 2), and subsequently to the liver and spleen (Step 3); neutrophils (PMN) recruited early in the infection kill bacteria in the colon and at peripheral sites, thereby reducing bacterial load (Step 4). Timely recruitment of neutrophils depends on production of chemokines such as KC via MyD88 signaling in non-hematopoietic cells, most likely colonic epithelia. Finally, an antibody response mounted by the adaptive immune system facilitates clearance of the bacteria (Step 5). MyD88 signaling is also required for optimal adaptive response. * Indicates steps in which MyD88 signaling is important.

Figure 1

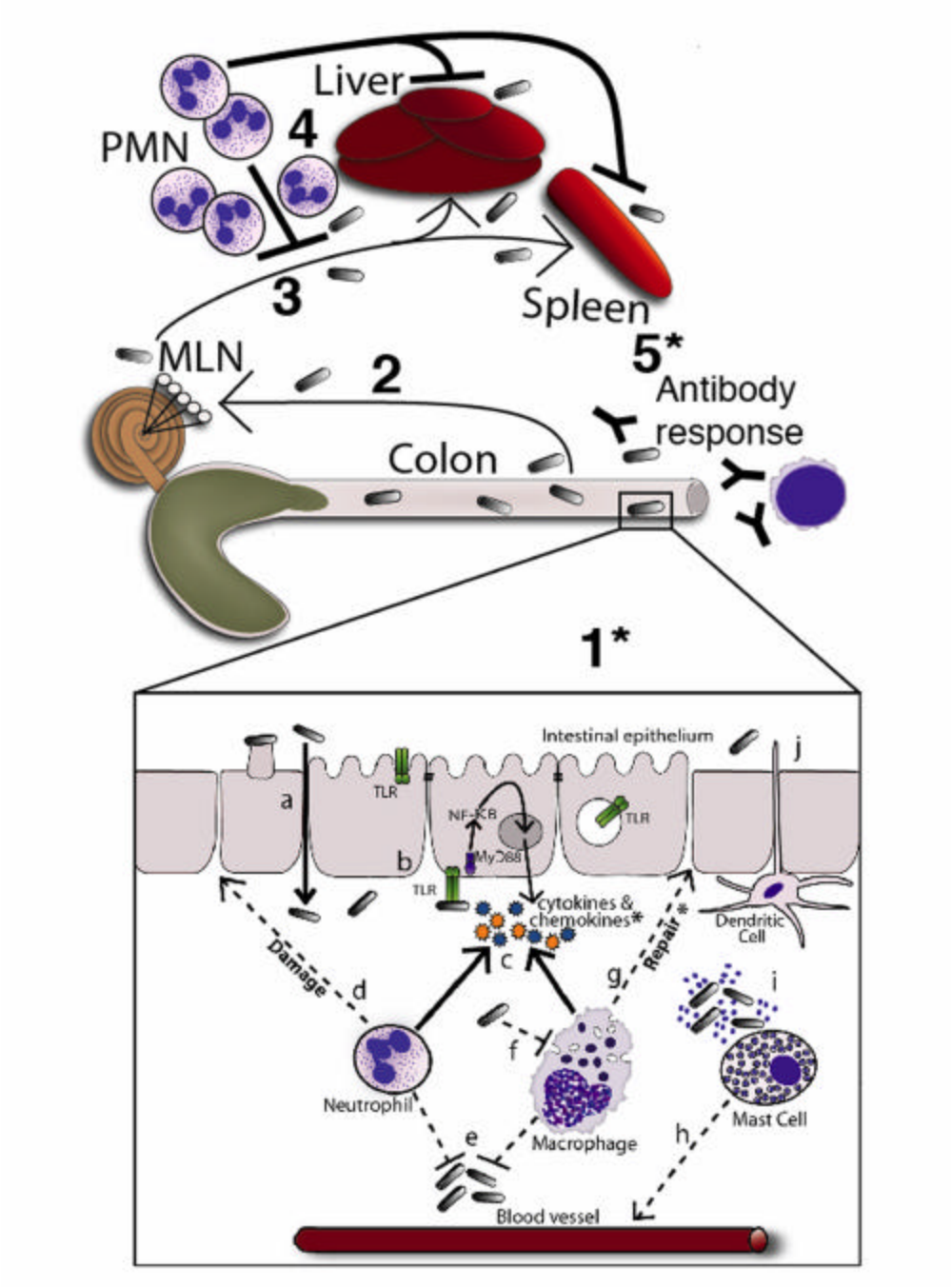
Liver
PMN
4
3
Spleen
MLN
2
5*
Antibody
response
Colon
1*
Intestinal epithelium
a
TLR
NF-κB
TLR
b
MyD88
TLR
cytokines &
chemokines*
c
Damage
d
Repair *
g
Dendritic
Cell
j
i
f
Neutrophil
Macrophage
Mast Cell
e
h
Blood vessel